PhD degree in Molecular Medicine

European School of Molecular Medicine (SEMM),

University of Milan and University of Naples "Federico II"

Faculty of Medicine

Settore disciplinare: BIO/11

PERSISTENT DNA DAMAGE AT TELOMERES, CAUSED BY TRF2-MEDIATED DNA REPAIR INHIBITION, TRIGGERS CELLULAR SENESCENCE AND IS ASSOCIATED WITH PRIMATES AGEING

Francesca Rossiello

IFOM, Milan

Matricola n. R08908

Supervisor Dr. Fabrizio d'Adda di Fagagna

IFOM, Milan

Internal co-supervisor Prof. Marco Foiani

IFOM, Milan

External co-supervisor Dr. Maria A. Blasco

CNIO, Madrid

Anno accademico 2012-2013

TABLE OF CONTENTS

List of Abbreviations

53BP1	p53 binding protein 1
ALT	alternative lengthening of telomere
AcH4	acetylated histone H4
ASO	antisense oligonucleotides
AT	ataxia-teleangectasia
ATCC	american type culture collection
ATM	ataxia telangiectasia mutated
ATR	ataxia telangiectasia and Rad3-related
ATRIP	ATR-interacting protein
B2M	Beta-2-microglobulin
BRCA1	breast cancer 1
BrdU	bromodeoxyuridine
CDK	cyclin-dependent kinase
CDS	coding DNA sequence
CLIP	cross-linking immunoprecipitation
DAPI	4',6-diamidino-2-phenylindole
DDR	DNA damage response
DDRNA	DNA damage response RNA
diRNA	DSB-induced RNA
DN	dominant negative
DNA-PKcs	DNA-PK catalytic subunit
DSB	double-strand break
ER	estrogen receptor

GR	glucocorticoid receptor
Gy	gray
HP1	heterochromatin protein-1
HR	homologous recombination
IR	Ionizing radiation
LNA	locked nucleic acid
lncRNA	long non-coding
MDC1	mediator of DNA damage checkpoint 1
MEF	mouse embryonic fibroblast
miRNA	microRNA
MRN	Mre11-Rad50-Nbs1
mRNA	messenger RNA
NBS	Nijmegen breakage syndrome
ncRNA	non-coding RNA
NHEJ	non-homologous end joining
OIS	oncogene-induced senescence
PFA	paraformaldehyde
piRNA	piwi interacting RNA
PNA	Peptide Nucleic Acid
POT1	protection of telomeres 1
pre-miRNA	precursor microRNA
pri-miRNA	primary microRNA
RAP1	repressor/activator protein 1
RNAi	RNA interference
ROS	reactive oxygen species
RPA	replication protein A

Rplp0	Ribosomal protein large P0
rRNA	ribosomal RNA
SA-β-gal	senescence-associated-β-galactosidase
SAHF	senescence-associated heterochromatin foci
SASP	senescent-associated secretory phenotype
s.d.	standard deviation
SDF	senescence-associated DNA-damage foci
SDS	sodium dodecyl sulphate
s.e.m.	standard error of the mean
shRNA	short hairpin RNA
siRNA	small interfering RNA
SISP	stress-induced premature senescence
snoRNA	small nucleolar RNA
snRNA	small nuclear RNA
SSB	Single-strand break
TERRA	telomeric repeat-containing RNA
TIF	telomere induced focus
TIN2	TRF1-interacting nuclear factor 2
TopBP1	topoisomerase II binding protein 1
TPP1	POT1 and TIN2 organizing protein
TRF1	telomeric-repeat-binding factor 1
TRF2	telomeric-repeat-binding factor 2
tRNA	transfer RNA
tTA	tetracyclin-controlled transactivator
UV	ultraviolet
VPA	valproic acid

Figures Index

Note about the figures

Figures 5, 7, 8, 9, 15, 17, 18, 19, 20, 21, 22, 23, 24, 26, 31, 32, 33 and 34, describe my original work that has been published, so they are considered as adapted from (Fumagalli, Rossiello et al., Nature Cell Biology, 2012).

1 Abstract

The DNA damage response (DDR) coordinates DNA repair events and transiently arrests cell-cycle progression until DNA damage has been removed. If the damage is not resolved, cells can enter an irreversible cell cycle arrest called cellular senescence. In irradiation-induced senescent cells a large fraction of persistent DDR markers are associated with telomeric DNA, both in cultured cells and in *in vivo* tissues.

The aim of my PhD project was to investigate the mechanism underlying this phenomenon. I showed that persistent DDR activation has a causative role for the senescence-associated cell cycle exit and that a double-strand break (DSB) within telomeric repeats is inducing a more protracted DDR activation compared with a non-telomeric one in human cells. The DDR persistency at telomeres is neither dependent on their heterochromatic state nor on TRF2 loss from telomeres during senescence establishment. Rather, TRF2 recruitment next to a DSB, in the absence of telomeric DNA, is sufficient to induce a more protracted site-specific DDR focus and to impair DSB repair in mouse cells. Ageing is associated with accumulation of markers of DDR activation. In terminally differentiated brain neurons from old primates, I observed DDR activation at telomeres that were not critically short.

Taken together, these results strongly suggest that TRF2 inhibits DNA repair at broken telomeres, contributing to the accumulation of unrepaired, DDR-positive telomeres during ageing. This can in turn trigger cellular senescence and impair tissue homeostasis providing a mechanism for ageing also in non-proliferating tissues.

Finally, I focused my attention on DICER and DROSHA-dependent DNA damage response RNAs (DDRNAs), novel components of the DDR machinery, which have been described to be necessary for DDR activation at DSBs. I showed that RNase A treatment as well as DICER or DROSHA down-regulation impair DDR activation at uncapped telomeres and that DICER and DROSHA may have a role in chromosomal fusions. Furthermore, in cells with dysfunctional telomeres, the inhibition of telomeric DDRNAs

using inhibitory oligonucleotide molecules with a complementary sequence can prevent DDR activation and senescent-associated cell cycle arrest.

These data indicate that at uncapped telomeres, DDRNAs with telomeric sequences are generated and that they are necessary for DDR activation and chromosomal fusions.

2 Introduction

2.1 The DNA damage response (DDR)

2.1.1 Different types of DNA damage

The integrity and stability of the genome is essential for the survival of an organism. Genomic DNA is challenged with different types of DNA damage (Jackson and Bartek, 2009). A major source of potential alterations in DNA is the generation of mismatches and small insertions or deletions during DNA replication. In addition cellular metabolism produces reactive oxygen species (ROS) such as superoxide anions, hydroxyl radicals and hydrogen peroxide derived from oxidative respiration and products of lipid peroxidation, leading to oxidative modifications of DNA. Also some spontaneous reactions can lead to hydrolysis of nucleotides, generating abasic sites, or deamination of cytosine, adenine, guanine or 5-methylcytosine, that are converted to uracil, hypoxanthine, xanthine and thymine, respectively. Among exogenous sources of DNA damage are the ultraviolet (UV) component of sunlight, ionizing radiation (IR) and various genotoxic compounds (Iliakis et al., 2003; Povirk, 1996; Rastogi et al., 2010). For example bleomycin is a glycopeptide antibiotic used also in cancer therapy, which once chelated to a metal ion, reacts with oxygen to produce superoxide and hydroxide free radicals that directly cleave DNA. Etoposide is an alkaloid derived from a plant toxin and inhibits DNA topoisomerase II preventing re-ligation of the DNA strands broken during DNA unwinding (Soubeyrand et al., 2010).

DNA crosslinks is a covalent linkage between the two strands and can be generated by bifunctional alkylating agents, such as psoralens, but also by UV and IR (Deans and West, 2011). Single-strand breaks (SSBs) are nicks in the sugar-phosphate backbone of one strand and can be caused by IR or ROS, while double-strand breaks (DSBs) are breakages of the sugar-phosphate backbone in both strands that can be generated when DNA is exposed to IR, radiomimetic drugs or ROS. They are also generated upon replication across a nick, as an intermediate of class switch and V(D)J recombination and as a result of

fork stalling following oncogene-induced replication stress (Di Micco et al., 2007; Soulas-Sprauel et al., 2007).

2.1.2 The DNA damage response pathway

The DNA damage response (DDR) is that set of cellular events that include the checkpoint functions and the DNA repair actions (Polo and Jackson, 2011). In the presence of DNA damage, DDR arrests the cell cycle progression to impede the propagation of altered genetic information (the checkpoint function), while it coordinates DNA damage repair to maintain genome integrity.

Powerful activators of the DDR are ruptures of the sugar-phosphate DNA backbone, leading to the exposure of single-stranded DNA or the generation of DSBs. These two types of lesions are sensed by specialized complexes that recruit and activate two large protein kinases, ataxia telangiectasia and Rad3-related (ATR) or ataxia telangiectasia mutated (ATM), respectively, at the site of the DNA lesion (Fig. 1) (Nam and Cortez, 2011; Shiloh and Ziv, 2013). They are members of the phosphatidylinositol 3-kinase-like family of serine/threonine protein kinases and phosphorylate their substrates on a serine or threonine that is followed by glutamine, the S/TQ motif (Bensimon et al., 2010; Langerak and Russell, 2011). The recruitment of either of these apical kinases to the lesion leads the local phosphorylation *in cis* of the histone H2AX at serine 139 (named γH2AX), a key step in the nucleation of the DDR. Indeed it acts as a recognition mark for the retention of other DDR proteins at sites of DNA damage (Martin et al., 2009), establishing a positive feedback loop, and fuelling the spreading of γH2AX along the chromatin up to megabases (Iacovoni et al., 2010). This results in the formation of cytologically detectable nuclear foci, containing multiple copies of the DDR proteins. Staining of DNA-damaged cells with antibodies against γH2AX or other DDR factors accumulating at DNA damage sites generates a distinctive nuclear pattern of discrete bright foci. As foci detection reveals the number and the position of the DNA lesions within a cell, immunocytological staining is generally considered a highly sensitive and informative approach because it allows the

detection of even a single focus and therefore informs on the activation of a cellular response at the single-cell level.

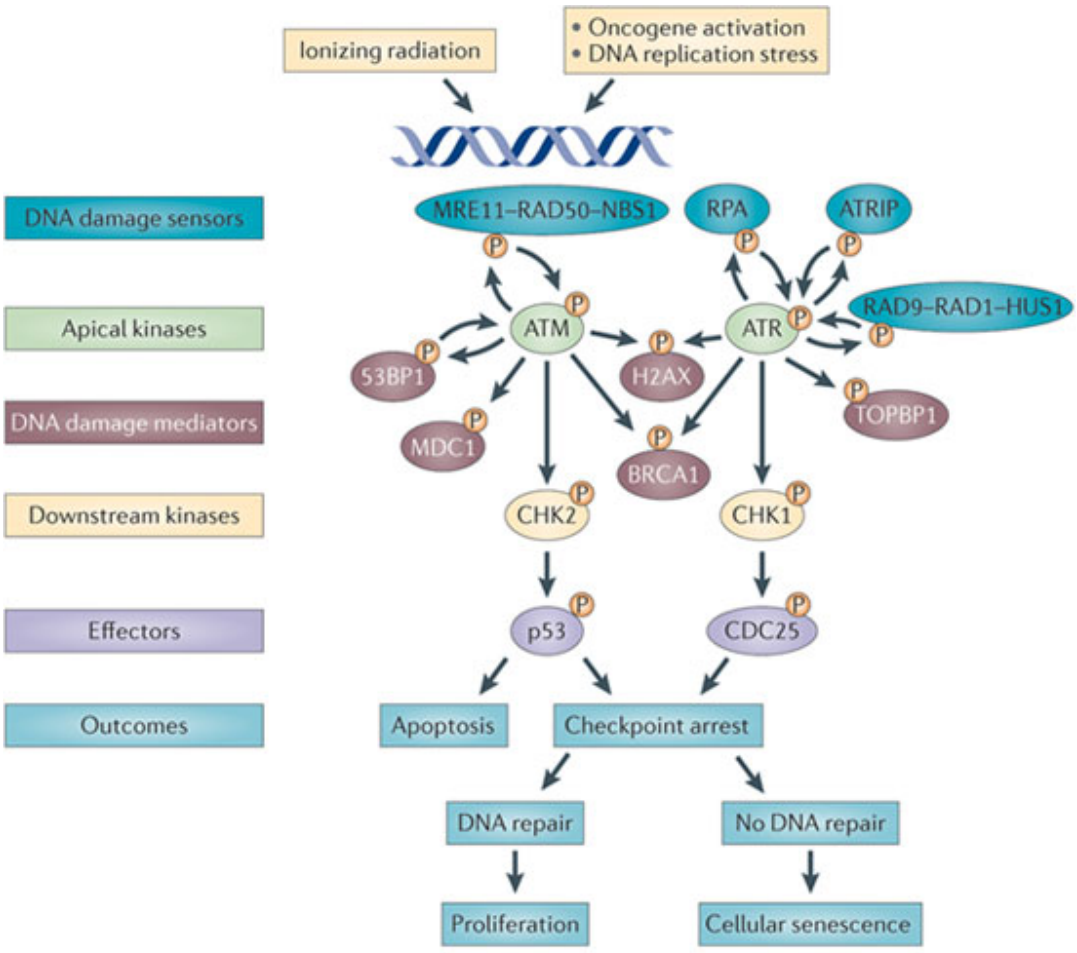

Adapted from (Sulli et al., 2012)

Figure 1. The DNA damage checkpoint response cascade.

DSBs are initially recognized by the MRN complex, while ssDNA is sensed by RPA and the RAD9–RAD1–HUS1 (9-1-1) complex. These DNA damage sensors recruit the apical kinases ATM and ATR, which is bound by ATRIP. These in turn phosphorylate (P) the histone variant H2AX on Ser139 (known as γH2AX) to recruit other components of the DDR cascade such as MDC1, 53BP1, BRCA1. The diffusible downstream kinases CHK2 (mainly phosphorylated by ATM) and CHK1 (mainly phosphorylated by ATR) spread the signal to effectors such as p53 and CDC25. There are three possible outcomes, cell death by apoptosis, transient cell cycle arrest followed by proliferation after DNA repair, or cellular senescence.

ATR exists in a complex with the ATR-interacting protein (ATRIP), both before and after exposure to stresses such as UV irradiation (Nam and Cortez, 2011). When single-stranded

DNA is exposed, the single-stranded DNA binding replication protein A (RPA) binds to it, generating a signal for ATRIP and ATR recruitment. In addition to ATR, several other protein complexes are recruited to ssDNA sites such as the RAD17- containing complex, which participates in the loading onto chromatin of the heterotrimeric 911 complex (constituted by RAD9, RAD1 and HUS1), and Claspin, a protein that is independently recruited to chromatin. ATR kinase activity is additionally boosted by the 911 complex and by topoisomerase II binding protein 1 (TopBP1), an amplifier of ATR kinase activity.

In the absence of DNA damage, ATM is maintained in an inactive dimeric structure in which the kinase domain is physically blocked (Shiloh and Ziv, 2013). The introduction of a DNA DSB leads to a conformational change in the ATM protein that stimulates the kinase to phosphorylate serine 1981, causing the dissociation of the homodimer. Active monomeric ATM is recruited to DSBs via an interaction with the MRN (Mre11-Rad50-Nbs1) complex that is rapidly recruited to the ends of broken DNA molecules and initially functions to facilitate holding the broken ends in close proximity. Then ATM phosphorylates many substrates, including NBS1 and the DDR mediators like p53 binding protein 1 (53BP1), the mediator of DNA damage checkpoint 1 (MDC1) and breast cancer 1 (BRCA1). This phosphorylation events fuel a positive feedback loop facilitating the recruitment of additional ATM molecules to the DSB site (Bekker-Jensen et al., 2005; Stucki et al., 2005).

Therefore, DSBs such as those generated by IR, primarily activate ATM, while RPA-coated ssDNA, products of perturbed DNA replication, triggers ATR activity. However, during S and G2 phases, resection activity at DSBs generates ssDNA, that provides a suitable substrate for ATR activation (Jazayeri et al., 2006).

Increase of local ATM and ATR activity determines phosphorylation of downstream protein kinases CHK2 and CHK1 respectively, although ATM can also phosphorylate CHK1 (Bekker-Jensen et al., 2006; Buscemi et al., 2004; Lukas et al., 2003). Activated

CHK1 and CHK2 diffuse in the nucleoplasm, phosphorylating their substrates throughout the nuclear space.

In addition to phosphorylation events, other reversible post-translational modifications like ubiquitylation and sumoylation are essential for the DDR activation, especially in response to DSBs (Jackson and Durocher, 2013). In particular, the ubiquitin E3 ligase RNF8 recognizes the phosphorylated MDC1 (Huen et al., 2007; Kolas et al., 2007; Mailand et al., 2007) and mediates ubiquitylation of histones H2A and H2AX at the DSB site. The ubiquitylated substrates are then bound by another E3 ligase, RNF168 (Panier et al., 2012). This results in the recruitment of key components of the DSB repair pathways, among which 53BP1 and BRCA1 (Al-Hakim et al., 2010).

2.1.3 Cell cycle and checkpoint activation

In response to DNA damage, the cell activates a transient proliferative arrest in order to fix the lesion, before the following cell division. DDR regulates cyclin-dependent kinases (CDKs) that are responsible for cell cycle progression at key stages of the cell cycle (Branzei and Foiani, 2008; Malumbres and Barbacid, 2009). In particular, between the G1 and S phases (G1/S checkpoint), within S phase (intra-S phase checkpoint) and between G2 and M phase (G2/M checkpoint).

- *The G1/S Checkpoint*. Cell cycle progression is driven by phosphorylation events mediated by CDK4-CyclinD, CDK6-CyclinD, CDK2-CyclinE, and CDK2-CyclinA complexes that sequentially phosphorylate pRB. These complexes are maintained active through dephosphorylation by CDC25A phosphatase. In the presence of DNA damage, entry into S phase is prevented by the phosphorylation of CDC25A by CHK2, resulting in its inactivation by both nuclear exclusion and ubiquitin-mediated proteolytic degradation. In addition, ATM and ATR directly phosphorylate serine 15 of p53, while the neighbouring serine 20 residue is phosphorylated by activated CHK1 and CHK2. The phosphorylation of p53 inhibits its nuclear export and degradation, allowing p53 levels to greatly increase. The accumulated p53 activates its target genes,

including the gene encoding the p21 CDK inhibitor, which specifically binds to and inhibits the S-phase-promoting CDK2-CyclinE complex, thereby maintaining the G1/S arrest.

- *The intra-S phase checkpoint*. The intra-S-phase checkpoint is activated by damage encountered by replication forks during the S phase or by unrepaired damage that escaped the G1/S. It can be initiated by the ATM/ATR-CHK2/CHK1-CDC25A-CDK2 pathway, very similar to that activated for the G1/S checkpoint. A second pathway requires the phosphorylation of SMC1 by ATM with the aid of BRCA1, FANCD2 and NBS1.
- *The G2/M checkpoint*. This checkpoint blocks the entrance in mitosis in the presence of DNA damage. ATM and ATR, through phosphorylation of CHK2 and CHK1, inhibit the entry into mitosis by down-regulating CDC25A and up-regulating Wee1, controlling CDK1-Cyclin B activity.

Checkpoint activation in stem cells can have a dual role in cancer and ageing depending on the cellular context (Sperka et al., 2012). In the presence of high levels of DNA damage, deletion of checkpoint genes can improve stem cell and tissue maintenance, and at the same time also induce damage accumulation in cancer stem cells protecting from tumour initiation. Conversely, in a low DNA damage background, increasing the gene dosage of checkpoint genes can lead to improved clearance of damaged cells, prolonged tissue maintenance and decreased carcinogenesis. If the damage is not repairable, checkpoint activation can induce cell death by apoptosis or a permanent cell cycle arrest called cellular senescence (see chapter 2.2).

2.1.4 The double-strand break repair pathways

Among the different types of DNA damage, DSBs are considered the most deleterious, because they can be responsible for cell death or chromosomal translocations leading to cancer. There are two major pathways for the repair of DSBs, the homologous recombination (HR) and the non-homologous end joining (NHEJ) (Chapman et al., 2012).

HR is an error-free mechanism as it uses a homologous chromosome as template for repair, so it can occur during S and G2 phases of the cell cycle (Karpenshif and Bernstein, 2012). An early event in HR is the resection of the DSB in the 5'-to-3' direction. The MRN complex has a DNA-binding activity, an endonuclease and 3'-5' exonuclease activity. It functions together with additional exo- and endo-nucleases such as BLM and EXO1, to resect DSBs and create 3'- ended single-stranded DNA that is required to initiate DNA strand invasion. RPA then coats the growing 3' overhang. The RAD51 recombinase is then loaded onto the ssDNA, displacing RPA, and catalyses strand exchange. The 3' ssDNA invades the intact homologous duplex DNA with the 3' OH group, using the intact homologous duplex as a template to repair the DSB (Chapman et al., 2012). Subsequently, a DNA polymerase extends the 3' terminus of the damaged molecule, DNA ligation takes place and RecQ helicases, such as the BLM and WRN proteins resolve Holliday junctions to obtain two intact DNA molecules.

NHEJ is active throughout the entire cell cycle, but is the only mode of repair during G0, G1 and early S phase when sister chromatids are unavailable (Lieber, 2010). Although NHEJ is highly efficient, its very simple mechanism of basic re-ligation, without proofreading, makes it prone to mutations. DNA ends are recognized by KU70/80 heterodimeric complex, followed by recruitment of DNA-PK catalytic subunit (DNA-PKcs) that phosphorylates itself and other targets among which the nuclease Artemis. Members of POLX family synthetize DNA and finally DNA ligase IV in association with its binding partners, XRCC4 and XLF, ligates the DNA ends.

In the absence of protein machinery involved in classical NHEJ (c-NHEJ), another pathway can contribute to DSB repair, the alternative NHEJ (a-NHEJ), also known as backup NHEJ (b-NHEJ) or microhomology-mediated end joining (MMEJ), because it exploits microhomology regions during joining (McVey and Lee, 2008; Nussenzweig and Nussenzweig, 2007; Wang et al., 2003). The mechanisms of a-NHEJ are not fully understood yet, however DNA ligase 3 and XRCC1 seem to play a major role.

KU70/80 heterodimer plays a major role in the repair pathway choice, promoting c-NHEJ, likely by inhibiting the access of the DNA end to RAD52 or PARP-1, components of HR and a-NHEJ pathways respectively (Fattah et al., 2010). RIF1 is also essential for the repair pathway choice; it is recruited by phosphorylated 53BP1 and promotes NHEJ at DSBs in G1 phase as well as at uncapped telomeres, while in S/G2 CtIP and BRCA1 displace 53BP1/RIF1 complex promoting HR (Chapman et al., 2013; Di Virgilio et al., 2013; Escribano-Diaz et al., 2013; Zimmermann et al., 2013).

2.1.5 Defects in DNA repair and checkpoint processes

The importance of the DDR signalling and DNA repair are evident, considering the variety of diseases linked to mutations or defects in these pathways. For example, inherited mutations in the ATM gene results in the syndrome ataxia-telangiectasia (AT), a rare human disease characterized by ataxia (dysfunction in movement coordination by the nervous system), telangiectasia (dilated blood vessels), immune defects, increased sensitivity towards IR, and cancer predisposition (Shiloh and Ziv, 2013). The Nijmegen breakage syndrome (NBS) is caused by mutations in the NBS1 gene, and it is characterized by symptoms similar to AT (Digweed and Sperling, 2004). In some patients with AT-like disorders, mutations in the MRE11 gene were identified (Stewart et al., 1999). Disruption of both alleles of ATR causes embryonic lethality in mice, however hypomorphic mutations in ATR cause the Seckel syndrome in humans (O'Driscoll et al., 2003). These patients show growth retardation, dwarfism, microencephaly and mental retardation. A human syndrome, called RIDDLE (Radiosensitivity, Immunodeficiency, Dysmorphic features and LEarning difficulties) is due to the mutation of ubiquitin ligase RNF168 that leads to an impaired recruitment of 53BP1 and BRCA1 to sites of DNA DSBs (Stewart et al., 2009; Stewart et al., 2007). Haploinsufficiency for H2AX results in detectable genomic instability and enhanced tumour susceptibility in the absence of p53 (Celeste et al., 2003). Homozygous loss of CHK1 is lethal, but CHK1 heterozygosity modestly enhances the tumorigenic phenotype of WNT1 transgenic mice (Liu et al., 2000). Lack of CHK2

enhances skin tumorigenesis induced by carcinogen exposure (Hirao et al., 2002) and increases tumour susceptibility in mouse models, in combination with mutations in other genes like BRCA1, NBS1 and MRE11 (Cao et al., 2006; McPherson et al., 2004; Stracker et al., 2008). The inheritance of a single mutated allele of either BRCA1 or BRCA2 markedly increases the incidence of breast and ovarian cancers in women (O'Donovan and Livingston, 2010).

2.2 Cellular senescence

2.2.1 General features of cellular senescence

Cellular senescence was first discovered by Hayflick and Moorhead in 1961, when they observed that human lung foetal fibroblasts in culture do not proliferate indefinitely, but can undergo a limited number of cell divisions, and eventually stop dividing, reaching the so-called Hayflick limit (Hayflick and Moorhead, 1961). Normal and primary cells in culture are in fact mortal and undergo cellular senescence in response to different types of stresses, like dysfunctional telomeres, DNA damage, and oncogene activation.

Cellular senescence is defined as a permanent loss of proliferative capacity, despite viability and metabolic activity. It is indeed distinct from quiescence, because it cannot be reverted by appropriate mitogenic stimuli and changes in the culturing conditions (Kuilman et al., 2010). Although there are no exclusive markers for senescent cells, some features are commonly used to identify them.

- *Growth arrest.* The lack of DNA replication is a typical characteristic of senescence establishment, although it does not distinguish senescent cells from quiescent or differentiated post-mitotic cells. It can be detected by the incorporation of 5-bromodeoxyuridine (BrdU), or by expression levels of proliferation markers, such as PCNA and Ki-67.
- *Morphology.* Senescent cells can be identified by an enlarged and flattened morphology with abnormally large cytoplasm.
- *Senescence-associated-β-galactosidase (SA-β-gal)*. Lysosomal β-galactosidase, encoded by GLB1 gene, is normally active at acidic pH 4.5. Its expression level increases during senescence due to an expansion in the lysosomal compartment, so its activity can be detected also in suboptimal conditions, at pH 6 (Dimri et al., 1995).
- *Senescence-associated DNA-damage foci (SDFs).* The DDR activation can be detected in the form of SDFs, which contain proteins that are associated with the DDR, like

γH2AX, 53BP1, ATM pS1981 and MDC1 (d'Adda di Fagagna et al., 2003; Di Micco et al., 2006; Herbig et al., 2004; Takai et al., 2003). These foci differ from the ones found in non-senescent cells because they are usually larger and long-lived. DDR plays an essential role both in senescence initiation and maintenance. In senescent cells the DDR is actively maintained and is necessary for the senescence establishment (d'Adda di Fagagna et al., 2003; Herbig et al., 2004; Sedelnikova et al., 2004; von Zglinicki et al., 2005). Indeed transient inactivation of ATM, alone or together with ATR, and combined CHK1 and CHK2 inactivation, lead to escape from senescence and re-entry into the S-phase of the cell cycle. In contrast with these observations, some reports describe that deep senescent cells eventually lose DDR foci (Bakkenist et al., 2004; Chen and Ozanne, 2006). This is against the hypothesis that DDR fuels and maintains cellular senescence. However, I will show that this can be at least partially explained by the cell type-specific response to stress (see chapter 4.1.3).

- *Activation of tumour suppressor networks.* The senescence growth arrest is established and maintained by p53 or p16-RB tumour suppressor pathways (Kuilman et al., 2010). Different cell types or species can activate one pathway or both, also in response to different stimuli. For example, IR and telomere dysfunction induce senescence primarily through the p53 and p21 pathway in fibroblasts (Brown et al., 1997). In other cell types, like melanocytes, senescence is mediated by p16-RB pathway (Haferkamp et al., 2009). There are also species-specific differences: for example, experimental uncapping of telomeres primarily engages the p53 pathway in mouse cells but both the p53 and p16-RB pathways in human cells (Smogorzewska and de Lange, 2002). p16 and p21 can both keep pRB in an active, hypophosphorylated form, thereby preventing E2F from transcribing genes that are needed for proliferation (Sherr and McCormick, 2002).
- *Senescent-associated secretory phenotype (SASP)*. The senescent status is often associated with a secretome that includes different cytokines and chemokines (Coppe

et al., 2008; Rodier et al., 2009). These factors can trigger modifications of the extracellular matrix or mediate local inflammation. They can bind receptors on the same cell that secreted them (autocrine effect) or on the surrounding cells (paracrine effect), fuelling the senescence state (Acosta et al., 2013).

- *Senescence-associated heterochromatin foci (SAHFs)*. In some senescent cells, the chromatin is reorganized into discrete foci (Narita et al., 2003). SAHFs are detected by the preferential binding of DNA dyes, such as 4',6-diamidino-2-phenylindole (DAPI), and the presence of heterochromatin-associated histone modifications like H3K9 methylation, and proteins, like heterochromatin protein-1 (HP1).

2.2.2 Replicative senescence

Senescence as a result of proliferative exhaustion in optimal culturing conditions is known as replicative senescence. Telomeres are the end of linear chromosomes, which lose 50–200 base pairs during each S phase (see chapter 2.3). Progressive telomere shortening eventually causes chromosome ends to be recognized as DNA breaks, to activate a consequent DDR and to enforce senescence. Thus cell proliferation inevitably arrest because of an intrinsic “clock” that is sensitive to the number of cell divisions rather than the time in culture. The causative role of telomere shortening in replicative senescence establishment was proven by reactivation of telomerase that prevents senescence and allows unlimited cell proliferation *in vitro* (Blackburn, 2000; Bodnar et al., 1998). Importantly, senescence is not determined by the average telomere length within a cell but by the presence of a few telomeres sufficiently short to trigger the senescent signal (Hemann et al., 2001; Herbig et al., 2004).

2.2.3 Stress-induced premature senescence

The Stress-induced premature senescence (SIPS) is a response to an external stress coming from the cell environment (Toussaint et al., 2000). Repeated or acute non-lethal doses of these stresses are required to efficiently induce accumulation of stress-induced senescent

cells. Cells undergoing SIPS share many cellular and molecular features with replicative senescent cells. Different types of stresses can induce the SIPS.

- *Culture shock-induced senescence.* An important example of SIPS comes from the biological behaviour of primary mouse embryonic fibroblasts (MEFs). Explanted MEFs stop dividing after only 15-30 cell divisions when placed in culture. Since telomeres are quite long in laboratory mouse strains, the proliferative block occurs well before detectable critical telomere shortening. Moreover, many somatic mouse tissues and cultured cells express telomerase activity (Prowse and Greider, 1995). Non-physiologic conditions including disruption of cell-cell contacts, lack of heterotypic interactions between different cell types, the medium-to-cell ratio, persistent RAS activation by mitogens, absence of appropriate survival factors, hyperoxia and plating on plastic are likely to induce stress responses (Sherr and DePinho, 2000). Among these factors, oxygen sensitivity is one of the major determinants of SIPS. MEFs do not senesce in physiological (3%) oxygen levels, but do so at 20% oxygen (Parrinello et al., 2003). Serum is also a recognized senescence-inducing factor. In fact, MEFs, glial and oligodendrocytes precursors have been shown to proliferate without apparent limits if grown in synthetic media without serum (Mathon et al., 2001; Tang et al., 2001; Woo and Poon, 2004). Moreover mitogenic stimuli have been shown to increase activation of DNA damage responses in senescent cells, likely to prevent senescent cells from entering the cell cycle (Satyanarayana et al., 2004).
- *UV and IR-induced senescence.* UV light is composed of UVA (320-400 nm), UVB (280-320 nm), and UVC (200-280 nm). UVB, in particular, is the most hazardous environmental carcinogen known in regard to human health. UVB irradiation is known to provoke oxidative stress through the generation of ROS that could be the cause of UV-induced SIPS (de Magalhaes et al., 2002). ROS removal by the use of free radical scavengers reduces the harmful effects of UVB irradiation resulting in a

significant delay in SIPS establishment (Ho et al., 2005). IRs are also inducers of SIPS. IR-treatment creates DSBs resulting in the activation of ATM-p53-p21 pathway within few hours from treatment. However, SIPS is not associated with telomeric shortening and IR does not appear to accelerate telomere erosion. Moreover expression of hTERT in different types of normal diploid cells undergoing SIPS by IR, as well as UV treatment and hydrogen peroxide exposure, did not prevent senescence induction. These data indicate that DNA lesions can induce senescence through a mechanism that is independent from telomere shortening (Gorbunova et al., 2002).

- *DNA damaging drug-induced senescence.* Many chemotherapy agents used to treat cancer, can induce SIPS, without affecting telomere length (Schmitt, 2003). Some examples are the DNA-intercalating doxorubicin, the topoisomerase I inhibitor camptothecin, the topoisomerase II inhibitor adriamycin, the cross-linking agent cisplatin, the anti-metabolite cytarabin. Moreover, chronic exposure to low concentrations of hydroxyurea, aphidicolin, or etoposide can also induce replication stress leading to irreversible cell cycle arrest after several population doublings and to checkpoint activation. Indeed, since replication stress stalls replication forks and some of the stalled forks can collapse, this leads to the generation of DSBs and the activation of the ATR/CHK1 pathway (Marusyk et al., 2007).

2.2.4 Oncogene-induced senescence

Oncogenes are mutant versions of normal genes that have the potential to transform cells in conjunction with additional mutations. Normal cells respond to many oncogenes by undergoing senescence. A common feature of the expression of various oncogenes *in vivo* and *in vitro* is the generation of a biphasic response: cells undergo an initial burst of cellular hyperproliferation followed by senescence establishment (Di Micco et al., 2006; Di Micco et al., 2007). Cellular senescence indeed prevents the expansion of a pool of cells bearing an activated oncogene and thus restrains the formation of a potential tumour.

Oncogene-induced senescence (OIS) was first described in cells expressing the constitutively activated and therefore oncogenic form of RAS, a cytoplasmic transducer of extracellular growth stimuli (Serrano et al., 1997). In the same way, activation or increased expression of other components of the RAS pathway, such as RAC1, RAF, MOS, MEK or the loss of the inhibitor of the RAS pathway PTEN can induce cellular senescence; a list of senescence-inducing gene is reviewed in (Evan and d'Adda di Fagagna, 2009). OIS and replicative senescence have some common features. For example, oncogenic RAS induces p16 and the formation of SAHFs (Kreiling et al., 2011; Narita et al., 2003; Zhang et al., 2005). In addition, in cells expressing oncogenes, DDR markers localize at DNA-replication sites, aberrant amounts of single-stranded DNA are generated and replicative fork progression is discontinuous and prone to pausing and/or collapse (Bartkova et al., 2006). Moreover, RAS activation induces re-replication, an event known to cause DNA damage and DDR activation and to increase the number of actives origins (Di Micco et al., 2006). Similarly, MYC boosts the number of active DNA replication origins; its deregulation induces DNA damage in a DNA replication-dependent manner (Dominguez-Sola et al., 2007). Therefore, all these observations suggest that oncogene-induced altered DNA replication is an important contributor to oncogene genotoxicity and senescence establishment.

2.2.5 Cellular senescence and ageing

Increasing evidence suggests the presence of senescent cells *in vivo*, and their contribution to organismal ageing. Telomere shortening has an impact on tissue ageing in various tissues (Tumpel and Rudolph, 2012), and senescent cells have been found in human skin fibroblasts (Dimri et al., 1995), in baboons skin fibroblasts (Herbig et al., 2006) and in mouse stem and somatic cells (Nijnik et al., 2007; Rossi et al., 2007; Sedelnikova et al., 2004; Wang et al., 2009). Different markers of senescence are used to identify senescent cells *in vivo*, among which the SA-β-gal activity, DDR activation, increased p16 expression, heterochromatin formation. Senescent cells can contribute to organismal

ageing by up-regulating genes that encode extracellular-matrix-degrading enzymes, inflammatory cytokines and growth factors, which stimulate chronic tissue remodelling and local inflammation, compromising tissue structure and function (Nelson et al., 2012). Notably, cells that express senescence markers are also found at sites of age-related pathologies, such as osteoarthritis and atherosclerosis (Chang and Harley, 1995; Price et al., 2002; Vasile et al., 2001). The causative effect of senescence on ageing is supported by different observations. p16 expression increases with age in the stem and progenitor cells of the mouse brain, bone marrow and pancreas, where it suppresses stem-cell proliferation and tissue regeneration. Consistently, the age-related decline can be prevented by the lack of p16 expression (Janzen et al., 2006; Krishnamurthy et al., 2006; Molofsky et al., 2006). Similarly, a genetically engineered mouse model in which p16-expressing cells are specifically cleared, show a delay in age-related pathologies, an attenuation of already established disorders, and increased lifespan (Baker et al., 2011).

Dysfunctional telomeres have been found in senescent cells *in vivo* in primates (Herbig et al., 2006; Jeyapalan et al., 2007), and loss of telomerase function in mice causes senescence and physiological impairment of many tissues (Ferron et al., 2004; Rudolph et al., 1999; Sahin and Depinho, 2010; Satyanarayana et al., 2004). Consistent with a causative role of replicative senescence in organism ageing, deletion of p21 in telomerase-deficient mice with dysfunctional telomeres improves hematolymphopoiesis, rescues the maintenance of intestinal epithelia and prolongs the lifespan (Choudhury et al., 2007). Moreover elongation of telomeres by reactivation of telomerase is sufficient to eliminate the degenerative phenotypes in multiple organs observed in telomerase knock out mice (Jaskelioff et al., 2011).

2.2.6 Cellular senescence and cancer

Cellular senescence is considered a potent tumour suppressive mechanism. Indeed OIS have been demonstrated to prevent cancer development *in vivo* both in humans and in mouse models (Dankort et al., 2007; Di Micco et al., 2006; Grandori et al., 2003; Lazzerini

Denchi et al., 2005; Michaloglou et al., 2005). Senescent cells are associated with benign dysplastic or pre-neoplastic lesions but not with malignant tumours suggesting that tumoral cells escaped the senescence barrier triggered by hyperproliferation (Collado and Serrano, 2010; Suram et al., 2012). They are also found in normal and tumour tissues following DNA-damaging chemotherapy (Collado and Serrano, 2010).

Also replicative senescence seems to play an important role in preventing cancer onset. Indeed cancer cells need a system to overcome telomere attrition and proliferate indefinitely. This is usually achieved by most human tumours through the expression of high levels of telomerase, that in human somatic tissues is absent (Meyerson, 2000). It has been shown that telomerase expression is necessary for full transformation of oncogene-expressing human cells (Hahn et al., 1999). This can be in part due to the ability of telomerase to prevent or suppress DDR activation at telomeres upon telomeric shortening and oncogene-induced replication stress (Gunes and Rudolph, 2013). Nevertheless, a transient telomere dysfunction promotes tumour initiation by generating chromosomal instability and polyploidy (Begus-Nahrmann et al., 2012; Davoli and de Lange, 2012; Rudolph et al., 1999). A minor fraction of human cancers (10–20%) are telomerase-negative and activate HR-based alternative lengthening of telomere (ALT) (Cesare and Reddel, 2010). ALT is also responsible for tumour relapse upon telomerase inhibition in mouse models (Hu et al., 2012).

Finally the inability to establish cellular senescence in mouse models deficient for p16 leads to increased cancer incidence (Janzen et al., 2006; Krishnamurthy et al., 2006; Molofsky et al., 2006).

All these results indicate that cellular senescence suppresses the development of cancer. However, it has been suggested that factors secreted by senescent cells can facilitate the development of cancer by promoting cell proliferation, mobility and differentiation and by modulating the immune response (Coppe et al., 2010). Thus cellular senescence has a dual

role in preventing uncontrolled proliferation leading to cancer, but also favouring tumour growth of surrounding cells.

2.3 Telomeres and telomere-binding proteins

2.3.1 Structure of the telomeres

Telomeres are nucleoprotein structures at the end of the linear chromosomes (Fig 2). They are made of three main components: long stretches of DNA tandem repeats (TTAGGG in vertebrates), telomere-associated proteins and non-coding RNA. The length of human telomeres is typically 9-15 Kb, whereas laboratory mouse strains chromosomes have longer telomeres, ranging from 10 to 60 Kb. Telomeres terminate in a 3' protruding single-stranded G-rich overhang, typically 50-300 nucleotides long (O'Sullivan and Karlseder, 2010). The overhang is generated through 5'-3' resection by Apollo and Exo1 nucleases (Wu et al., 2012) and is essential for TRF2-mediated invasion of preceding double-stranded DNA region to form a high-order structure known as t-loop (Griffith et al., 1999; Stansel et al., 2001). The G-rich end can also fold up into four-stranded G-quadruplex structure, an unusual DNA conformation based on a guanine quartet (Lipps and Rhodes, 2009).

Telomeres and subtelomeres are enriched for heterochromatic markers, such as H3K9me3, H4K20me3 and HP1. In addition, subtelomeric DNA is methylated. Both histone and DNA methylations act as negative regulators of telomere length, by inhibiting telomerase activity (Schoeftner and Blasco, 2009). The heterochromatin maintenance is regulated by the miR-290 family, which controls a subset of DNA methyltransferases; indeed mice deficient for Dicer1 show a decreased DNA methylation and increased telomere recombination and elongation (Benetti et al., 2008a).

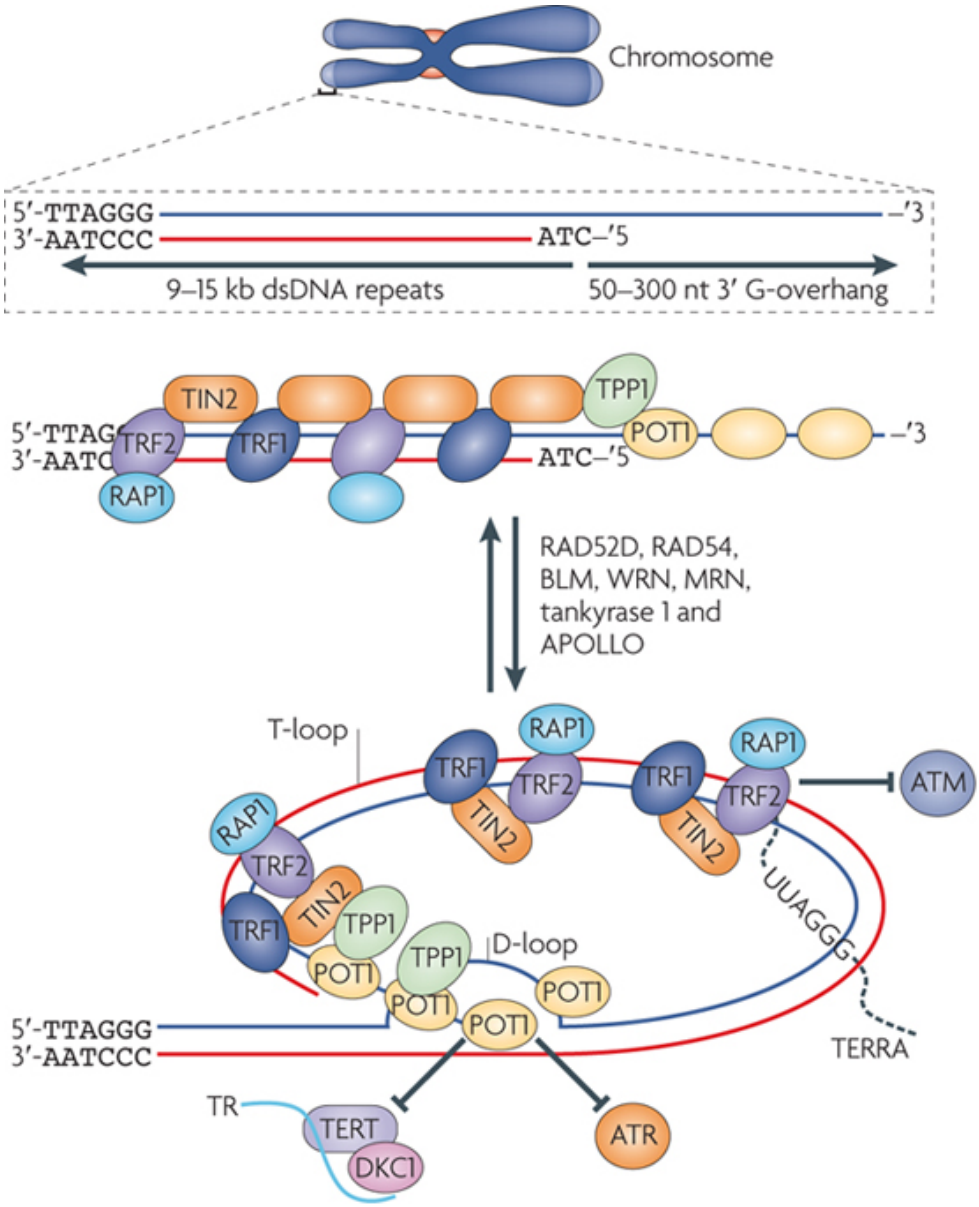

Adapted from (O'Sullivan and Karlseder, 2010)

Figure 2. Structure of the human telomeres.

Human telomeres are nucleoprotein complexes consisting of kilobases of TTAGGG repeats, with a 3' G-rich overhang, an RNA component called TERRA and the shelterin proteins TRF1, TRF2, RAP1, TIN2, TPP1 and POT1. These factors help the formation of a protective structure at chromosome ends, the t-loop. Activation of ATM is inhibited by TRF2, while ATR is inhibited by POT1. Telomerase is probably inhibited by the shelterin proteins.

2.3.2 Telomere-binding proteins

Telomeres are associated to a protein complex named shelterin, consisting of six components (de Lange, 2005): TRF1 and TRF2 (telomeric-repeat-binding factor 1 and 2), POT1 (protection of telomeres 1), RAP1 (also known as TERF2IP, telomeric repeat binding factor 2 interacting protein), TIN2 (TRF1-interacting nuclear factor 2) and TPP1 (POT1 and TIN2 organizing protein).

TRF1 and TRF2 directly associate as homodimers with the double-stranded telomeric DNA, through their MYB domain (Broccoli et al., 1997). TRF1 has been proposed to allow efficient replication of telomeres, preventing fork stalling (Martinez et al., 2009; Sfeir et al., 2009) and to act as a negative regulator of the telomere length, probably by controlling the access of telomerase (Ancelin et al., 2002; Munoz et al., 2009; van Steensel and de Lange, 1997). TRF2 maintains the t-loop structure and is mainly implicated in chromosome end protection, by preventing end-to-end fusions (Griffith et al., 1999; Stansel et al., 2001; van Steensel et al., 1998); it is also involved in the telomeric heterochromatin maintenance (Benetti et al., 2008b). POT1 coats the single-stranded overhang using two oligonucleotide/oligosaccharide binding folds and positively regulates telomere length in a telomerase-dependent manner (Baumann and Cech, 2001; Colgin et al., 2003). RAP1 binds to TRF2 and is involved in telomere-length regulation, telomere stability, and silencing of subtelomeric genes (Hardy et al., 1992; Lustig et al., 1990; Martinez et al., 2010). TIN2 connects TRF1 to TRF2 and can form a bridge with POT1 via TPP1, contributing to the stabilization of shelterin at telomeres (Ye and de Lange, 2004; Ye et al., 2004a; Ye et al., 2004b).

The CST complex, composed by Cdc13, Stn1 and Ten1, and first discovered in budding yeast, binds directly the 3’ overhang of telomeres and has structural similarity to the RPA heterotrimer (Giraud-Panis et al., 2010). Yeast Cdc13 protects the C-rich strand from degradation, interacts with the telomerase RNA component Est1, promoting telomere elongation, and with Pol1, preventing the formation of long C-strand (Qi and Zakian,

2000). Stn1 competes with telomerase for the binding to Cdc13, down-regulating telomerase activity (Chandra et al., 2001). Finally Ten1 enhances Cdc13 binding affinity to DNA (Qian et al., 2009). Stn1 and Ten1-related proteins have been found in higher eukaryotes, including humans, while the CTC1 protein is thought to have functions similar to Cdc13 (Miyake et al., 2009). The human CST complex binds only partially to the telomeres, and it has a role in the telomere protection, G-overhang control and in regulating Polα-Primase activity (Giraud-Panis et al., 2010).

Recently, a mass spectrometry-based screening identified HOT1 as a novel telomere-associated protein that directly binds to telomeric DNA (Kappei et al., 2013). Its recruitment is restricted to the actively elongated telomeres, where it promotes telomerase association.

2.3.3 Telomeric transcripts

Despite their heterochromatic structure, telomeres from yeast to humans are transcribed into telomeric repeat-containing RNA (TERRA) (Azzalin et al., 2007; Schoeftner and Blasco, 2008). TERRA are transcribed by RNA Polymerase II starting from promoters located in the subtelomeric regions through the telomeric repeats. They are polyadenilated, contain the G-rich telomeric sequence and are heterogeneous in size, ranging from around 0.1 to 9 Kb. Their expression levels are positively regulated by TRF1, which interacts with RNA Polymerase II, while heterochromatin is repressing their transcription (Schoeftner and Blasco, 2008). TERRA expression level is also regulated in a cell cycle dependent manner in human cells, reaching the maximum in G1 phase of the cell cycle and progressively decline in the S phase reaching their lowest levels in late S/G2 phase (Porro et al., 2010). The physiological functions of TERRA have not been completely elucidated yet, but some reports suggest that they can negatively regulate telomere length. *In vitro* experiments showed that TERRA block telomerase activity possibly by RNA duplex formation with the template region of Terc (Schoeftner and Blasco, 2008). However, in budding yeast, it has recently been shown that TERRA are able to induce telomerase

nucleation, favouring telomere elongation (Cusanelli et al., 2013). Consistently, long telomeres can inhibit TERRA expression by promoting heterochromatin formation (Arnoult et al., 2012). TERRA are also able to inhibit POT1 displacement by RAP1 during the G1 phase, allowing the protection of the telomeres (Flynn et al., 2011). However, in S phase, TERRA levels decrease, so the switch between POT1 and RAP1 can take place, in order to complete DNA synthesis. Finally, when TERRA accumulate again in G2, they promote again POT1 binding to telomeric DNA.

2.3.4 Mechanisms of telomere length maintenance

At each cell division telomere length is reduced due to the inability of the DNA replication machinery to copy the most distal telomeric sequences of the lagging-strand, and to the exonucleolytic processing needed to generate the overhang (Harley et al., 1990). This phenomenon is known as the "end replication problem" (Watson, 1972) and in most cases is solved by elongation of telomeric DNA by the telomerase enzyme. The telomerase complex consists of the reverse transcriptase catalytic subunit (TERT), the RNA component (TERC) used as a template to elongate the G-rich telomeric DNA strand, dyskerin that helps the assembly of the complex and TCAB1, involved in the localization of telomerase to the Cajal Bodies (Cohen et al., 2007; Greider and Blackburn, 1985; Mitchell et al., 1999; Venteicher et al., 2009). In humans, telomerase activity is restricted to the embryogenesis, while TERT expression is switched off in most somatic cells, with the exception of activated lymphocytes, adult stem cells and germ line (Wright et al., 1996). Telomerase function has been intensively studied in yeast, where it has been shown that telomere elongation is restricted to the S phase, when telomeres are replicated (Marcand et al., 2000). Furthermore, telomerase exhibits an increasing preference for telomeres as their length decline, suggesting that telomeres switch between non-extendible and extendible states. The repeat addition processivity varies between a few to >100 nucleotides, and is enhanced at extremely short telomeres, allowing cells to rapidly elongate them (Teixeira et al., 2004). Consistently, late generation heterozygous mice for

telomerase gene, have short telomeres, comparable with late generation Tert knock out mice, but do not display the associated phenotype, suggesting that a minimal amount of telomerase is sufficient to elongate the critically short telomeres (Chiang et al., 2010). Mutation and impaired activity of telomerase have been associated with ageing-associated phenotypes and many different types of human tumours (Bernardes de Jesus and Blasco, 2013).

Approximately 10–20% of human cancers maintain their telomeres by ALT (Cesare and Reddel, 2010). It has been reported that the telomeric 3′ overhangs exploit the HR machinery to invade other telomeric DNA, and use it as a template for DNA replication. Telomeres in ALT cells are heterogeneous in length; some of them are very short, but they can reach up to 100 Kb. Extrachromosomal telomeric DNA can be found in t-circle of 1–60 Kb.

2.3.5 Telomeres and the DDR

Despite their structural similarities, telomeres are not recognised as DSBs by the cellular DDR machinery. The shelterin complex is the main factor involved in this process, since the activation of the DDR apical kinases ATM and ATR is inhibited by TRF2 and POT1, respectively (Lazzerini Denchi and de Lange, 2007). In the absence of either of these proteins, DDR foci, containing the same proteins found at DSBs, are detectable at the telomeres. In *in vitro* experiments, TRF2 has been shown to inhibit NHEJ (Bae and Baumann, 2007; Bombarde et al., 2010). Consistently, TRF2 knock out in mouse cells leads to dramatic chromosomal fusions (Celli and de Lange, 2005; van Steensel et al., 1998), which can be mostly prevented by Ligase 4 and 53BP1 depletion, indicating that the NHEJ is the fundamental repair pathway acting at uncapped telomeres *in vivo* (Sfeir and de Lange, 2012). KU70/80 heterodimer is a component of the NHEJ, nevertheless it is found at the telomeres (d'Adda di Fagagna et al., 2001); its main function is to inhibit both a-NHEJ and HR events (Indiviglio and Bertuch, 2009). Also some shelterin proteins are able to repress the HR pathway; RAP1-free telomeres undergo recombination, even in the

absence of DDR activation (Sfeir and de Lange, 2012), while POT1 can suppress HR together with resection at telomeres (Palm et al., 2009).

2.4 The role of non-coding RNAs in DDR

2.4.1 Non-coding RNA

Non-coding RNAs (ncRNAs) are defined as RNA species that do not have protein coding potential. A variety of ncRNA exist with many different functions. They include ribosomal RNAs (rRNAs), transfer RNAs (tRNAs), small nuclear RNAs (snRNAs), small nucleolar RNAs (snoRNAs), long non-coding RNAs (lncRNAs) and small ncRNAs that are short (<200 nt), and can be further divided into microRNAs (miRNAs), small interfering RNAs (siRNAs) and piwi interacting RNAs (piRNAs). In addition to the well-defined classes of ncRNA, increasing amount of data have suggested that non-coding transcripts are generated from the vast part of the genome that was previously thought to be transcriptionally silent, a phenomenon known as pervasive transcription (Birney et al., 2007). Although the function of these transcripts is still unknown, it is likely that they play an active role in different biological processes.

2.4.2 DROSHA and DICER functions in ncRNA biogenesis

DROSHA and DICER are two important players of the RNA interference (RNAi) machinery (Fig. 3). DROSHA is a nuclear RNase III enzyme responsible for the initial processing of the miRNAs. It cleaves the primary miRNA (pri-miRNA), a transcript generated from the endogenous miRNA genes, that is generally longer than 1000 nt, and contains single or clustered double-stranded hairpins, with single-stranded 5′- and 3′-overhangs and 10 nt distal loops (Saini et al., 2007). The resulting precursor miRNA (pre-miRNA) associates with EXPORTIN-5 to be translocated to the cytoplasm (Lund and Dahlberg, 2006).

DICER is an endoribonuclease containing a helicase and an RNase III activity. It can cut pre-miRNAs as well as exogenous siRNAs into a duplex of 21-25 nt, with a 2 nt overhang at each 3′ terminus and a phosphate group at each recessed 5′ terminus (Schwarz et al., 2003). The resulting processed dsRNA is loaded into the RISC complex.

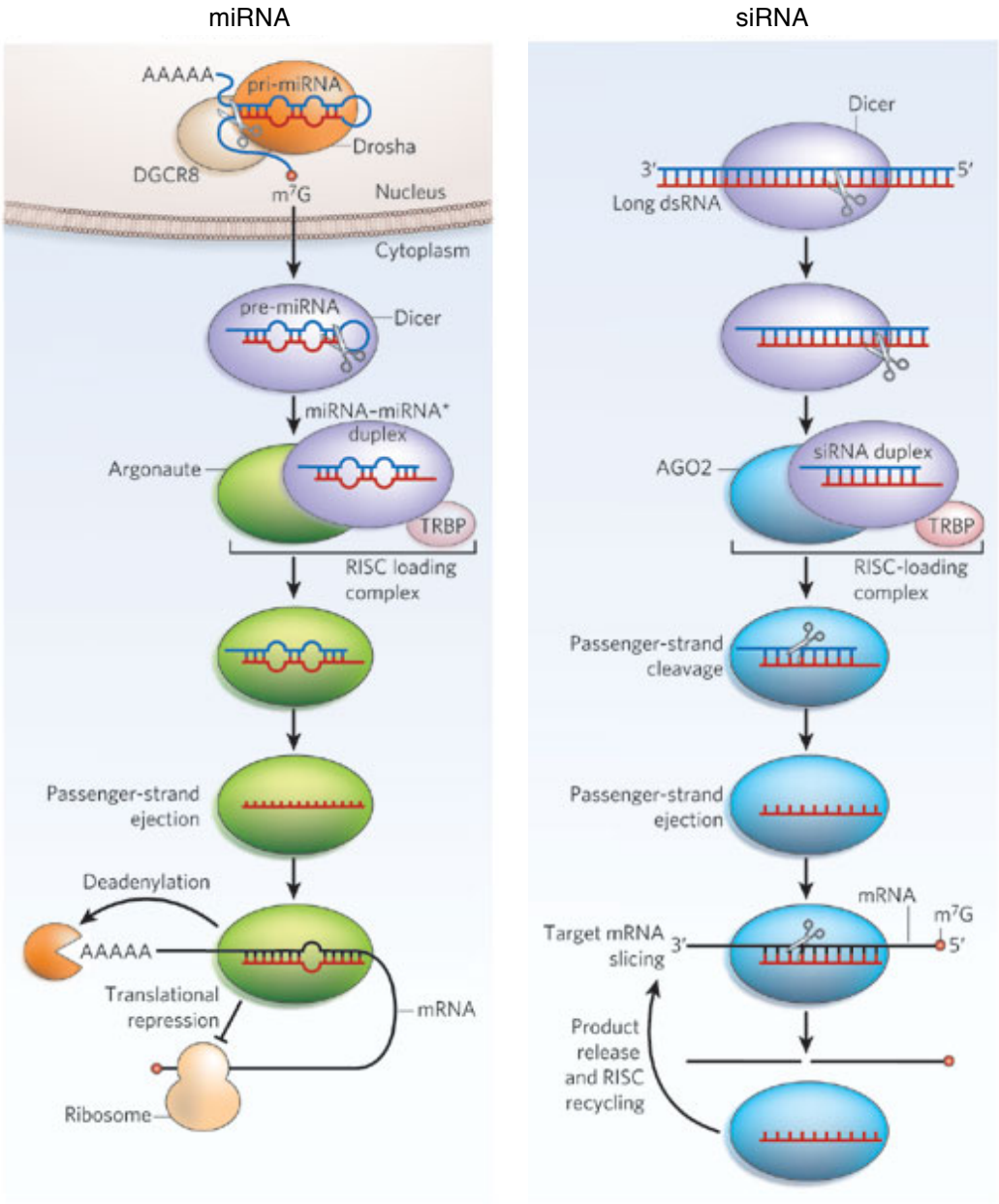

Adapted from (Jinek and Doudna, 2009)

Figure 3. Small ncRNA biogenesis.

miRNAs (left) are transcribed by endogenous genes in pri-miRNAs, which are initially processed by DROSHA/DGCR8 complex in the nucleus. In the cytoplasm, DICER cleaves the hairpin structure, generating the pre-miRNA, loaded on the RISC complex. Argonaute protein, bound to the guide strand, mediates the binding to the target mRNA, promoting translational repression and deanylation. dsRNA molecules resulting from viral RNA, convergent transcription, self-annealing transcripts or experimental transfection are processed by the siRNA pathway (right). DICER generates the siRNA duplex and AGO2 cleaves the target mRNA.

One of its components, Argonaute, binds the guide strand and mediates the cleavage of the complementary messenger RNA (mRNA) if the pairing is perfect. In alternative, it induces a translational repression followed by deadenylation and degradation. The Argonaute-binding protein GW182 is a key mediator in recruiting additional components that mediate translational repression and mRNA decay (Eulalio et al., 2008).

2.4.3 Interplay between ncRNAs and DDR

A link between ncRNA and DDR is recently emerging. DDR factors can indeed directly regulate the biogenesis of miRNAs by controlling their maturation: for instance ATM phosphorylates a panel of DROSHA interactors, including KSRP (Bensimon et al., 2010; Zhang et al., 2011), while BRCA1 interacts with DROSHA (Kawai and Amano, 2012). Some miRNAs target DDR genes such as ATM, DNA-PKcs, BRCA1, H2AX and RAD51 mRNAs (Hu et al., 2010; Lal et al., 2009; Moskwa et al., 2011; Wang et al., 2012; Yan et al., 2010).

However, recent evidence suggests a direct involvement of non-canonical small ncRNAs in the modulation of DDR and DNA repair events. In mammalian cells damaged by IR, enzymatic DNA cleavage or oncogene-induced replicative stress, DROSHA or DICER inactivation reduces the formation of DDR foci containing upstream signalling factors, such as the activated form of ATM, 53BP1 and MDC1, while γH2AX foci are not affected (Francia et al., 2012). The same effect is not observed upon down-regulation of GW proteins, downstream effectors of RNAi machinery, thus excluding a contribution of the canonical miRNAs biogenesis pathway. Many experimental data strongly indicate that DROSHA and DICER process a novel class of short RNAs (20-35 nt), generated at DSB site with the same sequence of the damaged locus. They are called DNA damage response RNAs (DDRNAs) and are necessary for the formation and maintenance of DDR foci (Francia et al., 2012). The recent finding that human DICER can shuttle between

cytoplasm and nucleus strongly suggests a local processing of DDRNAs at the DNA damage site (Doyle et al., 2013).

Similarly, in *Arabidopsis thaliana* and in human cells, 21-24 nt long RNAs, named DSB-induced RNAs (diRNAs), are involved in DNA repair by HR (Wei et al., 2012). They have the same sequence of the broken DNA, are transcribed by RNA Polymerase IV, and their biogenesis involves the components of the RNAi machinery Dicer-like proteins and Ago2. In *Drosophila melanogaster*, endogenous small interfering RNAs (endo-RNAs) are generated from a transfected linearized plasmid and they are able to silence transcription of homologous DNA sequences also *in trans* (Michalik et al., 2012). Finally in Neurospora crassa, small RNAs termed qiRNAs are transcribed from the rDNA locus in response to DNA damage (Lee et al., 2009). Although the mechanism of action of these RNAs is not clear yet, inactivation of proteins involved in their biogenesis increases the sensitivity to DNA damage.

3 Materials and Methods

3.1 Cell culture

BJ cells (The American Type Culture Collection, ATCC), WI-38 cells (ATCC) and all BJ-derived cell lines were grown in MEM supplemented with 10% foetal bovine serum, 1% L-glutamine, 1% non-essential amino acids, 1% sodium pyruvate. IMR-90 cells (ATCC) were grown in MEM supplemented with 15% foetal bovine serum, 1% L-glutamine, 1% non-essential amino acids, 1% sodium pyruvate. MRC-5, phoenix amphotropic (ATCC), HEK 293-T (ATCC) and Adeno-293 (Stratagene) cells were grown in DMEM, supplemented with 10% foetal bovine serum and 1% L-glutamine.

BJ hTERT cells are a BJ-derived cell line that stably expresses human TERT gene (Fumagalli et al., 2012). BJ hTERT shp53 cells are a BJ hTERT-derived cell line that stably expresses an shRNA against p53 (Di Micco et al., 2006). BJ hTERT shGFP and shKAP-1 were obtained by retroviral infection of BJ hTERT cells with pRetroSuper shGFP or pRetroSuper shKAP-1 (Ziv et al., 2006) and selected with puromycin (1 μg/ml). BJ hTERT GFP and TRF2 cells were obtained by lentiviral infection of contact-inhibited BJ hTERT. BJ hTERT I-SceI, Telo, and Telo + I-SceI cells were obtained by electroporation of BJ hTERT cells, selected with G418 (400 μg/ml). To have homogeneous cell populations, cells were plated sparsely and individual clones were obtained by ring cloning.

NIH 2/4 cells, a gift from Evi Soutoglou, IGBMC, Stransbourg, France (Soutoglou et al., 2007), were grown in DMEM supplemented with 10% TET system approved foetal bovine serum, 1% L-glutamine, hygromicin (400 μg/ml); they are a NIH 3T3-derived cell line transfected with the lac–ISceI–tet plasmid. To induce Tet-YFP and Tet-YFP-TRF2 binding to the TetO array, doxycycline (1 μg/ml) was added to the culture medium for 3 hours. To induce RFP-I-SceI-GR translocation to the nucleus, 16 hours post transfection Triamcinolone Acetonide (Sigma-Aldrich, 10 pM) was added to culture medium. 3 hours after treatment, cells were fixed for immunostaining (I-SceI ON) or washed with PBS to inactivate the endonuclease and fixed for immunostaining 24 hours later (I-SceI OFF).

MEFs CRE-ER TRF2$^{flox/flox}$ cells, a gift from Eros Lazzerini Denchi, SCRIPPS, La Jolla, California, USA (Celli and de Lange, 2005), were grown in DMEM supplemented with 10% foetal bovine serum and 1% glutamine; they are MEF-derived cell line in which both TRF2 alleles are loxP-flanked, and that stably expresses the CRE recombinase fused to the estrogen receptor (ER); for induction, cells were grown in the presence of 4-hydroxytamoxifen (600 nM) for 48 hours, to allow CRE-ER to translocate into the nucleus and to generate the TRF2$^{-/-}$ cell line.

T19 cells, a gift from Titia de Lange, Rockfeller University, New York, NY, USA (van Steensel et al., 1998), were grown in DMEM supplemented with 10% TET system approved foetal bovine serum, 1% L-glutamine, G418 (150 μg/ml) or hygromycin (90 μg/ml), alternatively; they are a HT1080-derived clonal fibrosarcoma cell line with a Tet-OFF system. They express the tetracyclin-controlled transactivator (tTA) and the dominant negative allele of TRF2 (TRF2ΔBΔM, containing aa 45-454 of the endogenous TRF2, lacking the basic and the myb domains) under the tetracycline-controlled promoter. Cells were grown in the presence of doxycycline (100 ng/ml), which impedes the binding of tTA to the promoter; expression of TRF2ΔBΔM was induced by removing doxycyclin from the medium, and telomere uncapping was established 7-8 days later.

All cells were grown under standard tissue culture conditions, at 37°C, 5% CO_2.

To inhibit ATM kinase activity, the inhibitor KU55933 (Tocris bioscience), or its solvent DMSO, was used at 10 μM concentration in cell culture medium for 72 hours. To induce a global chromatin relaxation, valproic acid (VPA, Sigma-Aldrich), or its solvent PBS, was used for 16 hours at 1, 10 or 50 mM concentration in cell culture medium.

3.2 Ionizing radiation

IR at different doses was used to generate acute DNA damage exogenously. IR refers to highly energetic particles or waves that can detach (ionize) at least one electron from an atom or molecule. IR-induced lesions include base damage, SSBs, DSBs and DNA cross-

links. DNA damage can be generated directly by IR or as secondary hits by free radical species. Examples of IR are energetic beta particles, neutrons, alpha particles, X- and Gamma Rays. X-rays are photons (electromagnetic radiations) emitted from electron orbits, such as when an excited orbital electron "falls" back to a lower energy orbit. The Gray (Gy) is the International System of Units of absorbed radiation dose, where 1 Gy is the absorption of 1 joule of radiation energy by 1 kilogram of matter. The radiation-generating machine (Faxitron X-Ray Corporation) is based on a high-voltage X-rays generator tube. To induce IR-dependent cellular senescence, I irradiated cultured cells with 20 Gy. Mice were irradiated with 8 Gy (total body IR) using GammaCell 200 and cobalt^{60} as a source.

3.3 Cell survival assay

Cells were plated in 6 multi-well plates, grown until confluency and irradiated or not with the appropriate dose of IR. At each time point cells were washed to remove culture medium, collected by trypsinization and counted in triplicate using a Burker chamber.

3.4 Retroviral infection

Retroviruses are single-stranded RNA viruses. They express a reverse transcriptase to retro-transcribe genomic RNA into DNA, which is then inserted into the genome at a random position by the viral integrase enzyme. The integrated vector is called provirus and it is transmitted to the progeny through cell divisions. Retroviruses used in cellular biology are replication-defective, thus they cannot produce infective particles. For cells that are not easy to transfect, like human fibroblasts, retroviral infection is an efficient way to express exogenous genes; nevertheless the primary drawback to the use of retroviruses is the requirement for cells to be actively dividing for transduction. Phoenix is a second-generation retrovirus producer cell line, based on the HEK 293T cell line that produces gag, pol and envelope proteins. The retroviral expression vectors provide the viral packaging signal (Ψ), the gene of interest under LTR promoter and an antibiotic resistance

marker. 48 hours before the transfection, packaging cells were plated at 1.8 million cells per 10 cm dish in cell growth medium. Phoenix amphotropic packaging cells were transfected by the calcium phosphate method. Calcium phosphate transfection is based on the formation of a precipitate containing calcium phosphate and DNA, which adheres to the cell surface and is internalized by endocytic process. Chloroquine, added to the medium at a final concentration of 40 μM for not more than 12 hours, increases retroviral titer by approximately two fold, by inhibiting lysosomal DNases by neutralizing vescicles pH. The precipitate is prepared by slowly mixing a HEPES-buffered saline solution containing sodium phosphate with a solution containing calcium chloride and high quality DNA (10 μg for each plate of phoenix cells). The HBS/DNA/$CaCl_2$ solution was added to the cells within 1-2 minutes of preparation. The day after the transfection the growth medium was replaced with 5 ml of fresh medium to concentrate viral particles in the supernatants and the target cells were plated at 50% of confluency. 48 hours post-transfection, viral supernatants were collected, filtered with 0.45 μm filter, to remove cells that were dead or detached from the plate, and supplemented with 8 μg/ml polybrene (this is a small, positively charged molecule that binds to cell surfaces and neutralizes surface charge, allowing the viral glycoproteins to bind more efficiently to their receptors). Supernatants were used to infect human primary fibroblasts. Four rounds of infections, of 4 hours each, distributed in 2 days, were carried out to have higher infection efficiency. After infection, cells were selected with the appropriate antibiotic.

3.5 Lentiviral infection

Lentiviruses are a subclass of retroviruses, with the ability to integrate into the genome of non-dividing as well as dividing cells. Thus lentiviral infection is amenable for contact inhibited or non-cycling senescent cells. Lentiviruses were produced by transfecting HEK 293T by calcium phosphate method with a vector expressing the gene of interest (10 μg for each plate of HEK 293T cells) together with the second-generation packaging vectors

expressing the gag, pol, rev and envelope genes. The day after the transfection the growth medium was replaced with 5 ml of fresh medium to concentrate viral particles in the supernatants. 48 hours post-transfection, viral supernatants were collected, filtered with 0.45 μm filter, to remove cells that were dead or detached from the plate, and supplemented with 8 μg/ml polybrene. Target cells were incubated with the supernatant for 8-16 hours. After infection, cells were selected with the appropriate antibiotic.

3.6 Adenoviral infection

Adenoviruses are non-enveloped viruses and have a dsDNA genome that does not integrate into the genome of the infected cells, thus it is not replicated during cell division. The recombinant adenoviral vectors are replication deficient and Adeno-293 cells, which express genes for viral particle assembly, are used to amplify viral particles. Adeno-293 cells were plated so they were at around 80% confluency the day of the infection and infected with the adenoviral particles (2 plaque forming units/cell) in medium without serum for 1 hour and 30 minutes. Infection medium was replaced with DMEM supplemented with 5% horse serum. 2-4 days later, cells were lysed by the virus and detached from the plate. Culture medium was treated with 3 cycles of freezing and thawing (putting it in liquid nitrogen and then in 37°C waterbath) to complete lysis of cells. It was centrifuged to eliminate cell debris and supernatant was stored as intermediate stock at -80°C. The intermediate stock was used for a second round of Adeno-293 infection to obtain the final stock. 1 ml of final stock was used to infect 1 well of 6 multi-well plates of target cells for 16 hours.

3.7 Electroporation

Pulsed electrical fields can be used to introduce DNA into a wide variety of cell lines that are refractive to other transfection techniques. BJ hTERT cells were trypsinized and around 300000 cells were resuspended in 10 μl resuspension buffer (MPK 1096 kit, Digital bio) containing 10 μg DNA. Plasmids were linearized prior to electroporation to facilitate

the correct integration in the genome. Cells were electroporated using a microporator device (Digital bio) with the following parameters: 1650 V, 1 pulse, 20 ms. Cells were plated in a 6 multi-well plate and transfected cells were selected with the appropriate antibiotic.

3.8 Transfection of plasmid DNA in NIH 2/4 cells

I plated cells in wells of 6 multi-well plates so that they were at around 90% confluency the day of the transfection. For each transfection reaction I mixed 250 µl of serum-free medium (Opti-MEM) with plasmidic DNA (2 µg final concentration) and 250 µl of Opti-MEM with 6 µl Lipofectamine 2000 transfection reagent (Life technologies). The two solutions were incubated 5 minutes at RT, then mixed and incubated for 20 minutes at RT to allow the formation of lipid complexes. The growth medium was removed from the cells and substituted with 1.5 ml of Opti-MEM. The mix was added to the cells that were left in the incubator for 6 hours, then transfection reaction was removed and fresh culture medium was added.

3.9 RNA interference

The RNAi pathway is used by the cells for post-transcriptional regulation of endogenous genes and to counteract viral invasion and transposon expansion. In cultured cells, short synthetic siRNAs are typically used. Alternatively, short hairpin RNA (shRNA) are used in vector-based approaches for supplying target sequence designed to form hairpins and loops of variable length, which are then processed to siRNAs by the cellular RNAi machinery and to produce stable gene silencing. For siRNA transfection, I plated cells in wells of 6 multi-well plates so that they were at around 30-50% confluency the day of the transfection. For each transfection reaction I mixed 250 µl of Opti-MEM with siRNA oligos (20 nM final concentration) and 250 µl of Opti-MEM with 4 µl Lipofectamine RNAiMAX transfection reagent (Life technologies). The two solutions were mixed and incubated for 20 minutes at RT to allow the formation of lipid complexes. The growth

medium was removed from the cells and substituted with 1.5 ml of fresh culture medium. The mix was added to the cells that were left in the incubator until the analysis. Knock down by siRNA transfection is transient, so biological effects are studied within 72 hours post transfection. I used SMARTpool siRNA (Thermo Scientific) for mouse Dicer 1 (M-040892-01), mouse Drosha (M-065630-03) and GFP (P-002048-01).

3.10 LNA transfection

Locked nucleic acid (LNA) oligos were transfected as described for siRNAs (see "RNA interference" section), with minor modifications. I used 200 nM of LNA oligos for each transfection reaction. LNA solution was incubated at 95°C for 5 minutes and chilled in ice for 5 minutes, to prevent the formation of secondary structures of the oligos. The sequences for LNAs are:

Cntl: ACTGATAGGGAGTGGTAAACT

Telo C: CCCTAACCCTAACCCTAACCC

Telo G: GGGTTAGGGTTAGGGTTAGGG

3.11 RNase A treatment

Cells grown on coverlips were washed with PBS, permeabilized with 0.6% Tween 20 in PBS for 15 minutes at RT, washed 3 times with PBS and treated with Ribonuclease A (RNase A, Sigma-Aldrich, 1 mg/ml) from bovine pancreas or acetylated bovine serum albumin (BSA, Sigma-Aldrich, 1 mg/ml) in PBS, for 30 minutes at room temperature (RT). Cells were washed with ice cold PBS twice and fixed with 4% paraformaldehyde (PFA) for 10 minutes or 1:1 methanol/acetone solution for 2 minutes. For the rescue experiment, after RNase A treatment, cells were washed twice with ice-cold PBS, treated with an incubation solution containing RNase inhibitor (RNase out, Invitrogen, 1 unit/μl) and the RNA Polymerase II and III inhibitor α-amanitin (Sigma-Aldrich, 0.4 μg/ml) for 15 minutes at RT. They were then incubated in the same solution with 200 ng of total cellular RNA, or tRNA, for additional 15 minutes at RT. They were fixed with 4% PFA for 10

minutes or 1:1 methanol/acetone solution for 2 minutes. In order to avoid the loss of small RNAs, total RNA from cells was extracted using mirVana kit (Life technologies) according to manufacturer's instructions.

3.12 Indirect immunofluorescence in cultured cells

The study protein sub-cellular localization at the single cell level I used specific antibodies by immunofluorescence techniques. Cells were grown on coverslips, washed twice for 5 minutes with PBS and fixed with either 1:1 methanol/acetone solution for 2 minutes at RT or with 4% PFA for 10 minutes at RT. In case of PFA fixation, cells were permeabilized with 0.2% Triton X-100 for 10 minutes at RT. Cells were incubated for 1 hour in blocking solution (PBG, 0.5% BSA, 0.2% gelatin from cold water fish skin) and then stained with primary antibodies diluted in PBG for 1 hour at RT in a humidified chamber. Cells were washed 3 times for 5 minutes with PBG and incubated with secondary antibodies diluted in PBG for 1 hour at RT in a dark humidified chamber. Cells were washed twice for 5 minutes with PBG, twice for 5 minutes with PBS and incubated with 4'-6-Diamidino-2-phenylindole (DAPI, 1μg/ml, Sigma-Aldrich, excitation wavelength 358nm, emission wavelength 461nm) for 2 minutes at RT. DAPI binds preferentially to AT clusters of DNA minor groove and it was used to visualize nuclei. Cells were briefly washed with PBS and water and coverslips were then mounted with mowiol mounting medium (Calbiochem), which is a polyvinyl alcohol solution containing an "anti fade" agent which is capable of reducing light-induced fading (photobleaching) of the fluorophore. Coverslips were air dried before microscope analysis.

3.13 Indirect immunofluorescence in mouse and baboon tissues

Frozen tissues placed in OCT were thawed, fixed for 20 minutes in 4% formaldehyde at RT and washed 3 times for 5 minutes with PBS. Samples were permeabilized with 0.5% Triton X-100 in PBS for 5 min at RT and washed twice for 5 minutes with PBS. Unspecific sites were blocked in 5% goat serum, 1% BSA diluted in PBS for 1 hour at RT.

Primary antibody diluted in 2.5% goat serum, 1% BSA in PBS was incubated over night at 4°C in a humidified chamber. Samples were washed 3 times for 10 minutes with PBS. Secondary antibody diluted in 1% BSA in PBS was incubated for 1 hour at RT in a dark humidified chamber. Samples were washed 3 times for 10 minutes with PBS. DAPI staining was used to detect nuclei and mowiol solution to mount coverslips. Mouse tissues were provided by Christian M. Beausejour, Université de Montréal & Centre Hospitalier Universitaire Sainte-Justine, Montréal, Canada; all *in vivo* manipulations were approved by the Comité Institutionnel des Bonnes Pratiques Animales en Recherche (CIBPAR) of CHU-Ste-Justine. Brain tissues from 3 mice (2 months old) were analyzed. Baboon tissues were provided by Utz Herbig, NJMS-UH Cancer Center (Newark, NJ, USA); all procedures were approved by the Institutional Animal Care and Use Committee (IACUC). The SBRF animal program has been accredited by the Association for the Assessment and Accreditation of Laboratory Animal Care, International (AAALAC) since 1973. Brain tissue from 4 old baboons (325-353 months old) and 2 young baboons (58 and 88 months old) were analyzed.

3.14 Immunofluorescence and Fluorescence In Situ Hybridization (ImmunoFISH)

ImmunoFISH technique combines the immunofluorescence with an antibody that recognizes a cellular antigene and FISH with a probe that detects the presence of specific DNA sequences on chromosomes in metaphase or interphase cells. The binding to its target can be identified by a distinct fluorescence signal. A Peptide Nucleic Acid (PNA) probe is a synthetic DNA/RNA analogue capable of binding to DNA/RNA in a sequence-specific manner obeying the Watson-Crick base paring rules. In PNA molecules, a neutral peptide/polyamide backbone keeps the distances between the bases exactly the same as in DNA and gives PNA excellent properties for hybridizing to DNA or RNA. In addition, PNAs are highly resistant to degradation by DNases, RNases, proteinases and peptidases

and are superior to DNA probes in terms of sensitivity and specificity. The fluorescence intensity of the spots is directly correlated to the length of the telomeres, thus it allows an exact measurement of the telomere length (Lansdorp et al., 1996).

Cells or tissues were fixed and probed as described in the corresponding immunofluorescence sections. Subsequently, after secondary antibodies incubation and washes, samples were fixed with 4% PFA and 0.1% Triton X-100 for 10 minutes at RT and reaction was then blocked with 100 mM Glycin, for 30 minutes at RT. Samples were washed 3 times with PBS and DNA was denaturated at 80°C for 5 minutes under a glass coverslip in the presence of the Cy3-conjugated telomeric PNA probe (Panagene, excitation wavelength 550 nm, emission wavelength 570 nm) in hybridization solution (70% formamide, 0.25% blocking reagent Roche, 10 mM Tris HCl pH 7.4, 0.5 μM telomeric PNA probe). The hybridization process took place in a dark humidified chamber at RT for 2 hours. Samples were washed twice for 15 minutes in wash solution I (70% formamide, 0.1% BSA, 10 mM Tris HCl pH 7.4) and twice for 5 minutes in wash solution II (100 mM Tris HCl pH 7.4, 150 mM NaCl, 0.08% Tween 20). They were stained with DAPI for 2 minutes, briefly washed with PBS and water and mounted with mowiol.

3.15 BrdU incorporation assay

To monitor DNA replication during S phase of the cell cycle, cells were incubated with 5-bromodeoxyuridine (BrdU, Sigma-Aldrich, 10 μg/ml) for 16-24 hours. BrdU is a synthetic nucleoside analogue of thymidine, and is incorporated into replicating DNA. Incorporation can be evaluated by immunofluorescence after DNA denaturation. Denaturation can be achieved by treatment with acids or alkali, or by a mild treatment with a nuclease that digest DNA to allow antibody access, simultaneously with antibody incubation. Cells, plated on coverslips, were fixed with 4% PFA for 10 minutes and permeabilized with 0.2% Triton X-100 for 10 minutes at RT. After blocking with PBG for 1 hour, cells were incubated with a mixture containing primary antibody (anti-BrdU, 1:20), DNase (Promega,

0.1 U/µl,), DNase buffer and $MgCl_2$ (3 mM) for 45 minutes at RT. Cells were washed 3 times with PBG and incubated with secondary antibody diluted in PBG for 40 minutes at RT. Cells were washed twice with PBG and twice with PBS. DAPI staining was used to detect nuclei and mowiol solution to mount coverslips.

3.16 BrdU detection under non-denaturing condition

This protocol has already been used to detect ssDNA upon replicative stress (Ye et al., 2010). Cells were incubated with BrdU (Sigma-Aldrich, 10 µg/ml) for 24 hours, so that virtually all cells had the chance to incorporate the nucleotide analogue. Cells grown on coverslips were washed twice with ice-cold PBS and treated with ice-cold cytoskeleton buffer (10 mM Pipes pH 6.8, 100 mM NaCl, 300 mM sucrose, 3 mM $MgCl_2$, 1 mM EGTA, 0.5% Triton X-100) for 5 minutes on ice and subsequently with cytoskeleton stripping buffer (10 mM Tris HCl pH 7.4, 10 mM NaCl, 3 mM $MgCl_2$, 1% Tween 40, 0.5% sodium deoxycholate) for 5 minutes on ice. Cells were washed 3 times for 5 minutes with ice-cold PBS, fixed with 4% formaldehyde for 20 minutes at RT and permeabilized with 0.5% Triton X-100 for 15 minutes at RT. They were washed 3 times for 5 minutes with PBS and unspecific epitopes were blocked with 5% BSA in PBST (0.1% Tween 20 in PBS) for 45 minutes at RT. They were incubated with primary antibody diluted in PBST-2% BSA for 1 hour at RT in a humidified chamber and washed 3 times for 5 minutes in PBST. They were incubated with secondary antibody diluted in PBST-2% BSA for 45 minutes at RT in a dark humidified chamber and washed twice for 5 minutes in PBST and once for 5 minutes in PBS. DAPI staining was used to detect nuclei and mowiol solution to mount coverslips. As a control for the efficient BrdU incorporation, additional coverslips cells were also stained for BrdU signal in denaturing conditions (see “BrdU staining under non-denaturing condition” section).

3.17 Senescence-associated-β-galactosidase assay

The activity of SA-β-gal is a widely used biomarker of cellular senescence, because β-galactosidase is specifically active at pH 6.0 in senescent cells, while its activity at this pH is poorly detectable in pre-senescent, quiescent or immortal and transformed cells (Dimri et al., 1995). Cells were grown on coverslips, washed in PBS, fixed in 4% PFA for 10 minutes at RT, washed again and incubated at 37°C in the absence of CO_2 with fresh SA-β-gal stain solution (1 mg/ml 5-bromo-4-chloro-3-indolyl beta-D-galactopyranoside, 0.5 M phosphate buffer at pH 6.0, 5 mM potassium ferrocyanide, 5 mM potassium ferricyanide, 150 mM NaCl, 2 mM $MgCl_2$). Staining was evident after 2-4 hours and maximal after 12-16 hours. At the end of the incubation time, cells were washed with PBS, fixed with 4% PFA for 10 minutes at RT, permeabilized with 0.2% Triton X-100 for 10 minutes at RT, washed with PBS, incubated with DAPI for 2 minutes, washed with PBS and mounted with mowiol. SA-β-gal staining is detected in senescent human fibroblasts as a local perinuclear blue precipitate.

3.18 Imaging

Immunofluorescence and immunoFISH images were acquired using a wide field Olympus Biosystems Microscope BX61 or a Leica TCS SP2 AOBS confocal laser microscope. To allow a more accurate signals discrimination and detection of co-localization events, confocal sections were obtained by acquisition of optical z-sections at different levels along the optical axis. Co-localization between DDR and telomeres was assessed by ImageJ software with co-localization ImageJ plug-in on confocal 3D stacks. Two points were considered co-localizing if their respective intensities were higher than the threshold of their channels, and if the ratio of their intensity was higher than the ratio setting value. Comparative immunofluorescence analyses were performed in parallel with identical acquisition parameters. Telomere length was analyzed by quantification of telomeric signal fluorescence intensities by ImageJ software. SA-β-gal images were acquired using a wide

field Olympus Biosystems Microscope IX 81. Comparative imaging analyses were performed in parallel with identical acquisition parameters.

3.19 Immunoblotting

Cells were lysed in Laemmli sample buffer (2% sodium dodecyl sulphate (SDS), 10% glycerol, 60 mM Tris HCl pH 6.8). SDS is an anionic detergent, which denatures secondary and tertiary protein structures providing a uniform negative charge along the length of the polypeptide, thus allowing separation by electrophoresis only by molecular weight. The amount of proteins in the samples was measured by the biochemical Lowry protein assay. Copper (II) ions in alkaline solution react with protein to form complexes, and with the Folin-phenol reagent, a mixture of phosphotungstic acid and phosphomolybdic acid in phenol. The product becomes reduced to molybdenum/tungsten blue and can be detected colorimetrically by absorbance at 750 nm. A tracking dye, bromophenol blue, was added to the protein solution to allow the tracking of the proteins through the gel during the electrophoretic run. Disulfide linkages were reduced by adding β-mercaptoethanol and proteins were further denatured by heating at 95°C for 5 minutes. 50 µg of whole cell extracts were resolved by SDS polyacrylamide gel electrophoresis (SDS-PAGE). Protein solution run is performed in two layers of gel, namely stacking or spacer gel and resolving or separating gel. The stacking gel is a large pore 4% polyacrylamide gel in which proteins are concentrated. It is prepared with Tris HCl buffer at pH 6.8. This gel is cast over the resolving gel, which is a small pore polyacrylamide gel. The Tris HCl buffer used is at pH 8.8. Resolving gel is used for separating different range of proteins. I commonly used 6% gel for > 100 kDa proteins, 10% gel for 40-100 kDa proteins and 15% gel for < 40 kDa proteins. After running in running buffer (25 mM Tris HCl, 0.2 M glycine, 0.1% SDS, pH 8.3), the proteins were transferred to nitrocellulose membrane by a wet electroblotting transfer method with transfer buffer (25 mM Tris HCl, 0.2 M Glycine, 20% methanol). Following protein

transfer, membranes were temporarily stained with Ponceau to assess the transfer efficiency. Ponceau is a negative stain, which binds to the positively charged amino groups of the protein and it also binds non-covalently to non-polar regions of the protein. Blocking of unspecific sites and primary and secondary antibody incubations were carried out in 5% milk in TBST (0.1% Tween in Tris-Buffered Saline). All the washes between incubations were performed in TBST. The primary antibody is specific for the protein of interest, whereas the secondary antibody is a modified antibody, which is linked to the horseradish peroxidase enzyme that, in the presence of the acridan-based substrate, produces localized light in the region where the antibody is bound to the membrane. The localized light, which is emitted from the bands, was detected by photosensitive photographic film. This method of detection is called chemiluminescence.

3.20 Quantitative reverse PCR (qRT-PCR)

Total RNA from cultured cells was extracted with RNeasy Mini Kit (Qiagen), according to manufacturer's instructions and quantified with NanoDrop spectrophotometer (Thermo Scientific). 1 µg of RNA was retrotranscribed using SuperScript VILO cDNA Synthesis Kit, according to manufacturer's instructions. A volume corresponding to 10 ng of initial RNA was used for each qPCR reaction.

The Real Time PCR Instrument allows real time detection of PCR products as they accumulate during PCR cycles. In the initial cycles of PCR, the low fluorescence defines the baseline for the plot of fluorescence signal *vs* cycle number. A fixed fluorescence threshold can be set above the baseline. The parameter Ct (threshold cycle) is defined as the cycle number at which the fluorescence becomes higher than the fixed threshold. Thus, the higher the initial amount of the sample, the sooner accumulated product is detected in the PCR process as a significant increase in fluorescence, and the lower the Ct value. Ct values are very reproducible in replicates because the threshold is detected in the exponential phase of the PCR, where there is a linear relation between log of the change in

fluorescence and cycle number. When the Ct values were higher than 35, PCR result was classified as undetermined.

The Sybr Green-based qPCR experiments were performed on a Roche LightCycler 480 sequence detection system in triplicate. Sybr Green binds to all double-stranded DNA species present in the sample, thus during the reaction the fluorescence intensity increases proportionally to the amount of PCR product. Ribosomal protein large P0 (Rplp0) was used as a control gene for normalization. qPCR primers were:

Dicer1 Fw: GCAAGGAATGGACTCTGAGC

Dicer1 Rv: GGGGACTTCGATATCCTCTTC

Drosha Fw: CGTCTCTAGAAAGGTCCTACAAGAA

Drosha Rv: GGCTCAGGAGCAACTGGTAA

Rplp0 Fw: TTCATTGTGGGAGCAGAC

Rplp0 Rv: CAGCAGTTTCTCCAGAGC

The Taqman-based qPCR experiments and the following analyses were carried in triplicate by the Real Time PCR unit (Cogentech) at the IFOM-IEO Campus, Milan, Italy, using the ABI 7900HT sequence detection system and 7500 Real-Time PCR system (Life Technologies). A gene-specific probe carrying two dyes, the fluorescent reporter and the quencher, hybridizes to the amplicon during the PCR reaction. The two fluorescent dyes interact whenever the probe is intact, causing the quencher dye to quench the reporter dye. During the amplification, the Taq DNA polymerase cleaves the 5′ end of the probe, releasing the quencher dye resulting in an increase in fluorescence. The change in reporter dye fluorescence is quantitative for the amount of PCR product. Beta-2-microglobulin (B2M) was used as a control gene for normalization. The following assays were used from Applied Biosystems: Hs00606991_m1 (KI-67), Hs99999907_m1 (B2M).

3.21 Plasmids and cloning

Retroviral vectors pRetroSuper shGFP and pRetroSuper shKAP-1 were gifts from Penny Jaggo, University of Sussex, Brighton, UK. Lentiviral vectors expressing GFP and TRF2, and packaging vectors Gag/Pol 8.91 plasmid (encoding for gag, pol and rev genes) and VSV-G (encoding for envelope elements) were gifts from Eric Gilson, IRCAN, Nice, France. Telo plasmid is a pSP73 plasmid containing 135 TTAGGG repeats and was a gift from Titia de Lange, Rockfeller University, New York, NY, USA; I-SceI + Telo plasmid was generated by cloning the I-SceI restriction site in the Telo plasmid; I-SceI plasmid was generating from the I-SceI + Telo plasmid, removing the TTAGGG repeats. Cherry-LacI, CFP-LacI, YFP-Tet and RFP-ISceI-GR vectors (Soutoglou et al., 2007; Soutoglou and Misteli, 2008) were gifts from Evi Soutoglou, IGBMC, Strasbourg, France. LacI vector was generated from the Cherry-LacI plasmid, removing the Cherry coding DNA sequence (CDS). LacI-TRF2 vector was generated by in frame cloning of the TRF2 CDS (amino acids 29-446) in the LacI vector. LacI-TRF1 vector was generated by in frame cloning of the TRF1 CDS (amino acids 1-378) in the LacI vector. YFP-Tet-TRF2 was generated by in frame cloning of the TRF2 CDS (amino acids 29-446) in the YFP-Tet vector. Adeno GFP was a gift from Elisabetta Dejana, IFOM, Milan, Italy. Adeno I-SceI was a gift from Philip Ng, Baylor College of Medicine, Huston, Texas, USA).

3.22 Antibodies

Anti-γH2AX (Millipore 05-636, 1:200); anti-ATM pS1981 (mouse, Rockland 200-301-400, 1:400; rabbit, Abcam ab2888, 1:300; mouse, Millipore 05-740, 1:100); anti-pS/TQ (Cell Signalling 2851, 1:200); anti-53BP1 (mouse, a gift from Thanos Halazonetis, University of Geneva, Geneva, Switzerland, 1:20; rabbit, Novus NB100-304, 1:200); anti-MDC1 (a gift from Jiri Bartek, IMG, Prague, Czech Republic, 1:20); anti-BrdU (denaturing conditions: Becton Dickinson 347580, 1:20; non-denaturing conditions: Abcam ab6326, 1:200); anti-CENP-C (a gift from Andrea Musacchio, Max Planck

Institute, Dortmund, Germany, 1:1000); anti-CREST (Antibodies Incorporated 15-234, 1:100); anti-CHK2 pT68 (Cell Signalling 2661, 1:100); anti-TRF2 (Upstate 05-521, 1:500); anti-LacI (Abnova PAB10255, 1:400); anti-FLAG (Sigma-Aldrich F3165, 1:500); anti-KAP-1 (Abcam ab10484, 1:1000); anti-AcH4 (a gift from Saverio Minucci, IEO, Milan, Italy, 1:1000); anti-H3 (Abcam ab10799, 1:1000); anti-Vinculin (Signa-Aldrich V9131, 1:2000); anti tubulin (Sigma-Aldrich T5168, 1:2000); anti GFP (Abcam ab290, 1:2500). As secondary antibodies I used goat anti-rabbit Alexa 405 IgG (Life Technologies, 1:100, excitation wavelength 401 nm, emission wavelength 421 nm); donkey anti-mouse or anti-rabbit Alexa 488 IgG (Life Technologies, 1:100, excitation wavelength 495 nm, emission wavelength 519 nm); donkey anti-rat FITC IgG (Jackson Immuno Research, 1:50, excitation wavelength 495 nm, emission wavelength 519 nm); donkey anti-mouse or anti-rabbit Cy3 IgG (Jackson Immuno Research, 1:400, excitation wavelength 550 nm, emission wavelength 570 nm), donkey anti-mouse or anti-rabbit Alexa 647 IgG (Life Technologies, 1:100, excitation wavelength 650 nm, emission wavelength 665 nm).

3.23 Statistical analyses

Results are shown as means plus minus standard error of the mean (s.e.m.) or standard deviation (s.d.) as indicated. p-values were calculated by chi-square test with 1 degree of freedom for qualitative data.

4 Results

4.1 Irradiation-induced cellular senescence is associated with a persistent DNA damage response activation at the telomeres

4.1.1 Ionizing radiations induce persistent DNA damage and cellular senescence

The generation of DNA damage is a harmful event for cells, because it can lead to cell death and genomic instability. Different repair pathways have evolved to cope with various endogenous or exogenous DNA lesions. Surprisingly, previous work in the lab showed that not all the DNA damage could be repaired. In this regard, early passage contact-inhibited BJ cells, were exposed to high dose (20 Gy) of IR. Since the cells did not proliferate, no telomere shortening, a potential trigger of cellular senescence (Bodnar et al., 1998) could occur. To study DDR activation, cells were fixed at different time points following irradiation and stained for nuclear foci containing the phosphorylated histone H2AX (γH2AX) and proteins phosphorylated by the activated form of ATM or ATR (pS/TQ) (Fig. 4a). Despite an efficient wave of repair leading to a dramatic reduction in the number of DDR foci per cell, not all of them disappeared and, even four months post-irradiation, some foci could still be detected and most cells were DDR-positive (Fig 4b,c). These few but persisting DDR signalling events were responsible for the establishment of cellular senescence in these cells (hereafter named IrrSen), as shown by inability to incorporate BrdU, upon release from contact inhibition, and high SA-β-gal activity (Fumagalli et al., 2012). However it was not clear whether the inability to repair in full the DNA damage was a consequence of the acute high dose of IRs used in the experiment. In order to address this point, I irradiated contact-inhibited BJ hTERT cells with a single high dose (20 Gy), or a fractionated low dose repeated each day (2 Gy x 10) or a single low dose (2 Gy) of IR. Thirty days after treatment, I fixed irradiated and non-irradiated cells and immunostained them for 53BP1 as a DDR marker (Fig. 5a). Cells irradiated with 20 Gy both in a single or fractionated dose showed a comparable number of persistent 53BP1 foci and comparable fraction of 53BP1-positive cells.

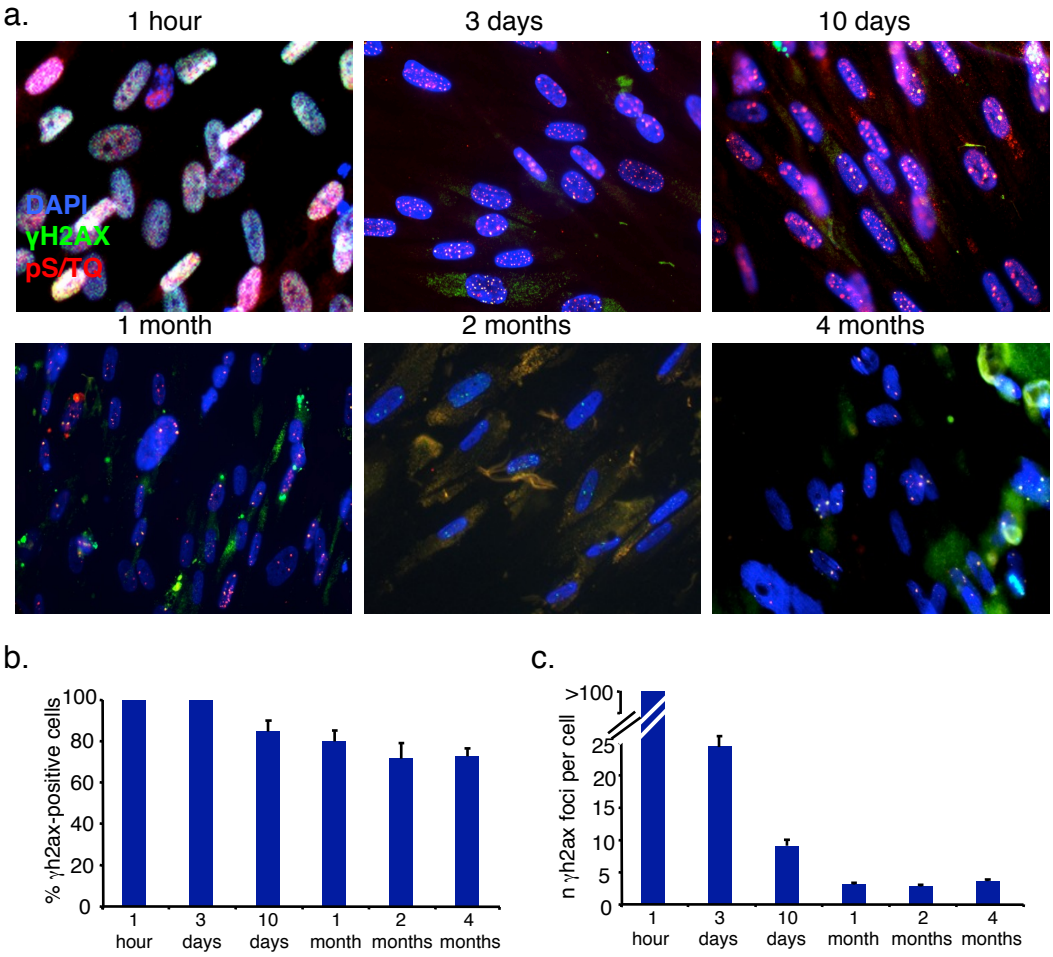

Results by Marzia Fumagalli; adapted from (Fumagalli et al., 2012)

Figure 4. Ionizing radiations induce persistent DNA damage response activation in human cells.

BJ cells were irradiated with 20 Gy and stained at the indicated time points following irradiation. (**a**) Representative images of γH2AX and pS/TQ immunostaining, acquired by widefield microscopy. (**b**) Quantification of γH2AX-positive cells and (**c**) number of γH2AX foci per cell. (For the quantification shown, around 100 cells per sample from 1 experiment were analysed; error bars represent s.e.m.).

Of note, also in cells irradiated with 2 Gy, some persistent 53BP1 foci were still detectable, although in a lower fraction of cells (Fig. 5b,c). This suggests that, independently from the type of irradiation, while the majority of DDR foci are transient and thus inconsequential for cell proliferation, few DDR foci resist repair and seem sufficient to maintain cellular senescence and impair the ability of cells to recover and proliferate.

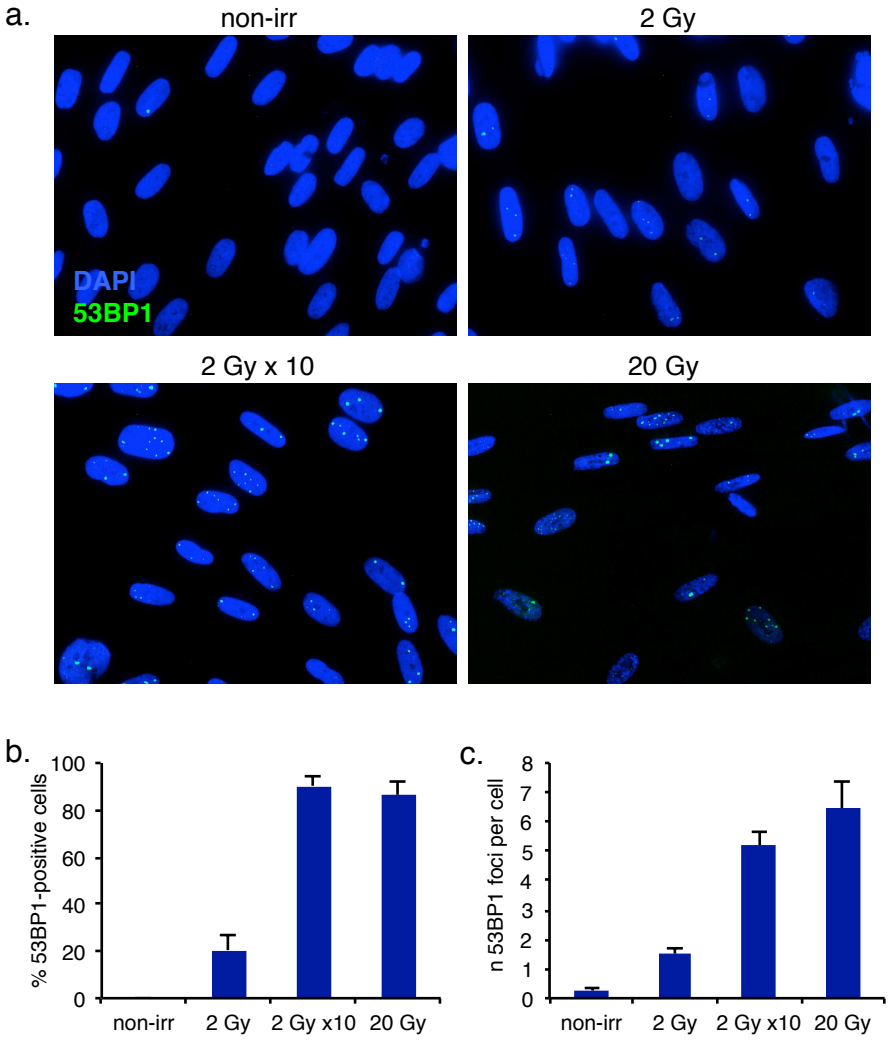

Figure 5. Ionizing radiations induce persistent DNA damage response, independently from the amount of DNA damage.

BJ hTERT cells were irradiated with 2 Gy, 2 Gy per day for 10 days, and 20 Gy and stained 30 days later. (**a**) Representative images of 53BP1 immunostaining, acquired by widefield microscopy. (**b**) Quantification of 53BP1-positive cells and (**c**) number of 53BP1 foci per cell. (For the quantification shown, around 200 cells per sample from 1 experiment were analysed; error bars represents s.e.m.).

4.1.2 Irradiation-induced cellular senescence is ATM-dependent

It has been previously shown that an active DDR is necessary for initiation and maintenance of replicative and oncogene-induced senescence (d'Adda di Fagagna et al., 2003; Herbig et al., 2004). Thus I asked whether a similar mechanism was in place also in IR-induced senescence. I treated IrrSen BJ hTERT cells with an inhibitor of ATM kinase activity and monitored ATM inhibition by the loss of ATM-dependent CHK2 phosphorylation (CHK2 pT68). In virtually all cells the CHK2 pT68 signal disappeared

after 24 hours of treatment (Fig. 6). Inhibition of ATM caused a prompt escape from senescence, already two days after the treatment, as shown by an increase in BrdU incorporation rates (Fig. 7).

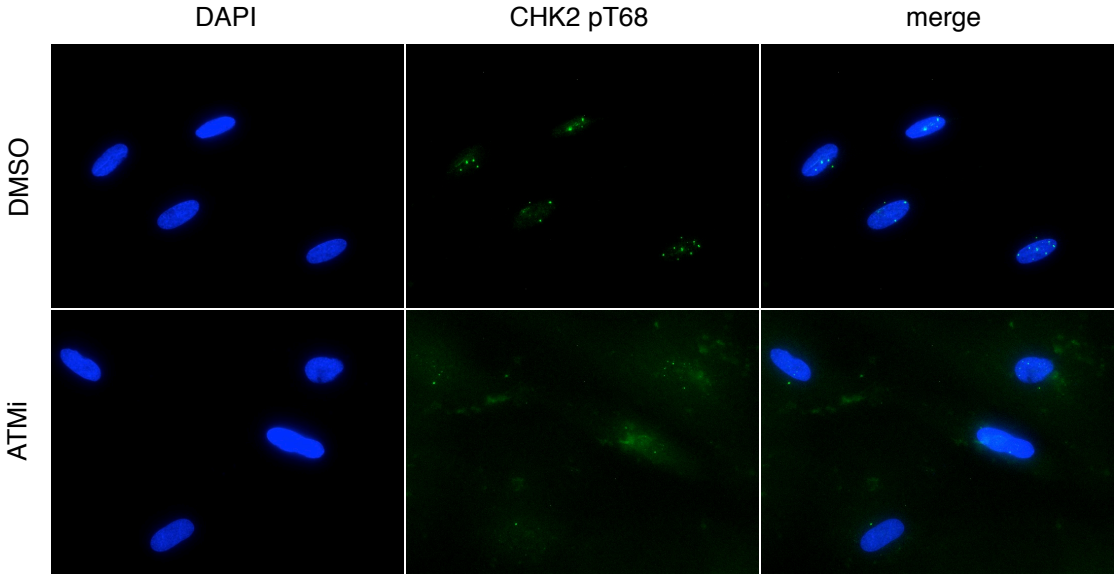

Figure 6. CHK2 phosphorylation is lost upon treatment with an ATM inhibition in IrrSen cells.

IrrSen BJ hTERT cells were treated with the ATM inhibitor KU55933 (ATMi; 10 μM) or vehicle alone (DMSO). Representative images of CHK2 pT68 immunostaining, acquired by widefield microscopy. Upon ATMi treatment, ATM-dependent CHK2 phosphorylation is lost, indicating ATM inhibition.

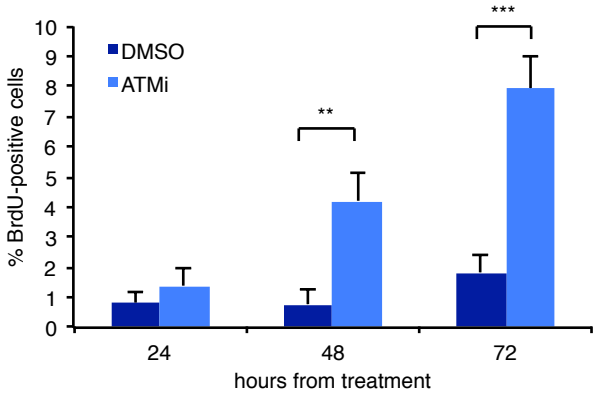

Figure 7. ATM inhibition leads to increased proliferation in IR-induced senescent cells.

IrrSen BJ hTERT cells were treated with the ATM inhibitor KU55933 (ATMi; 10 μM) or vehicle alone (DMSO). Quantification of BrdU-positive cells after 24 hours BrdU pulses at the indicated time points after ATMi treatment (** p-value < 0.01, *** p-value < 0.001, calculated by chi square test; for the quantification shown, around 600 cells per sample were analysed; n = 3 independent experiments; error bars represent s.e.m.).

As an independent evidence of re-entry in the cell cycle, I analysed the expression levels of KI-67, a marker of cell proliferation. Consistent with the previous result, the mRNA levels of KI-67 were five fold higher in treated cells, compared with controls (Fig. 8). These data reveal that, as for the replicative senescence, a sustained DDR is constantly and actively maintained and that this signalling is necessary for IR-induced senescence maintenance.

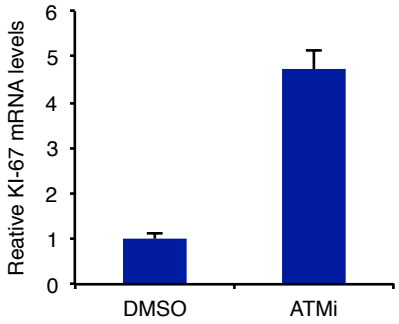

Figure 8. ATM inhibition leads to increased expression levels of the proliferation marker KI-67.

IrrSen BJ hTERT cells were treated with the ATM inhibitor KU55933 (ATMi; 10 μM) or vehicle alone (DMSO). Triplicate qPCR reactions with Taqman chemistry show an increase of KI-67 mRNA levels in ATMi-treated cells. (Error bars represent s.d.).

In addition, consistent with a published report (Rodier et al., 2011), IrrSen cells showed focal accumulation of the activated form of CHK2, which co-localized with persistent H2AX foci, whereas freshly irradiated cells show a more diffuse nuclear staining (Fig. 9). This suggests that DNA damage that is not promptly resolved causes downstream DDR factors (such as CHK2) to be retained longer at lesion sites. A focal accumulation of CHK2 pT68 signal co-localizing with telomeres has already been observed for replicative senescent cells (Herbig et al., 2004).

4.1.3 Differential DDR activation in different cell type during senescence establishment

In apparent contrast with our and other groups' results (d'Adda di Fagagna et al., 2003; Herbig et al., 2004; Sedelnikova et al., 2004), some published reports described that initially upon senescence establishment DDR foci are detectable, but then are lost in deep senescent cells (Bakkenist et al., 2004; Chen and Ozanne, 2006). The novel results

described here about IR-induced senescence support the former hypothesis that DDR foci persist.

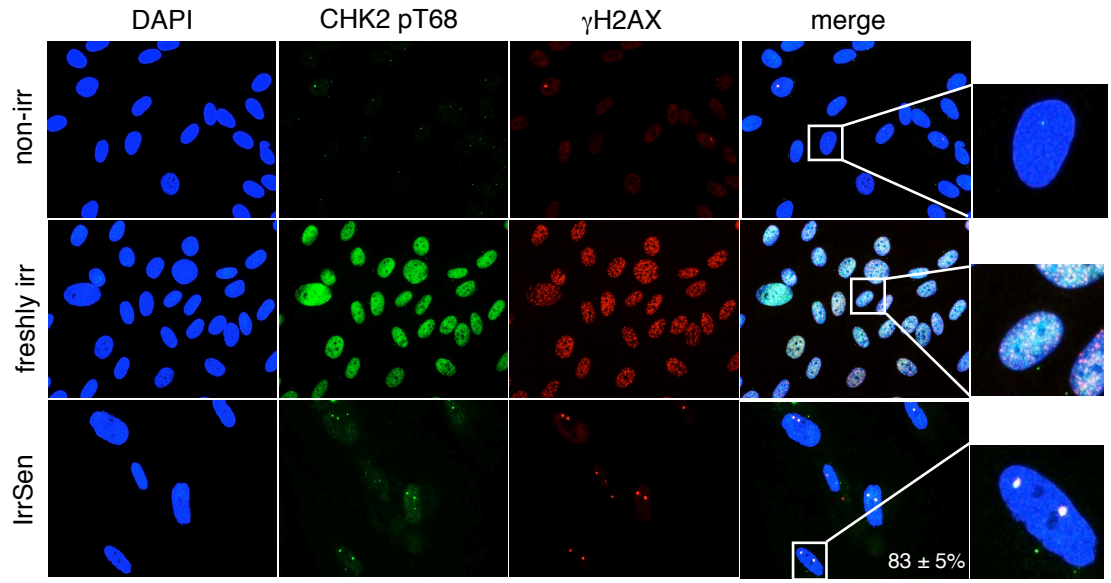

Figure 9. Activated CHK2 forms discrete nuclear foci that co-localize with persistent γH2AX only in IrrSen cells.

Representative images of CHK2 pT68 and γH2AX immunostaining, acquired by widefield microscopy. Twenty minutes (freshly irr) after IR (1 Gy), CHK2 pT68 shows a diffuse staining. Differently, in IrrSen BJ hTERT cells, it accumulates in foci co-localizing with γH2AX. The percentage of co-localization between CHK2 pT68 and γH2AX (± s.e.m.) is indicated.

I therefore decided to extend my analysis to other normal human fibroblasts cell lines, IMR-90 (that were used in the above mentioned studies), and WI-38. I irradiated early passage, contact-inhibited BJ, WI-38 and IMR-90 cells and stained them for 53BP1 as a DDR marker. These cells showed a comparable number of DDR foci immediately (one hour) after low dose irradiation (Fig. 10a). Differently, at later time points (3, 10 and 30 days) post irradiation (20 Gy), while WI-38 had an apparent similar kinetics of DDR foci resolution compared to BJ, IMR-90 showed a reproducibly lower number of 53BP1 foci per cell and lower fraction of 53BP1-positive cells at various time points (Fig. 10b-c). This is consistent with what was observed in replicative senescent cells (Bakkenist et al., 2004;

Chen and Ozanne, 2006), and it suggests that the presence of persistent DDR foci upon senescence establishment can be cell line-specific.

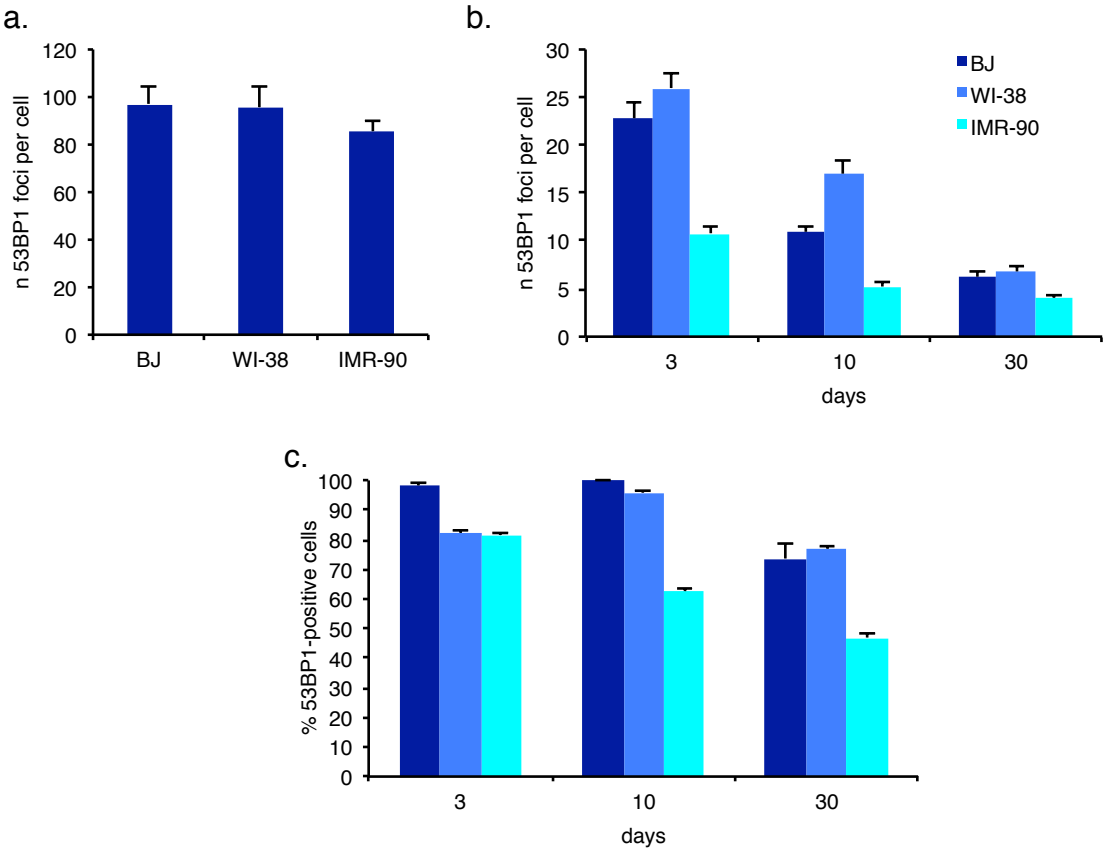

Figure 10. Different cell lines show an apparently differential persistence of DNA damage response activation upon senescence establishment.

(**a**) BJ hTERT, WI-38 and IMR-90 cells were irradiated with 1 Gy and stained 10 minutes later. Quantification of number of 53BP1 foci per cell. (For the quantification shown, around 50-100 cells per sample from 1 experiment were analysed; error bars represent s.e.m.). (**b-c**) BJ hTERT, WI-38 and IMR-90 cells were irradiated with 20 Gy and stained for 53BP1 as a DDR marker thirty days later. Bar graphs show the quantification of 53BP1-positive cells and number of 53BP1 foci per cell. (For the quantification shown, around 50-100 cells per sample were analysed; n = 2 independent experiments; error bars represent s.e.m.).

This apparent inconsistency among cell lines could be explained by the higher sensitivity to stress of IMR-90 compared to the other cell types. To address this, I exposed the three cell lines to high doses of IR and observed their survival at different time points following irradiation. I observed a massive cell death in IMR-90 upon irradiation and, to a minor

extent, also in non-irradiated cells, while in BJ hTERT and WI-38 cell number remained almost constant (Fig. 11).

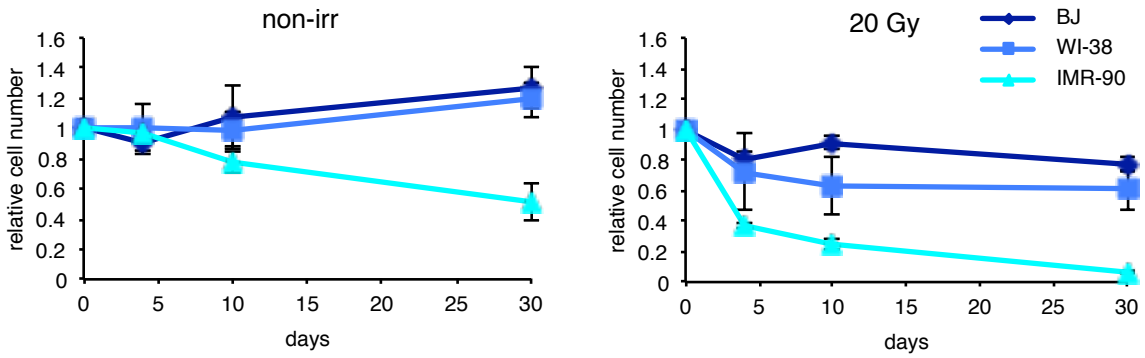

Figure 11. Apparent differential DNA damage response activation during senescence correlates with cell survival upon DNA damage.

BJ hTERT, WI-38 and IMR-90 cells were irradiated or not with 20 Gy. Graphs show the average cell number of triplicates at different time points, in irradiated cells and non-irradiated controls (error bars represent s.e.m.).

I tested the hypothesis that these cells died by apoptosis, but the absence of detectable levels of cleaved caspase-3 by immunoblot staining suggested that this was not the case (Fig. 12).

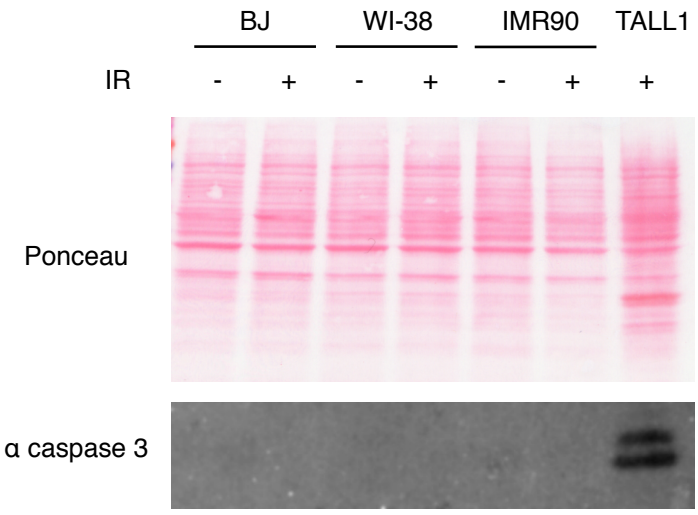

Figure 12. IR-induced cell death is not associated with apoptosis marker.

BJ hTERT, WI-38 and IMR-90 cells were irradiated with 20 Gy and protein lysates were collected 30 days later. Cleaved caspase-3 signal was detected only in irradiated TALL-1 cells, used as a positive control for apoptosis activation. Ponceau staining was used as a loading control.

Thus the difference in DDR activation at the time of senescence establishment could be explained by a cell-specific sensitivity to stress likely associated with culture shock, so that the cells with more unrepaired DNA damage preferentially die. We conclude that indeed DDR foci in senescent cells are persistent, rather it is the prolonged cell viability of some cell lines that does not allow their accurate study in time.

4.1.4 Persistent DNA damage response foci localize preferentially at telomeres, independently from the amount of DNA damage

The molecular bases that distinguish reparable, transient DDR foci from irreparable, persistent DDR foci were unknown. Telomeres are genomic loci made of repetitive DNA sequences coated by specific proteins that inhibit DNA repair at chromosome termini to prevent chromosomal fusions and genome instability (O'Sullivan and Karlseder, 2010). We hypothesized that they could be genomic loci that resist cellular DNA-repair activities when a DSB occurs within the telomere length. This hypothesis is supported by *in vitro* assays using human cell extracts, in which NHEJ is inhibited at telomeric DNA ends (Bae and Baumann, 2007; Bombarde et al., 2010). Previous experiments in our group aimed to test this hypothesis. Therefore, interphase BJ cells were stained for the DDR factor 53BP1, in conjunction with FISH using a telomeric Cy3-conjugated PNA probe (immunoFISH) at different time points following exposure to IR (Fig. 13a). Optical z-sections acquired by confocal microscopy were used to perform a manual 3D analysis, followed by a software-based quantification. We showed that while the number of 53BP1 foci per cell progressively declined with time, the fraction that co-localized with a telomeric signal gradually increased up to 30%. In contrast, this was not evident looking at the co-localization between the DDR marker and another repetitive DNA region, the centromeres, visualized by CENP-C staining (Fig. 13b). A very similar result was reproduced using MRC-5 cells, another human fibroblast cell line (Figs. 13c,d).

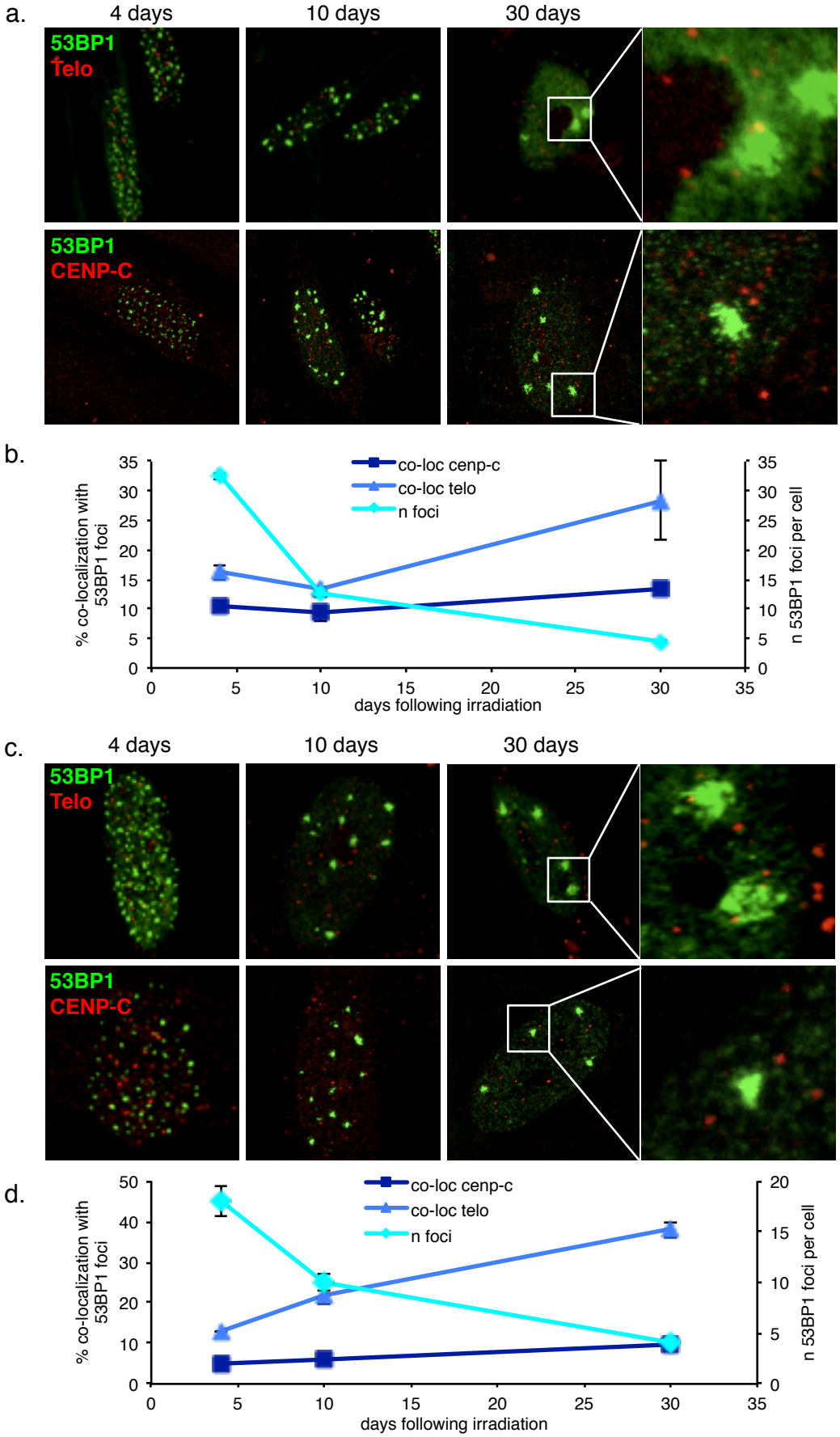

Results by Marzia Fumagalli; adapted from (Fumagalli et al., 2012)

Figure 13. Persistent DDR preferentially co-localizes with telomeric DNA in human cells.

Contact-inhibited BJ (**a,b**) and MRC-5 (**c,d**) cells were irradiated and analysed at the indicated time points. (**a,c**) Representative images acquired by confocal microscopy show co-localization between 53BP1 and telomeres, detected using a telomeric PNA probe (Telo), or centromeres detected by antibodies raised against a centromeric protein (CENP-C). (**b,d**) Quantification of the percentage of co-localizations between 53BP1 foci and telomeric (Telo) or centromeric (CENP-C) regions, and the average number of 53BP1 foci per cell. (For the quantifications shown, around 50-200 cells per time point from 1 experiment were analysed; error bars represent s.e.m.).

The length of the human genome is around 3 billions bp, while each telomere is around 10 Kb long. Thus the observed extent of co-localization is highly significant, since telomeric DNA in human cells accounts for around 0.014% of the genome.

To extend this observation *in vivo*, mice were irradiated with a sub-lethal dose of total body IR (8 Gy) and hippocampal sections were stained 6 hours and 12 weeks after irradiation for 53BP1 and the telomeric PNA probe or the centromeric marker CREST (Fig. 14a). Consistent with observations in cultured cells, with time, hippocampal neurons are able to repair most of the DDR foci and 12 weeks after irradiation the percentage of co-localization of DDR with the telomeric signals increased up to 40%, while the fraction co-localizing with the centromeres remained constant (Fig. 14b).

To make sure that the accumulation of DDR markers at telomeres was not due to the high acute dose of IR, I performed the same co-localization analysis between telomeres and 53BP1 in BJ hTERT cells irradiated with 20 Gy, 2 Gy per day for 10 days, and 2 Gy (Fig 15a). IR is expected to generate DNA damage and DDR foci randomly in the genome. When most of DNA damage is repaired, the fraction of persisting DDR foci at telomeres should be constant and independent from the initial amount of DNA damage. Indeed, 30 days after irradiation, cells showed a comparable fraction of 53BP1 foci co-localizing with the telomeric PNA probe, in the three different conditions (Fig. 15b), despite the different number of DDR foci per cell (Fig. 5).

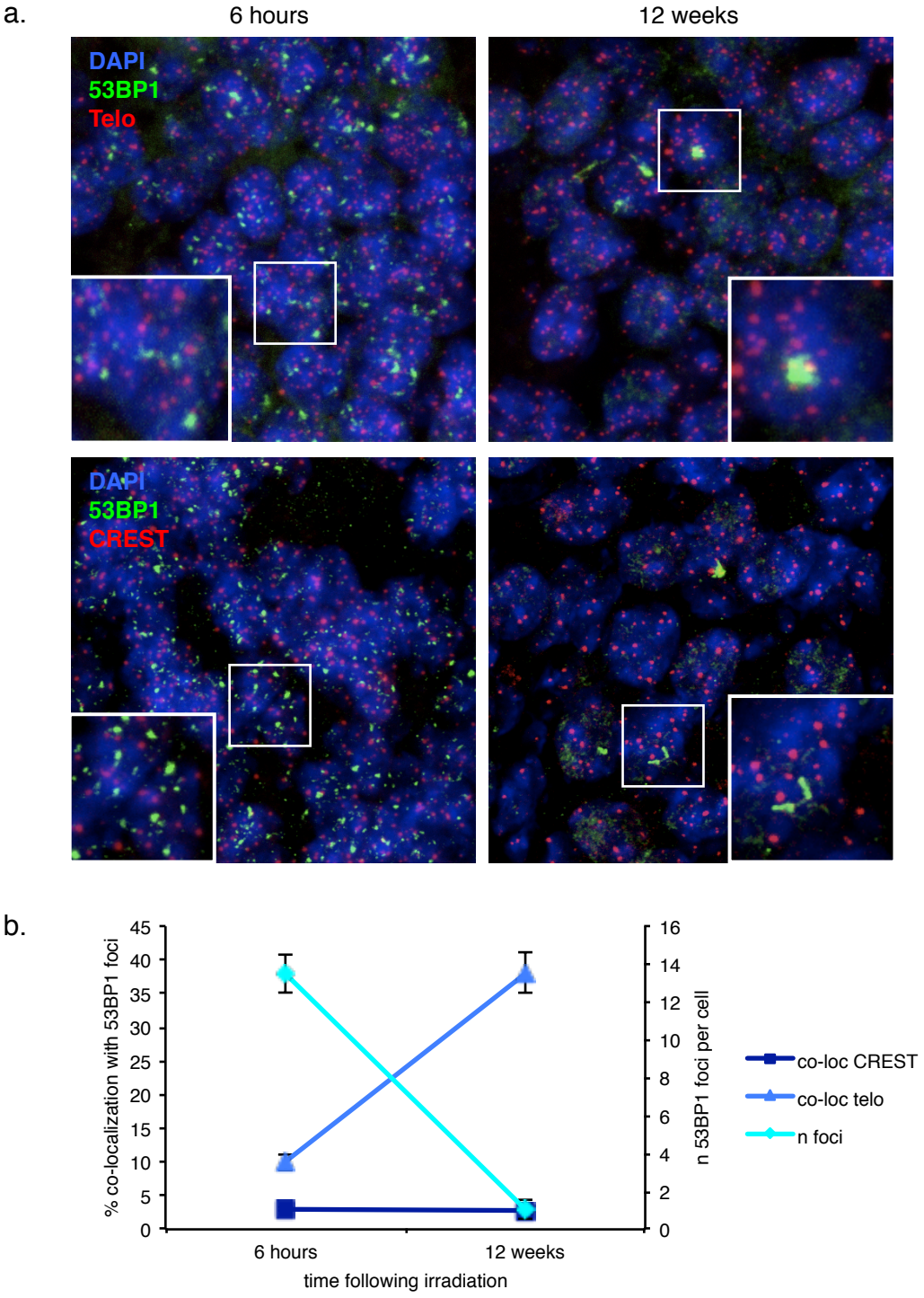

Results by Marzia Fumagalli; adapted from (Fumagalli et al., 2012)

Figure 14. Persistent DDR preferentially co-localizes with telomeric DNA *in vivo*, in mouse hippocampal neurons.

Hippocampal neurons from adult mice were analysed at the indicated timepoints post IR (8 Gy). (**a**) Representative images acquired by confocal microscopy show co-localization between 53BP1 and telomeres, detected using a telomeric PNA probe (Telo), or centromeres detected by a specific antibody (CREST). (**b**) Quantification of the percentage of co-localizations between 53BP1 foci and telomeric (Telo) or centromeric (CREST) regions, and the average number of 53BP1 foci per cell. (For the quantification shown, around 400

cells per time point were analysed; samples from 3 individual mice were analysed; error bars represent s.e.m.).

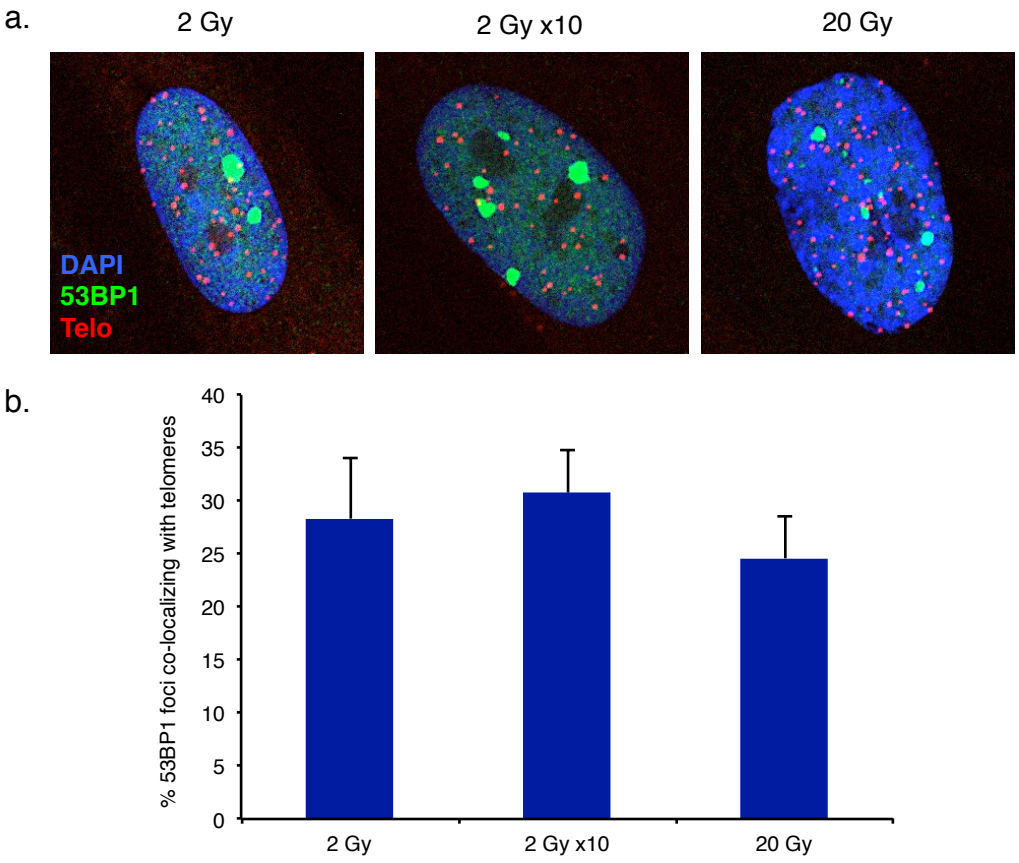

Figure 15. Persistent DDR foci localize preferentially at telomeres in cells irradiated with low dose or fractionated IR.

BJ hTERT cells were treated with the indicated dose of IR and stained 30 days later. (**a**) Maximum projections of Z-stacks acquired by confocal microscopy show co-localizations between DDR foci, detected as 53BP1 foci, and telomeres, detected using a telomeric PNA probe (Telo). (**b**) Quantification of 53BP1 foci co-localizing with telomeres upon the different irradiation treatments. (For the quantification shown, around 20 cells per sample from 1 experiment were analysed; error bars represent s.e.m.).

4.1.5 In human cells a DNA double-strand break close to telomeric repeats results in a more persistent DNA damage response

Since a high fraction of persistent DDR foci co-localized with telomeric DNA, I hypothesized that this was the consequence of the impaired capability of telomeric DSB to

be repaired. In order to directly address this, I generated three stable cell lines by electroporation of different constructs in BJ hTERT cells. The first plasmid carried a site for the restriction endonuclease I-SceI a yeast endonuclease that recognizes a 18-nucleotide long sequence not found in the mammalian genome. This site was flanked by 135 telomeric repeats (Telo + I-SceI). Importantly, I cloned the I-SceI site downstream the telomeric repeats because *in vitro* assays showed that the telomeric effect in inhibiting NHEJ was directional and toward the 3' direction (Bae and Baumann, 2007). I also generated stable cell lines carrying the telomeric repeats only (Telo), or the I-SceI site with no telomeric DNA (I-SceI), to be used as controls (Fig. 16a). I isolated and cultured homogeneous clonal cell populations till confluency, then infected them with an adenovirus expressing the I-SceI endonuclease and analyzed the DDR activation in the form of 53BP1 foci. One day after the infection most cells were DDR-positive, even in Telo cells, that did not have an I-SceI site (Fig. 16b). This is likely due to adenoviral infection *per se* – also cells infected with a GFP-expressing adenovirus showed a similar DDR activation. Seven days after the infection, around 40% of GFP-expressing cells were still DDR-positive. This experiment had the important limitation that the DNA damage site could not be visualized in the nucleus. Thus I could not distinguish the specific DDR focus generated by the I-SceI endonuclease from the ones caused by the adenoviral infection, complicating the interpretation of the experimental results. However, considering a background level of DDR, based on the GFP-infected cells, the Telo + I-SceI cells showed a slightly higher percentage of DDR-positive cells compared to the I-SceI and Telo cells, consistent with our model (Fig. 16b). Similarly, looking at the number of DDR foci per cell, both cell lines carrying an I-SceI site showed a similar DDR activation one day after the infection, while seven days later, the presence of telomeric repeats induced a more persistent DDR compared to the other samples (Fig. 16c). Although the results shown here were not dramatic, they are consistent with the hypothesis that accumulation of DNA damage at the telomeres might be due to their irreparability.

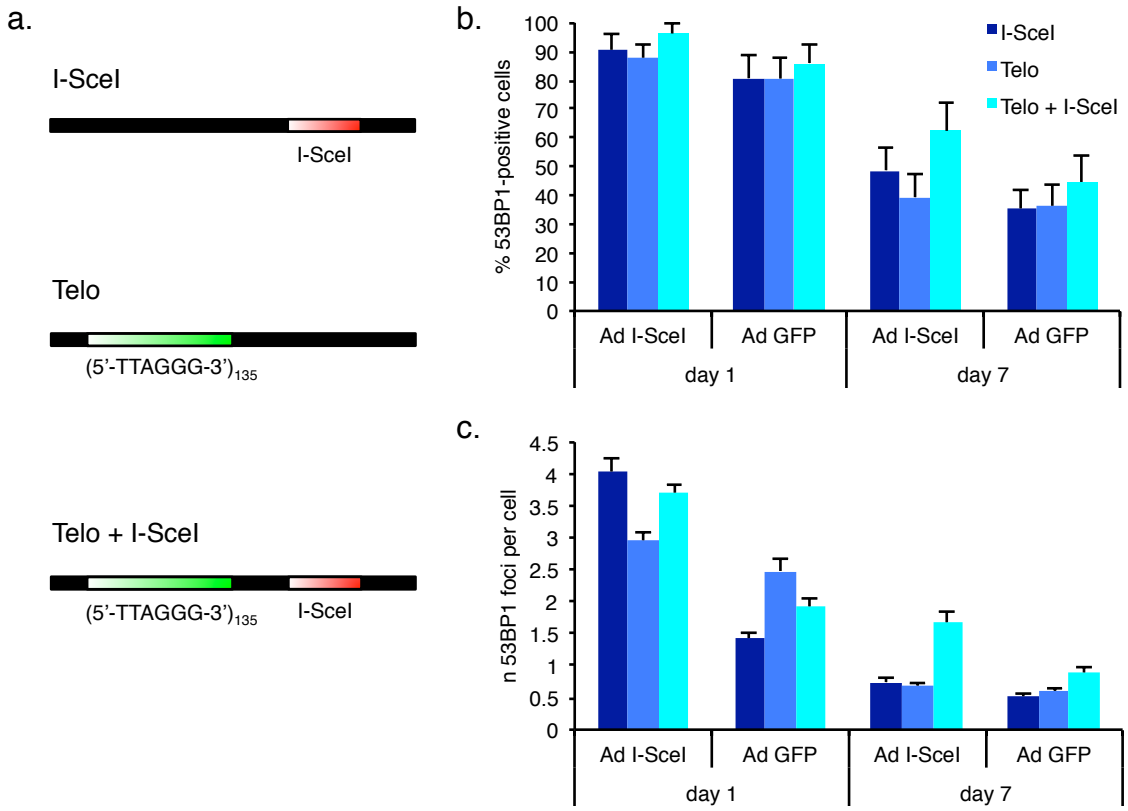

Figure 16. Telomeric repeats close to a double-strand break induce a more persistent DNA damage response activation.

(**a**) Schematic of the integrated constructs studied in BJ hTERT cells. BJ hTERT cells were electroporated to integrate one of the three following constructs: I-SceI, which carries an integrated cut site for the I-SceI endonuclease, Telo, a 810 bp of telomeric repeats, and Telo + I-SceI which has an I-SceI site next to the telomeric repeats. (**b-c**) Stable cell lines carrying the indicated constructs were infected with an I-SceI- or GFP-expressing adenovirus and immunostained for 53BP1 at the indicated time points post infection. Bar graphs show the percentage of 53BP1-positive cells and the number of 53BP1 foci per cell. (For the quantification shown, around 40 cells per sample from 1 experiment were analysed; error bars represent s.e.m.).

4.2 Inhibition of repair at the telomeres is mediated by the telomere-binding protein TRF2

4.2.1 Persistent DNA damage at the telomeres is not caused by its heterochromatic state

Next I tried to investigate the molecular mechanisms at the basis of telomere irreparability. Telomeres are made of constitutive heterochromatin (Blasco, 2007) and it has been shown that heterochromatic DSBs are generally repaired more slowly than euchromatic DSBs (Goodarzi et al., 2008). Thus I tested if persistent DDR at telomeres was related to the heterochromatic structure of chromosome ends.

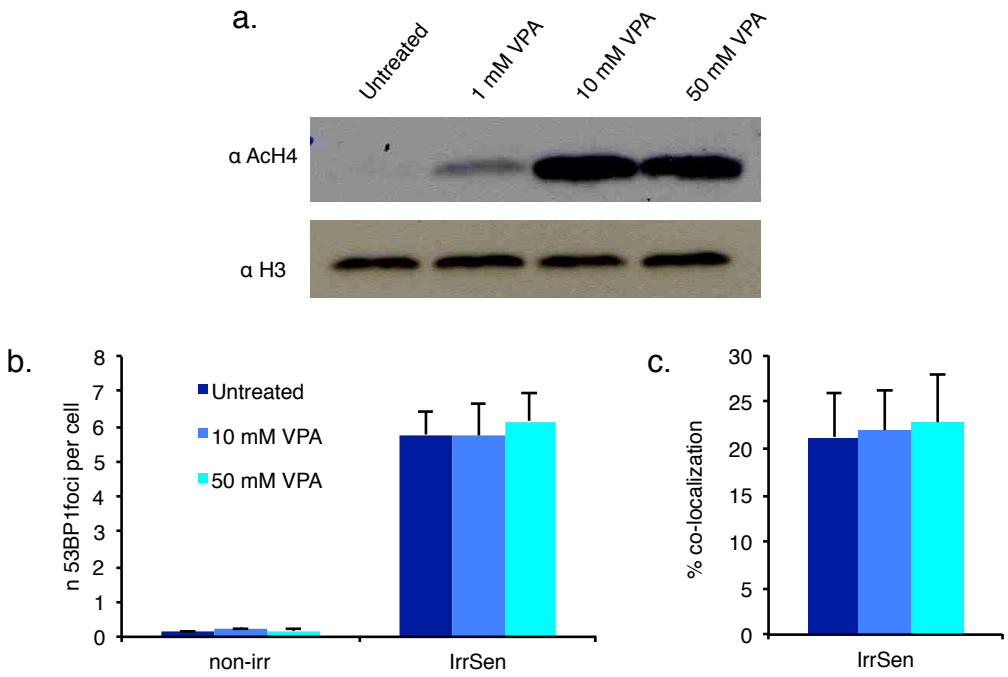

Figure 17. Heterochromatin disruption by VPA treatment does not significantly affect the number of persistent DDR foci and their localization at telomeres.

BJ hTERT cells were treated with the indicated concentration of VPA, irradiated with 20 Gy and analysed 30 days later. (**a**) Immunoblot shows the increased levels of acetylated histone H4 (AcH4) in treated cells, compared to untreated control. H3 was used as a loading control. (**b**) Quantification of the number of 53BP1 foci per cell, in cells treated with the indicated doses compared to untreated control. (For the quantification shown, around 100 cells per sample from 1 experiment were analysed; error bars represent s.e.m.). (**c**) Quantification of 53BP1 foci co-localizing with telomeres, in cells treated with the indicated doses compared to untreated control. (For the quantification shown, around 30 cells per sample from 1 experiment were analysed; error bars represent s.e.m.).

I perturbed constitutive heterochromatin treating cells with different concentrations of a histone deacetylase inhibitor, valproic acid (VPA) (Marchion et al., 2005). The global relaxation of chromatin was monitored by increased acetylation of histone H4 (Fig. 17a). I then exposed these and control cells to IRs. Thirty days after irradiation treated cells showed no significant difference in terms of number of persistent 53BP1 foci per cell or their co-localization with telomeres (Fig. 17b,c), suggesting that VPA treatment could not prevent accumulation of persistent DDR foci at the telomeres.

KAP-1 is a mediator of ATM-dependent DNA repair activity in heterochromatin (Goodarzi et al., 2008). I reasoned that, if KAP-1 was necessary for the DNA repair also at the telomeres, like in other heterochromatic regions, knock down of this co-factor could further increase the accumulation of persistent DDR foci at the telomeres. I exposed stable KAP-1 knocked down and control cells (Fig. 18a) to IRs and analyzed them one month later. Again no difference was evident in the number of 53BP1 foci per cells or their fraction co-localizing with telomeres (Fig. 18b,c). Thus, persistent DDR at telomeres cannot be explained as a consequence of their heterochromatic structure.

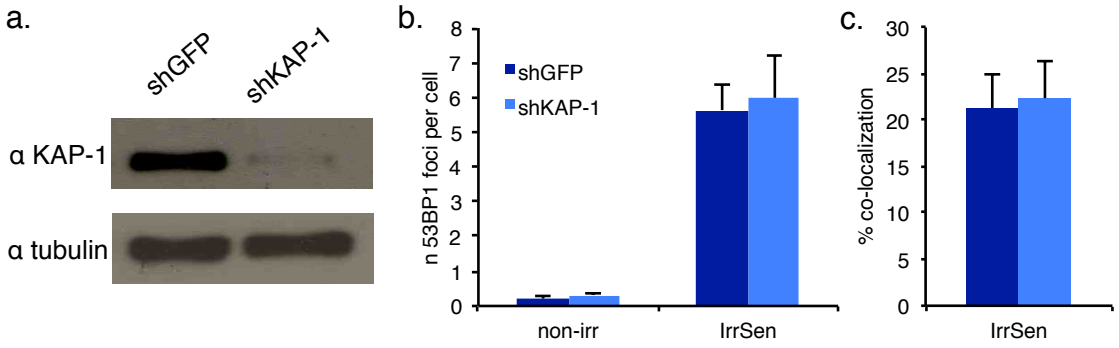

Figure 18. KAP-1 knock down does not significantly affect the number of persistent DDR foci and their localization at telomeres.

BJ hTERT cells were infected with shGFP or shKAP-1 expressing lentiviruses, irradiated with 20 Gy and analysed 30 days later. (**a**) Immunoblot shows the expression of KAP-1 in shGFP or shKAP-1 BJ hTERT cells. Tubulin was used as a loading control. (**b**) Quantification of the number of 53BP1 foci per cell. (For the quantification shown, around 100 cells per sample from 1 experiment were analysed; error bars represent s.e.m.). (**c**) Quantification of 53BP1 foci co-localizing with telomeres. (For the quantification shown, around 30 cells per sample from 1 experiment were analysed; error bars represent s.e.m.).

4.2.2 Persistent DNA damage at the telomeres is not caused by a dramatic TRF2 down-regulation or mislocalization

TRF2 is one of the six components of the shelterin complex, which directly binds to telomeric DNA (Broccoli et al., 1997). Its loss triggers DDR activation at telomeres and chromosomal fusions (d'Adda di Fagagna et al., 2003; Takai et al., 2003; van Steensel et al., 1998). Furthermore, during replicative senescence it is down regulated through preoteasome-mediated degradation (Fujita et al., 2010). I therefore tested whether persistent DDR foci at telomeres were associated with TRF2 loss also during IR-induced senescence. The total TRF2 protein level was around 64% in IrrSen cells compared to non-senescent controls (Fig. 19), a much weaker down-regulation compared to the one reported in replicative senescence.

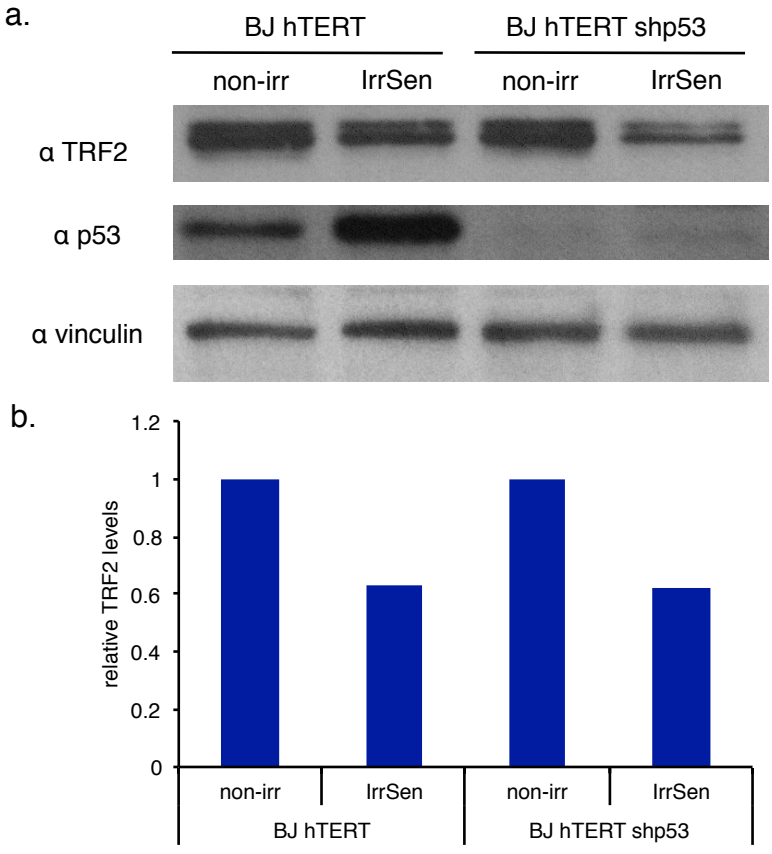

Figure 19. TRF2 expression is not significantly altered in IrrSen cells.

BJ hTERT and BJ hTERT shp53 cells were irradiated with 20 Gy and analysed 30 days later. (**a**) Immunoblot shows TRF2 and p53 protein levels. Vinculin was used as a loading control. (**b**) Quantification of TRF2 levels in IrrSen cells, compared to non-irradiated cells, normalized on vinculin.

Since in replicative senescence TRF2 down-regulation is mediated by p53 and prevented by p53 knock down (Fujita et al., 2010), I checked TRF2 protein levels in stable shp53 cells. Interestingly, I observed the same relative down regulation as in p53 proficient cells. One possible explanation for this difference could also partially reflect the increased volume of the cytoplasm in senescent cells that can change the cytosolic (vinculin) *vs* nuclear (TRF2) protein ratio. In addition, one copy of the gene is sufficient to protect telomeres, and DDR foci at telomeres are evident only upon removal of both alleles (Celli and de Lange, 2005). However I wanted to experimentally rule out the possibility that DDR accumulation at telomeres was induced by the observed partial TRF2 down-regulation.

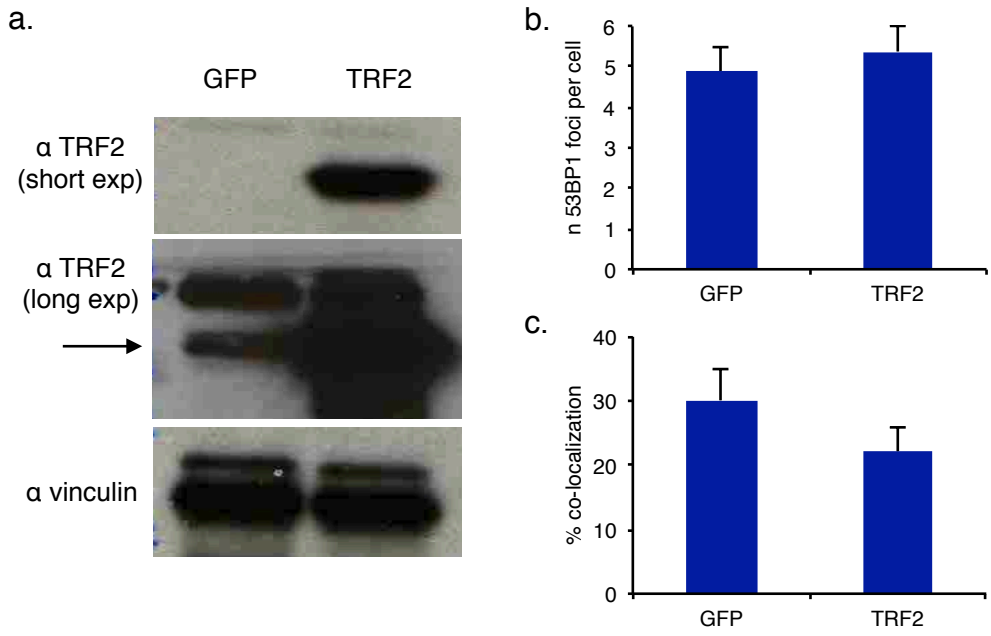

Figure 20. TRF2 over-expression does not significantly affect the number of persistent DDR foci per cell and their localization at telomeres.

BJ hTERT cells were infected with either TRF2 or GFP expressing lentiviruses, irradiated with 20 Gy and analysed 30 days later. (**a**) Immunoblot showing TRF2 expression in TRF2 and GFP over-expressing BJ hTERT cells. Vinculin was used as a loading control. Arrow shows endogenous TRF2 in GFP over-expressing sample. (**b**) Quantification of the number of 53BP1 foci per cell. (For the quantification shown, around 100 cells per sample from 1 experiment were analysed; error bars represent s.e.m.). (**c**) Quantification of 53BP1 foci co-localizing with telomeres. (For the quantification shown, around 50 cells per sample from 1 experiment were analysed; error bars represent s.e.m.).

Thus I over-expressed TRF2 or GFP by lentiviral infection in BJ hTERT cells (Fig. 20a) before exposing them to IR. In TRF2 over-expressing cells I could still find persistent DDR foci at telomeres, to a similar extent compared to control cells (Fig. 20b,c).

Most importantly, TRF2 over-expression did not alter the establishment of cellular senescence. Indeed 30 days after irradiation, both in non-irradiated and in IrrSen cells, the BrdU incorporation rate was not affected at all compared to GFP-expressing cells (Fig. 21). Similarly, another marker of cellular senescence, the SA-β-gal activity, was detected at a very similar level despite TRF2 over-expression (Fig. 22).

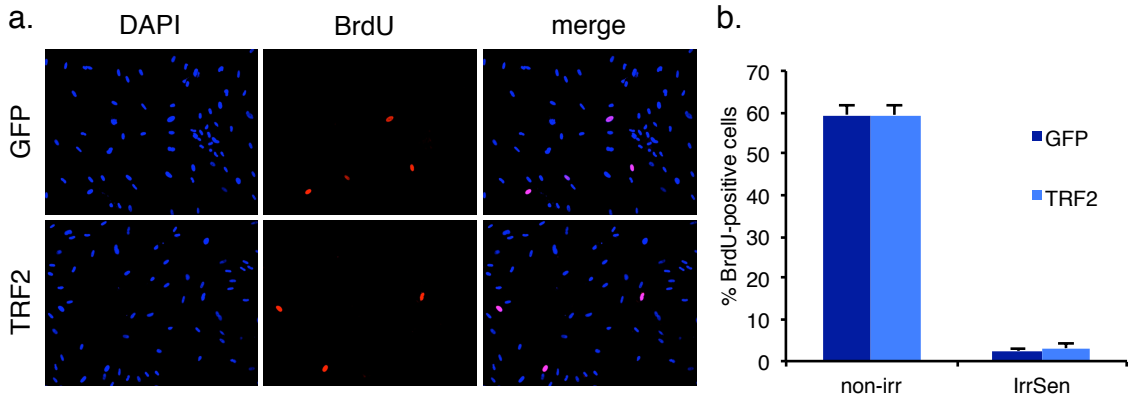

Figure 21. Effects of TRF2 over-expression on senescent-associated proliferative arrest.

TRF2 and GFP over-expressing BJ hTERT cells were irradiated with 20 Gy and analysed 30 days later. (**a**) Representative images of BrdU immunostaining under denaturing condition acquired by widefield microscopy. (**b**) Quantification of BrdU-positive cells in non-irradiated and IrrSen cells. (For the quantification shown, around 400 cells per sample from 1 experiment were analysed; error bars represent s.e.m.).

Beyond its expression levels, also TRF2 localization at telomere is essential for telomere protection (van Steensel et al., 1998). Since TRF2 is recruited at DNA damage sites (Bradshaw et al., 2005), one possibility is that upon irradiation TRF2 moves from telomeres to the sites of DNA damage, causing deprotection of telomeres. However immunoFISH staining of IrrSen cells showed that the vast majority of telomeres, detected by a telomeric PNA probe, co-localized with TRF2 (Fig. 23a). Furthermore, around 41%

of persistent ATM pS1981 foci, co-localized with TRF2 (Fig. 23b), suggesting that the DDR-positive telomeres were not the ones that lost TRF2 protection.

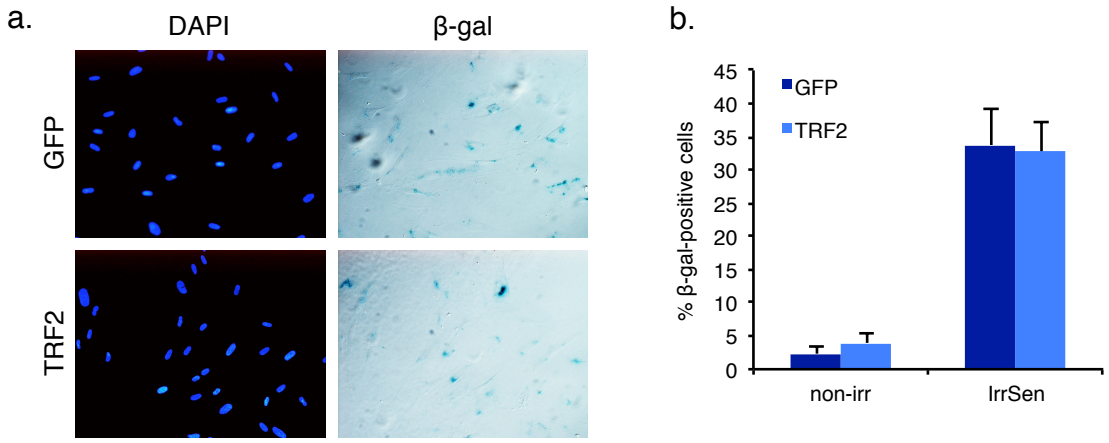

Figure 22. Effects of TRF2 over-expression on senescent-associated beta-galactosidase staining.

(**a**) Representative images of SA-β-gal staining acquired by widefield microscopy. (**b**) Quantification of SA-β-gal positive cells, in non-irradiated and IrrSen cells. (For the quantification shown, around 50 cells per sample from 1 experiment were analysed; error bars represent s.e.m.).

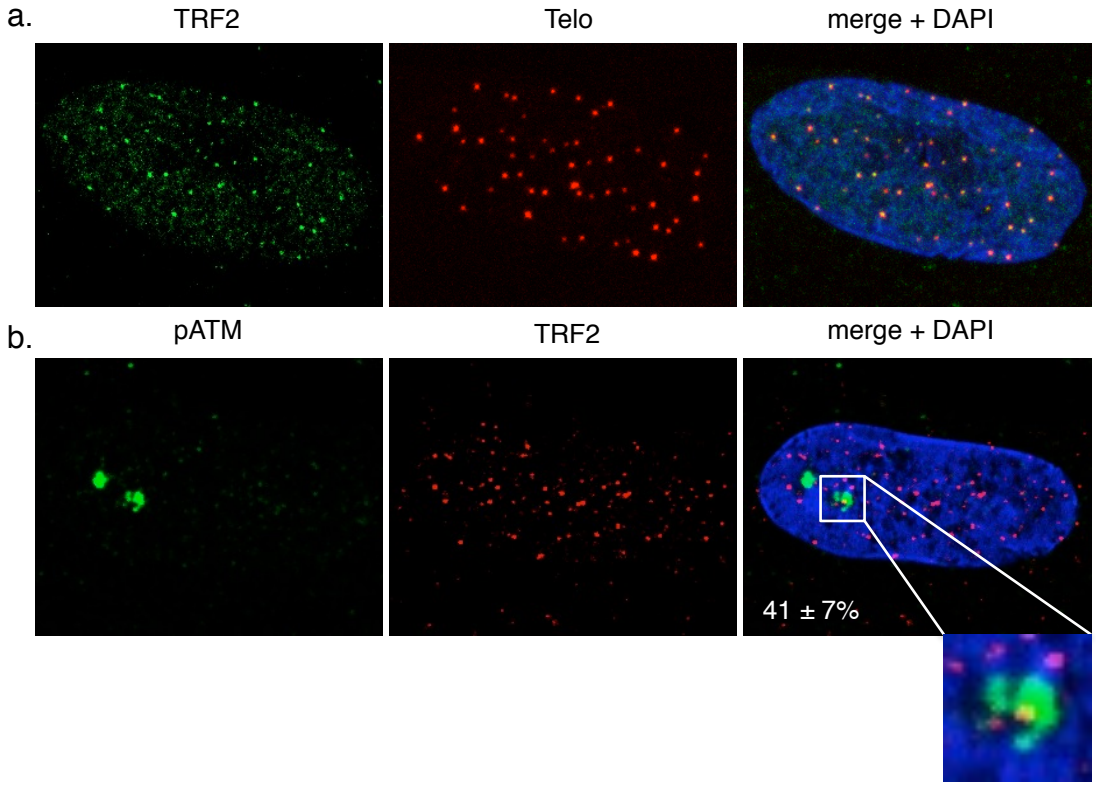

Figure 23. TRF2 and DDR foci co-localization analysis with telomeric DNA in IrrSen cells.

Maximum projections of Z-stacks acquired by confocal microscopy show co-localizations between TRF2 and telomeres, detected using a telomeric PNA probe (Telo) (**a**) and TRF2 and ATM pS1981 foci (**b**) in IrrSen BJ hTERT cells. The percentage of co-localization (± s.e.m.) is indicated.

In conclusion, these results strongly indicate that IR-induced senescence and persistent DDR at the telomeres are not due to TRF2 loss.

4.2.3 Ectopic TRF2 localization to a non-telomeric DNA double-strand break is sufficient to induce a more prolonged DNA damage response in mouse cells

Irreparability of telomeric DNA damage could be a feature of telomeric DNA *per se* or could be mediated by the proteins that bind to it. Among the telomere-binding proteins TRF2 is a very good candidate for repair inhibition. Indeed it has been previously shown to prevent chromosomal fusions *in vivo* (van Steensel et al., 1998) and to inhibit NHEJ *in vitro* (Bae and Baumann, 2007; Bombarde et al., 2010). To address this issue I took advantage of a published cellular system, NIH 2/4 cells (Fig. 24a and (Soutoglou et al., 2007)).

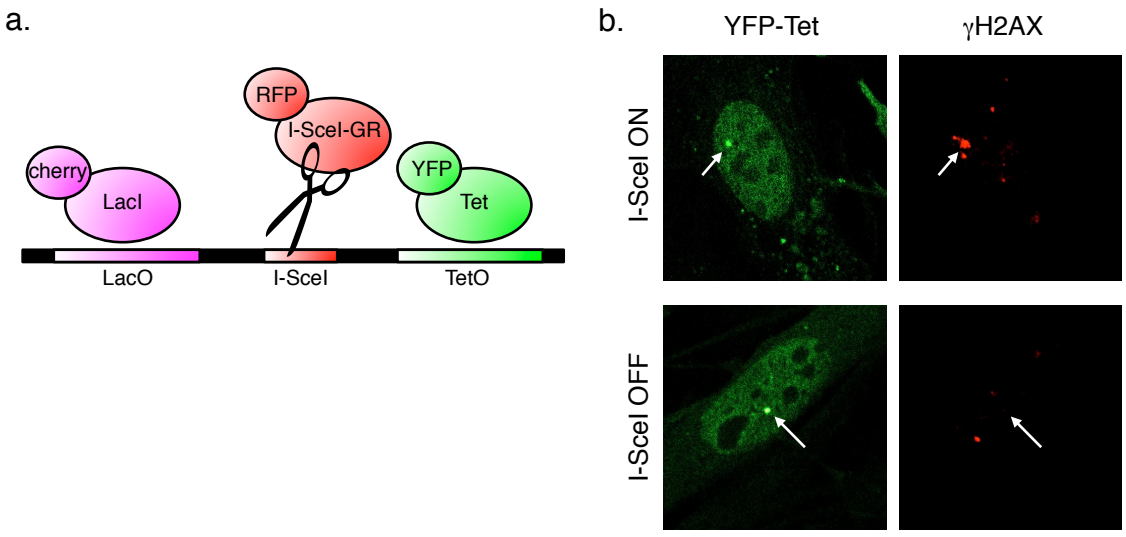

Figure 24. I-SceI endonuclease can be activated and inactivated in a cellular system.

(**a**) Schematic of the integrated locus studied in NIH 2/4 cells. Upon transfection, Cherry-LacI binds to the lactose operator (LacO) repeats, YFP-Tet binds to the tetracycline operator (TetO) repeats, and RFP-I-SceI-GR cuts the specific site between the two sets of repeats. (**b**) Representative images of γH2AX immunostaining and YFP-Tet signal, acquired by confocal imaging. I-SceI ON corresponds to 3 hours after RFP-I-SceI-GR induction with triamcinolone acetonide (10 pM), I-SceI OFF corresponds to 24 additional hours after removal of inducing agent.

They are immortalized mouse fibroblasts, carrying a single integrated cut site for the endonuclease I-SceI, flanked by lactose operator repeats on one side and by tetracycline operator repeats on the other. This locus could be visualized as a nuclear spot using the Cherry-LacI or the YFP-Tet proteins binding to the corresponding array. To validate this system I transiently transfected NIH 2/4 cells with an inducible version of I-SceI endonuclease, fused to the glucocorticoid receptor (GR), and YFP-Tet constructs. Upon addition of the GR ligand triamcinolone acetonide, I-SceI translocated to the nucleus, generating a DSB that could be detected by γH2AX focus co-localizing with the YFP-Tet signal (I-SceI ON). After removal of TA, I-SceI was again restricted to the cytoplasm, allowing the cells to repair the DSB (I-SceI OFF). This could be monitored by the disappearance of the γH2AX focus (Fig. 24b). I used the Cherry-LacI plasmid to generate the LacI construct, then I added a truncated TRF2 CDS, lacking its DNA binding domain, to generate the LacI-TRF2 construct. The two proteins were over-expressed upon transient transfection in NIH 2/4 cells (Fig. 25a) and importantly they both co-localized with YFP-Tet protein at the I-SceI site (Fig 25b).

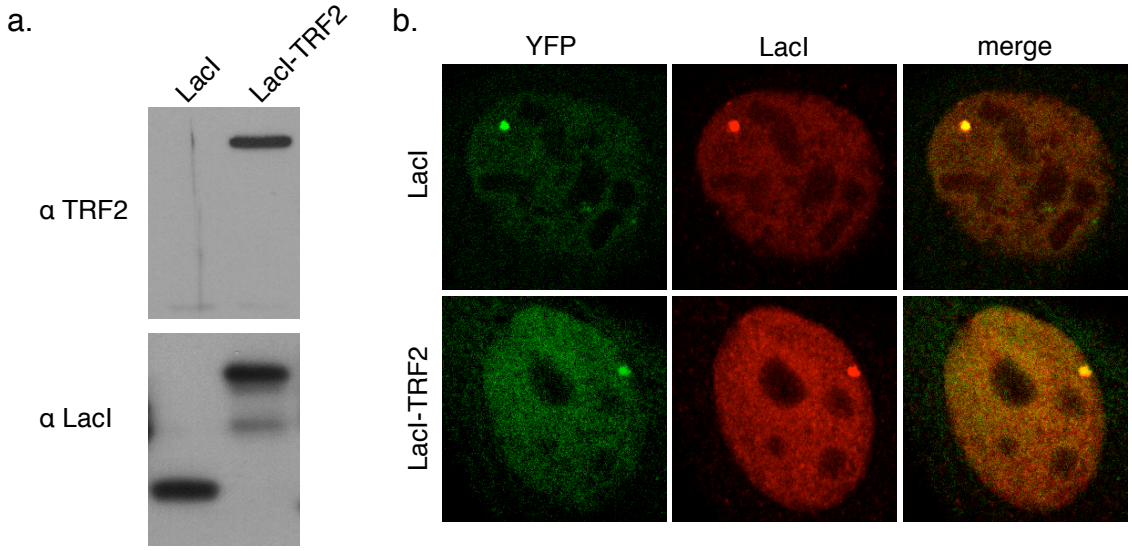

Figure 25. LacI and LacI-TRF2 proteins localization at the I-SceI locus.

NIH 2/4 cells were transfected with YFP-Tet and either LacI or LacI-TRF2 expressing plasmids. (**a**) Immunoblot with anti-LacI and TRF2 antibodies shows LacI and LacI-TRF2 over-expression. (**b**) Representative images of LacI immunostaining and YFP-Tet signal, acquired with confocal microscope.

The expression of LacI-TRF2 enabled the accumulation of TRF2 next to an exposed non-telomeric DNA end, which resembled a telomere bearing telomeric proteins but lacking telomeric DNA. After I-SceI activation a local DDR was triggered, as shown by γH2AX focus formation co-localizing with YFP-Tet signal. Following I-SceI inactivation, in cells expressing LacI alone, the percentage of DDR-positive cells at the locus studied was significantly reduced from 65% to 22%. Differently, in LacI-TRF2-expressing cells, DDR focus persisted in a significantly larger fraction of cells when compared with the LacI control (40% *vs* 22%, respectively; Fig. 26). This strongly suggested that TRF2 is sufficient to induce a more protracted DDR at a non-telomeric DSB.

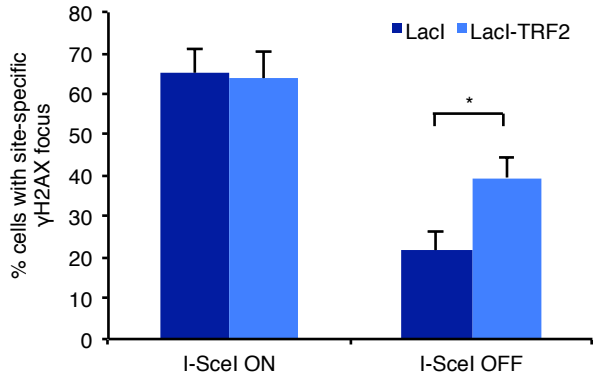

Figure 26. Ectopic TRF2 modulates DDR focus persistence at a non-telomeric DSB.

NIH 2/4 cells were transfected with RFP-I-SceI-GR, YFP-Tet and either LacI or LacI-TRF2 expressing plasmids. Quantification of cells positive for γH2AX at the I-SceI locus expressing LacI or LacI-TRF2, as detected by immunostaining and confocal microscopy. I-SceI site was detected as a distinct focus double-positive for YFP-Tet and anti-LacI antibody signals (* p value < 0.05, calculated by chi square test; for the quantification shown, around 100 cells per sample were analysed; n = 3 independent experiments; error bars represent s.e.m.).

After the generation of a DSB, a broken telomere should be coated by telomeric proteins, included TRF2, on both DNA ends. In order to better recapitulate the physiological conditions I cloned the truncated TRF2 CDS to the YFP-Tet plasmid, generating the YFP-Tet-TRF2 construct. Upon transient transfection in NIH 2/4 cells, the fusion protein was

over-expressed (Fig. 27a) and co-localized with the anti-LacI signal at the I-SceI site (Fig 27b).

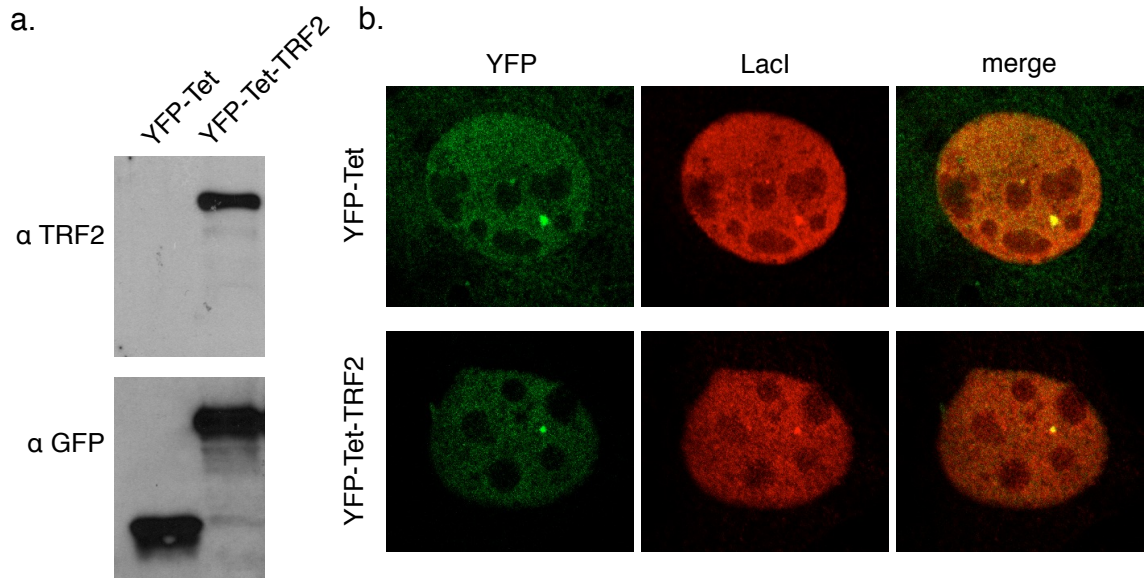

Figure 27. YFP-Tet-TRF2 protein localization at the I-SceI locus.

NIH 2/4 cells were transfected with LacI and either YFP-Tet or YFP-Tet-TRF2 expressing plasmids. (**a**) Immunoblot with anti-GFP and TRF2 antibodies shows YFP-Tet and YFP-Tet-TRF2 over-expression. (**b**) Representative images of LacI immunostaining and YFP signal, acquired with confocal microscope.

Unexpectedly, after I-SceI cut, the targeting of TRF2 at both DNA ends reduced the fraction of DDR-positive cells, compared to control cells. Nonetheless, 24 hours after I-SceI inactivation, TRF2 over-expressing cells retained the DDR focus in a higher fraction (Fig. 28). I could speculate that the presence of TRF2 at both sides of the I-SceI locus interfered with the I-SceI cut, because of steric hindrance, slowing down the cut kinetics. At later time points (I-SceI OFF), this effect was no more evident, leading to the expected more protracted DDR activation mediated by TRF2. The transient nature of the experiment did not allow me to further extend the studied time points, so I decided to target TRF2 to only one side of the DSB for the following experiments. Indeed in *in vitro* experiments it has been shown that the telomeric repeats inhibit NHEJ only in 5' to 3' direction (Bae and Baumann, 2007), making unnecessary the coating of both ends with TRF2.

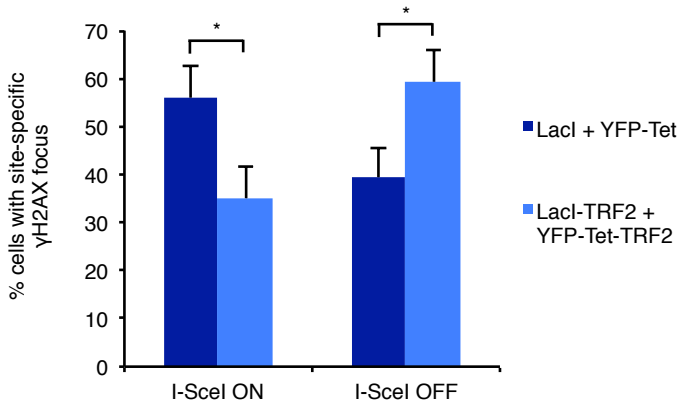

Figure 28. Ectopic TRF2 localization on both sides of DSB is inducing a more persistent DDR activation.

NIH 2/4 cells were transfected with RFP-I-SceI-GR, LacI and either YFP-Tet or YFP-Tet-TRF2 expressing plasmids. Quantification of cells positive for γH2AX at the I-SceI locus, as detected by immunostaining and confocal microscopy. I-SceI site was detected as a distinct focus double-positive for YFP and anti-LacI antibody signals (* p value < 0.05, calculated by chi square test; for the quantification shown, around 50 cells per sample were analysed; n = 2 independent experiments; error bars represent s.e.m.).

4.2.4 DDR focus persistence mediated by TRF2 is specific and it acts in cis only

The LacI protein is smaller than the fusion product LacI-TRF2 (39 kDa *vs* 84 kDa), thus one possibility is that TRF2 is inhibiting the repair activity of the cell by steric hindrance.

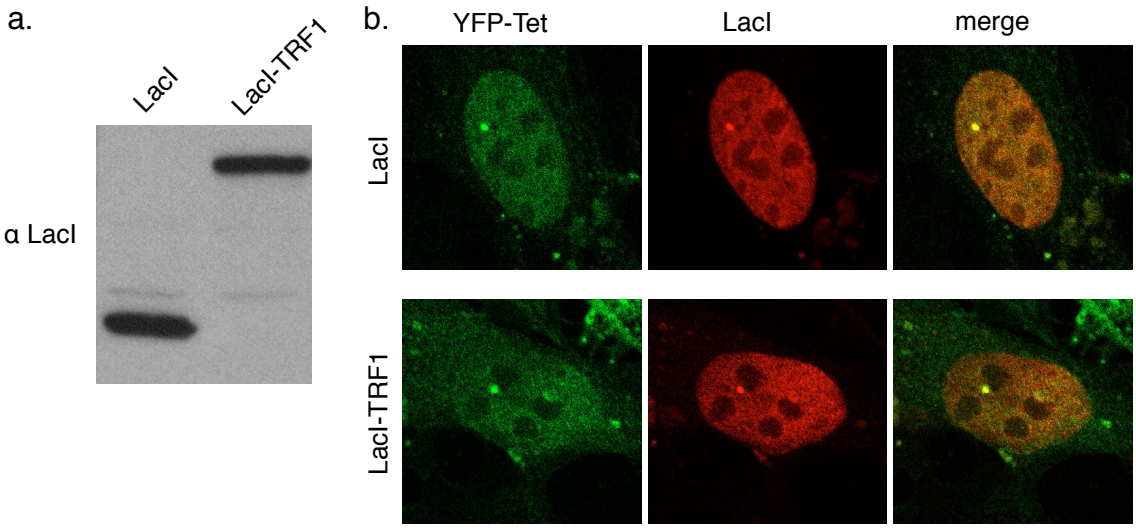

Figure 29. LacI-TRF1 protein localization at the I-SceI locus.

NIH 2/4 cells were transfected with YFP-Tet and either LacI or LacI-TRF1 expressing plasmids. (**a**) Immunoblot with anti-LacI antibody shows LacI and LacI-TRF1 over-expression. (**b**) Representative images of LacI immunostaining and YFP signal, acquired with confocal microscope.

To exclude this I repeated the experiment using different constructs, the LacI fused to Cyan Fluorescent Protein (Soutoglou et al., 2007) (CFP-LacI, 66 kDa) or to another telomere binding protein, TRF1 (LacI-TRF1, 84 kDa). I generated this fusion protein using the LacI construct and the truncated TRF1 CDS, lacking its DNA binding domain, and I checked the expression and the localization to I-SceI site of the LacI-TRF1 protein in NIH 2/4 cells (Fig. 29).

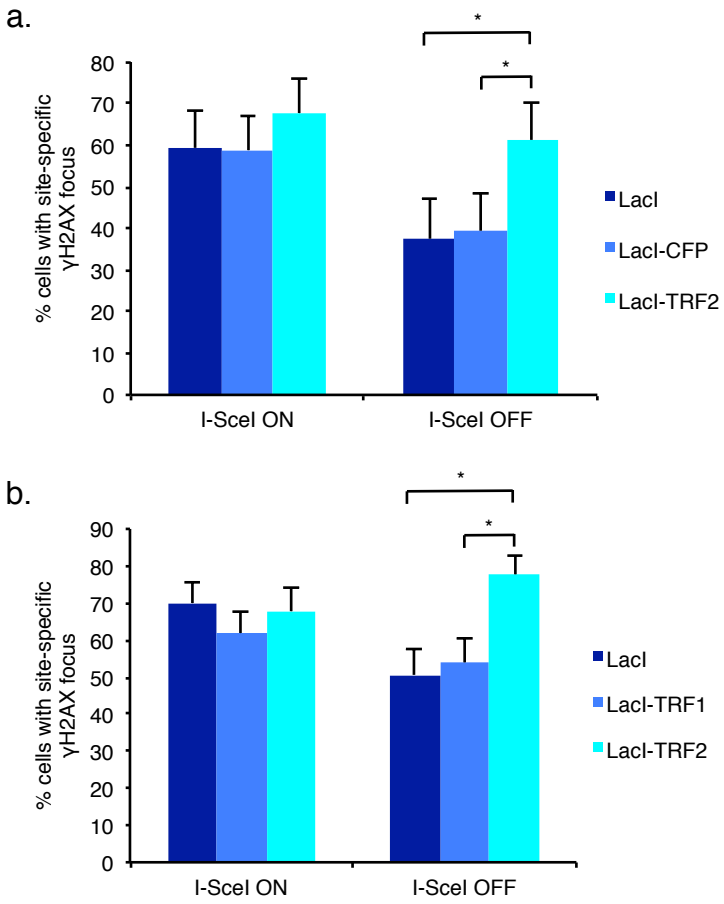

Figure 30. TRF2 effect on I-SceI site is specific and not due to steric hindrance.

NIH 2/4 cells were transfected with RFP-I-SceI-GP, YFP-Tet and either LacI, LacI-CFP, LacI-TRF1 or LacI-TRF2 expressing plasmids. (**a**) Quantification of cells positive for γH2AX at the I-SceI locus expressing LacI, LacI-CFP or LacI-TRF2, as detected by immunofluorescence and confocal microscopy. (* p value < 0.05, calculated by chi square test; for the quantification shown, around 30 cells per sample from 1 experiment were analysed; error bars represent s.e.m.). (**b**) Quantification of cells positive for γH2AX at the I-SceI locus expressing LacI, LacI-TRF1 or LacI-TRF2, as detected by immunofluorescence and confocal microscopy. (* p value < 0.05, calculated by chi square test; for the quantification shown, around 60 cells per sample were analyzed; n = 2 independent experiments; error bars represent s.e.m.).

Then I studied the DDR focus formation and disappearance in cells expressing either LacI, LacI-CFP, LacI-TRF1 or LacI-TRF2 proteins. Again, the presence of TRF2 induced a more persistent γH2AX focus compared to all the other controls (Fig. 30), suggesting that its action is specific and not due to steric hindrance. Furthermore, the ability to induce a more persistent DDR focus at a DSB site seems to be limited to the TRF2 protein only as TRF1, another component of the shelterin complex, did not behave differently from the LacI control. Next I investigated whether the increased persistency of the DDR focus at the I-SceI site was due to an impact of TRF2 over-expression on the global DDR activation of the cell.

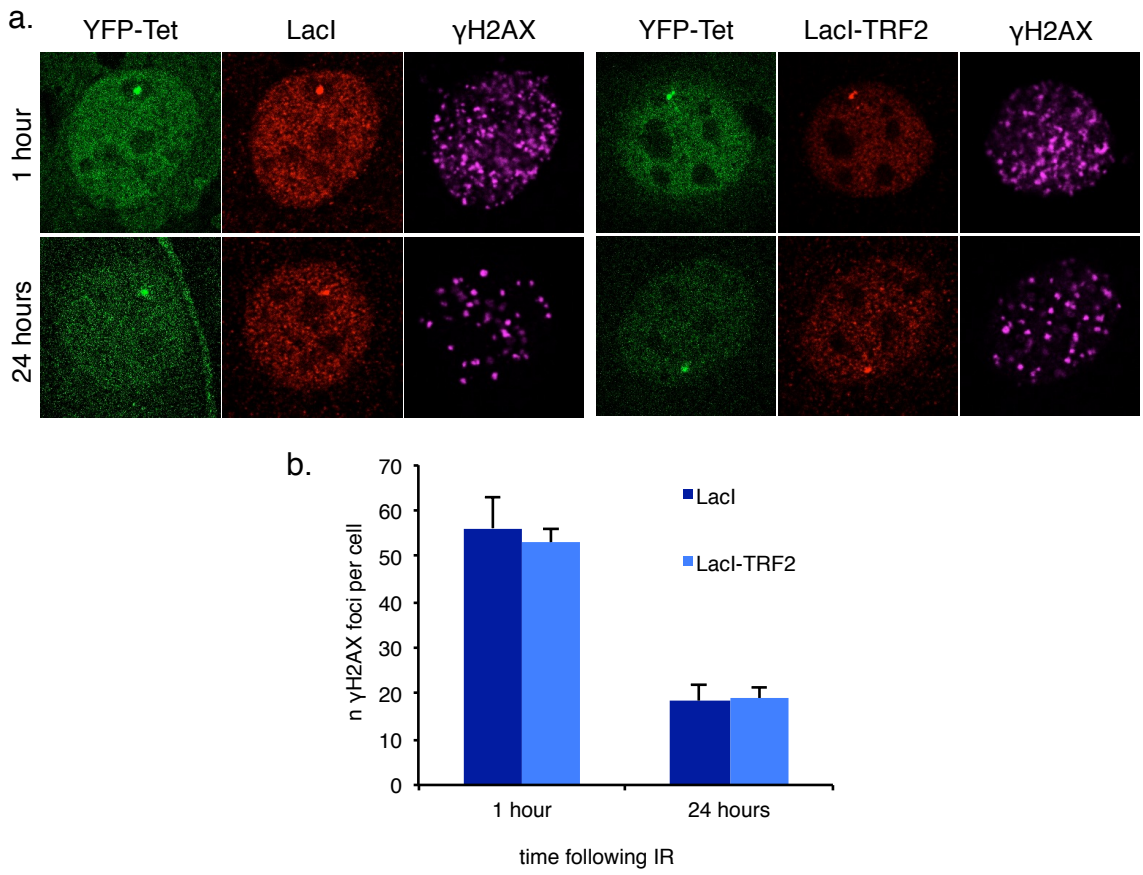

Figure 31. TRF2 acts in modulating DDR focus persistence only *in cis*.

NIH 2/4 cells were transfected with YFP-Tet and either LacI or LacI-TRF2 expressing plasmids, irradiated (2 Gy) 24 hours later and analysed at the indicated time points following irradiation. (**a**) Representative images of γH2AX and LacI immunostaining and YFP signal acquired by widefield microscopy at the indicated time points after irradiation. (**b**) Quantification of the number of γH2AX foci per cell. (For the quantification shown, around 30 cells per sample from 1 experiment were analysed; error bars represent s.e.m.).

Cells over-expressing LacI or LacI-TRF2 were irradiated to generate DNA damage randomly in the genome. The DDR foci resolution kinetics was not affected by TRF2 over-expression (Fig. 31), showing that TRF2 acts locally *in cis* only.

4.2.5 TRF2 inhibits physical double-strand break repair

The more persistent site-specific γH2AX focus induced by TRF2 indicates that the DDR machinery is switched off less efficiently, but it did not give any information about the repair of the DSB. To address this point, I adapted a protocol for BrdU staining under non-denaturing conditions to my experimental setup. This protocol was initially optimized for detection of single-stranded DNA during replicative stress (Ye et al., 2010). When I-SceI generated a site-specific DSB, as monitored by γH2AX focus formation, a co-localizing BrdU punctuated signal is detectable because of the exposed DNA ends. After I-SceI inactivation, the repair activity of the cell re-joined the two DNA ends, so the BrdU signal could not be detected anymore (Fig. 32a). In NIH 2/4 cells over-expressing LacI or LacI-TRF2, the generation and repair of physical DNA damage, monitored by BrdU signal, mirrors the DDR-focus formation, (Fig. 32b). This strongly suggests that TRF2 is sufficient to inhibit not only the DDR focus disappearance, but also the DNA repair of DSBs, providing a mechanism for irreparability of telomeric DNA damage. This result further supports the *in vivo* evidence in *Saccharomyces cerevisiae*, showing that Rap1, which directly bind telomeric DNA in budding yeast, is required for NHEJ inhibition at telomeres (Marcand et al., 2008).

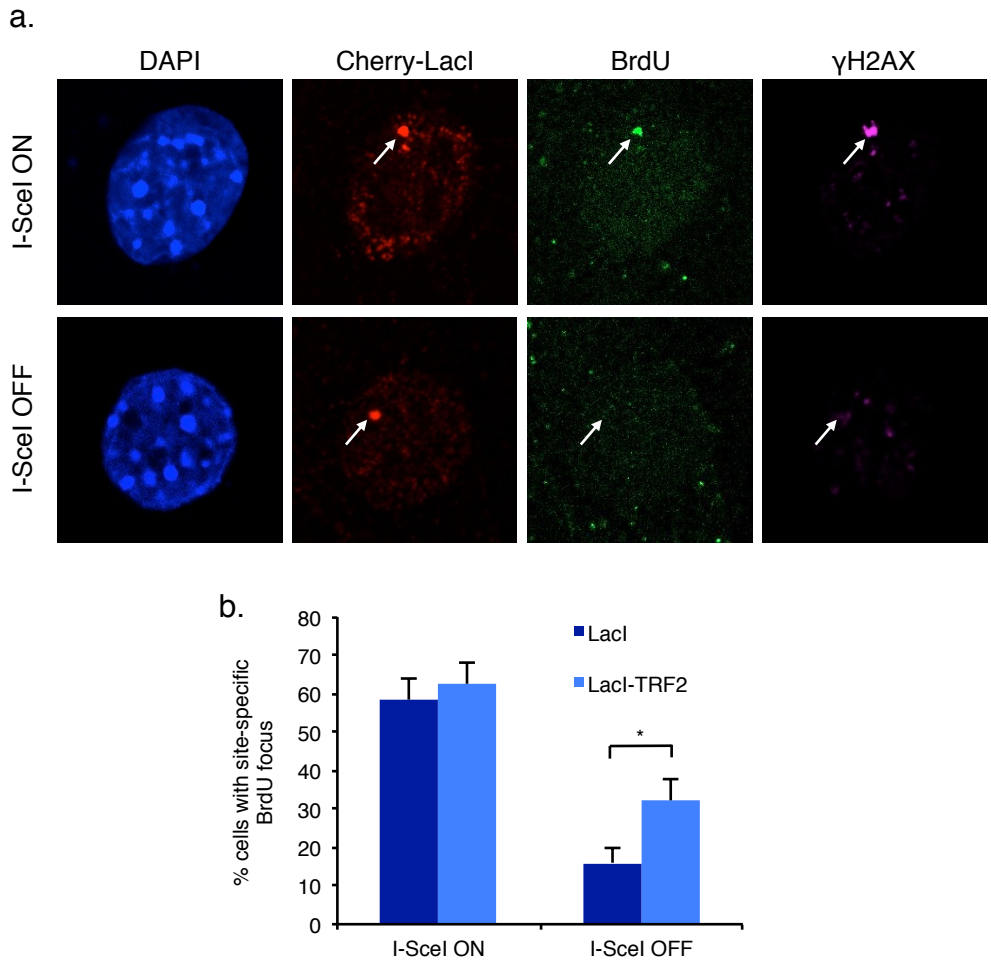

Figure 32. Ectopic TRF2 modulates DNA repair at a non-telomeric DSB.

NIH 2/4 cells were transfected with RFP-I-SceI-GP, YFP-Tet and either Cherry-LacI, LacI or LacI-TRF2 expressing plasmids and were incubated with BrdU (10μg/ml) for 16 hours. (**a**) Representative images of LacI, γH2AX and BrdU immunostaining under non-denaturing conditions, acquired by confocal microscopy. (**b**) Quantification of cells expressing LacI or LacI-TRF2 positive for BrdU signal at the I-SceI-locus, as detected by immunostaining and confocal microscopy. Values were normalized on the fraction of cells that had incorporated BrdU. (* p value < 0.05, calculated by chi square test; for the quantification shown, around 100 cells per sample were analysed; n = 2 independent experiments; error bars represent s.e.m.).

4.3 Persistent DNA damage accumulates at the telomeres, also in a non-proliferating tissue of aged primates

The results shown about the irreparability of telomeric DNA damage can be relevant also for the ageing field. Indeed it has been shown that ageing primates accumulate DDR foci co-localizing with telomeres *in vivo* (Herbig et al., 2006; Jeyapalan et al., 2007; Nijnik et al., 2007; Rossi et al., 2007). This observations have been made only in proliferating tissues such as dermal fibroblasts, stem cells and progenitors, so it was unclear whether such DDR was triggered solely by telomere shortening. I therefore decided to extend these observations studying the accumulation of endogenous DNA damage *in vivo*, in aged baboons. I analysed hippocampus, which is made of non-proliferating, terminally differentiated neurons, so they are not expected to undergo progressive telomere attrition. I performed a staining for the DDR marker 53BP1 of hippocampal samples from young and old baboons. I observed that a higher fraction of cells stained positive for 53BP1 in old samples compared to the young ones, confirming that also in non-proliferating tissues endogenous DNA damage could accumulate during ageing (Fig. 33).

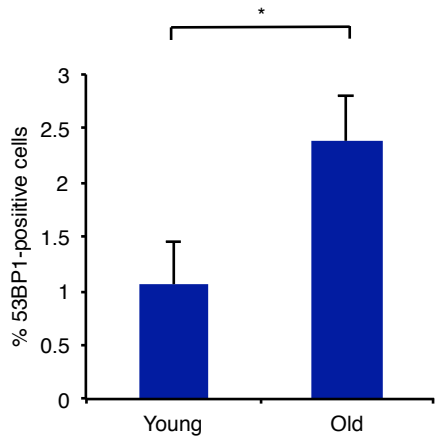

Figure 33. DDR activation in hippocampus of primates during ageing.

Quantification of 53BP1 foci-positive cells in hippocampal neurons of 4 old baboons, compared to 2 young ones (* p-value < 0.05, calculated by chi square test; error bars represent s.e.m.).

Then I also looked at the co-localization between 53BP1 foci and telomeres in the old baboons (Fig. 34a). The use of PNA probe in immunoFISH experiments generated discrete signals amenable for quantization, as the fluorescence intensity of the spots was directly correlated to the length of the telomeres. So I could plot the distribution of total telomeres accordingly to their length and compare it to the length of DDR-positive telomeres. 53BP1 foci did not co-localized preferentially with the critically short telomeres (Fig. 34b), consistently with the hypothesis that DNA damage is accumulating at the telomeres because they are irreparable and not because of their shortening.

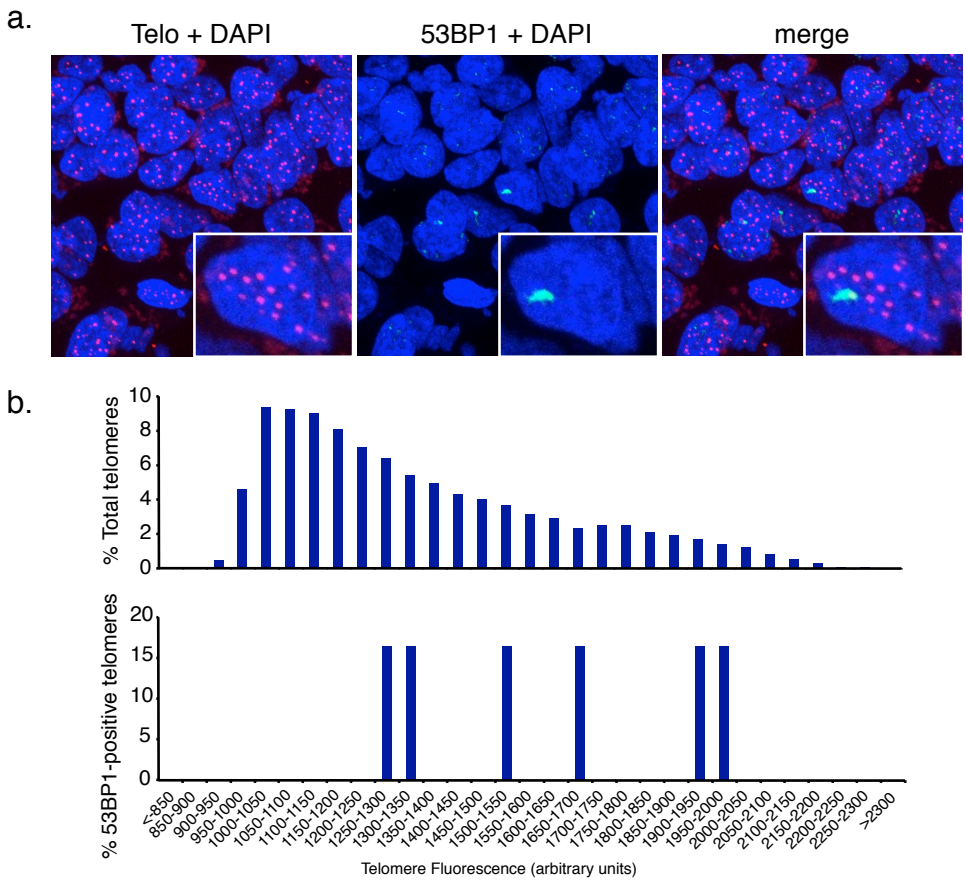

Figure 34. DDR-positive telomeres in hippocampus of aged primates are not the critically short telomeres.

(**a**) Maximum projections of Z-stacks acquired by confocal microscopy show 53BP1 foci and telomeres, detected using a telomeric PNA probe (Telo) in hippocampal neurons of aged baboons. (**b**) Relative distribution of total telomere lengths (upper histogram) and of 53BP1-focus-positive telomere lengths (lower histogram), according to telomeric probe signal intensity (Telomere Fluorescence Arbitrary Units) in hippocampal neurons from aged baboons. (Telomeres from 4 individual baboons were analysed).

4.4 DDRNA are necessary for DNA damage activation and maintenance at uncapped telomeres

4.4.1 Telomere induced foci are RNA-dependent

A report published by our group described an unexpected link between the DDR and components of the RNAi machinery. Indeed we characterized a new class of 21-22 nucleotides-long DICER and DROSHA RNA products in mammalian cells. These short RNAs (named DNA damage response RNAs or DDRNAs) have the sequence of the damaged locus and are necessary for DDR activation and maintenance specifically at that locus (Francia et al., 2012). Short RNAs with a similar biogenesis have been observed and tentatively implicated in DNA repair also in other model systems like *Arabidopsis Thaliana* (diRNAs (Wei et al., 2012)) and *Drosophila* (endo-siRNAs (Michalik et al., 2012)). Telomeres are the ends of linear chromosomes, but they are not recognized by the cellular DDR machine as DSBs because they are protected by the shelterin component TRF2 (de Lange, 2005). Removal of this protection makes the telomeres to be not distinguishable from normal DSBs and causes DDR activation specifically at the telomeres. This may lead to cellular senescence, chromosomal fusions and genome instability (Sfeir and de Lange, 2012). Since nothing was known about the role of DDRNAs at deprotected, DDR-positive telomeres, I decided to explore the potential role of DDRNAs at dysfunctional telomeres. For this purpose, I used CRE-ER TRF2$^{flox/flox}$ MEFs (Celli and de Lange, 2005). Cells were grown in presence of 4-hydroxytamoxifen for 48 hours to induce CRE recombinase localization into the nucleus, thus generating a TRF2-knockout (TRF2$^{-/-}$) cell line. TRF2 removal promptly induced telomere induced foci (TIFs) (Fig. 35 and (Celli and de Lange, 2005)).

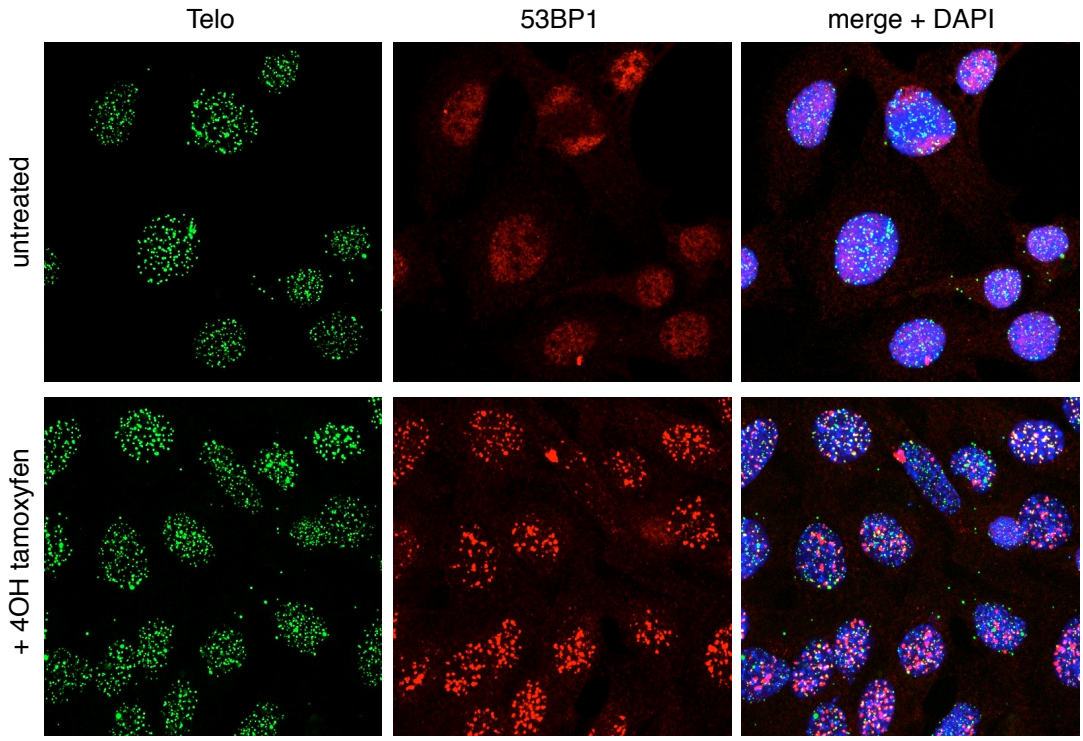

Figure 35. TRF2$^{-/-}$ MEFs show DDR activation at telomeres.

MEFs CRE-ER TRF2$^{flox/flox}$ cells were treated with 4-hydroxytamoxifen (0.6 μM) for 48 hours to induce TRF2 knock out. Representative images, acquired by confocal microscope, show co-localization of 53BP1 and telomeres, detected using a telomeric PNA probe (Telo).

I then permeabilized living MEFs TRF2$^{-/-}$ with a mild detergent and treated them with RNase A or BSA as a control. Consistent with our previous results (Francia et al., 2012), I observed that γH2AX foci were not affected, while 53BP1 foci were sensitive to RNase A treatment (Fig. 36). Thus, like other DSB lesions, also at uncapped telomeres RNA is necessary for the maintenance of 53BP1 foci. Next, I tested whether DDR foci could be allowed to reform in RNase A-treated cells by adding back RNA. For this purpose I extracted total cellular RNA using a specific kit in order to retain also short RNAs. Telomere-uncapped cells were treated with RNase A, and incubated in the presence of α-amanitin, an inhibitor of RNA Polymerase II, to block transcription, which would allow spontaneous transcription and focus reformation (Francia et al., 2012). I added RNA coming from TRF2$^{-/-}$ MEFs, and yeast tRNA as a control. Interestingly, only cellular RNA

coming from damaged cells could partially rescue 53BP1 foci after RNase A treatment (Fig. 37).

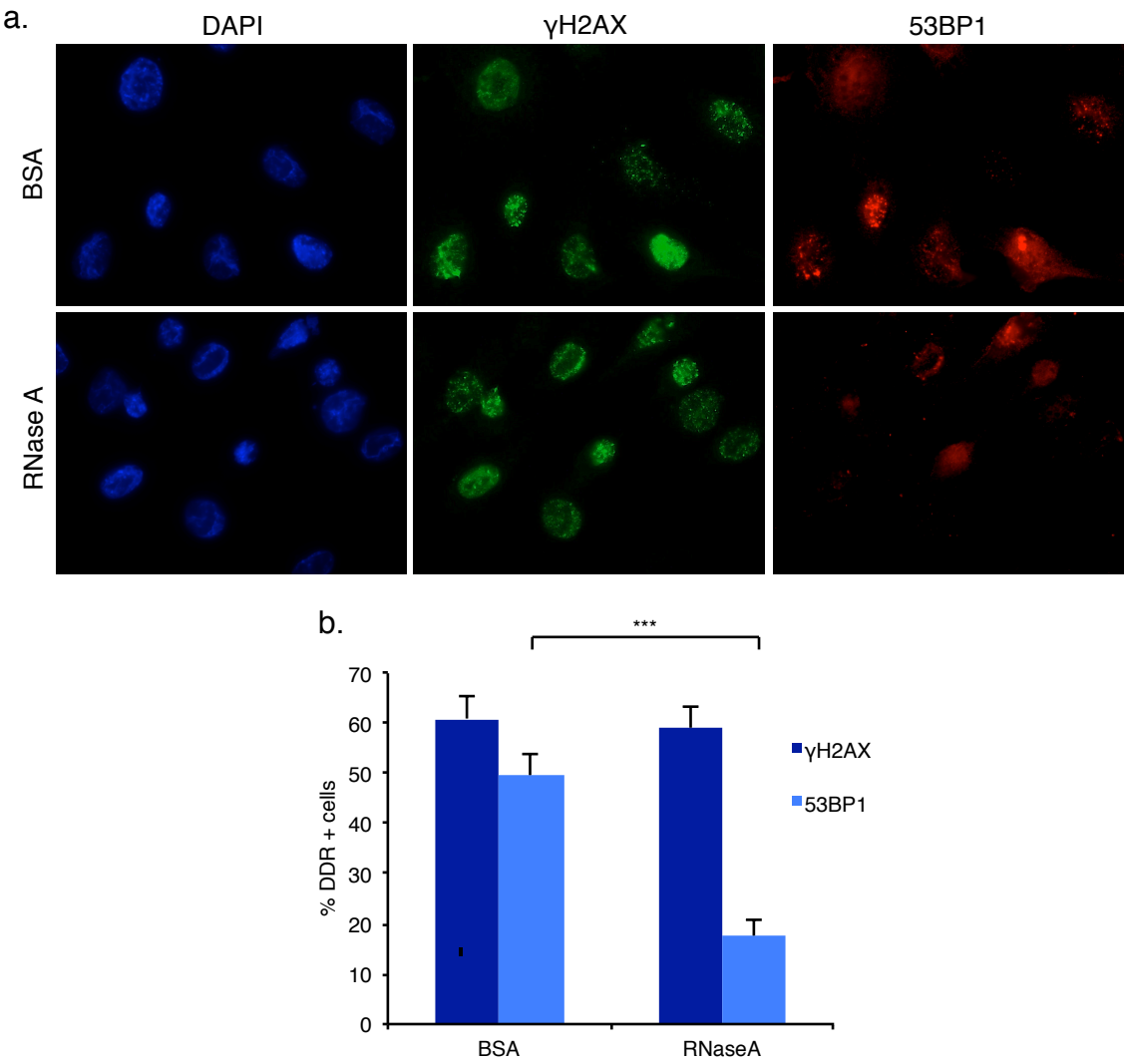

Figure 36. RNase A treatment impairs 53BP1 localization at uncapped telomeres.

TRF2$^{-/-}$ MEFs cells were permeabilized and treated with BSA or RNase. (**a**) Representative images, acquired by widefield microscope, show that γH2AX foci are stable, while 53BP1 foci disassemble upon RNase A treatment. (**b**) Quantification of γH2AX and 53BP1 foci in RNase A and BSA treated cells. (*** p value < 0.001, calculated by chi square test; for the quantification shown, around 150 cells per sample were analysed; n = 2 independent experiments; error bars represent s.e.m.).

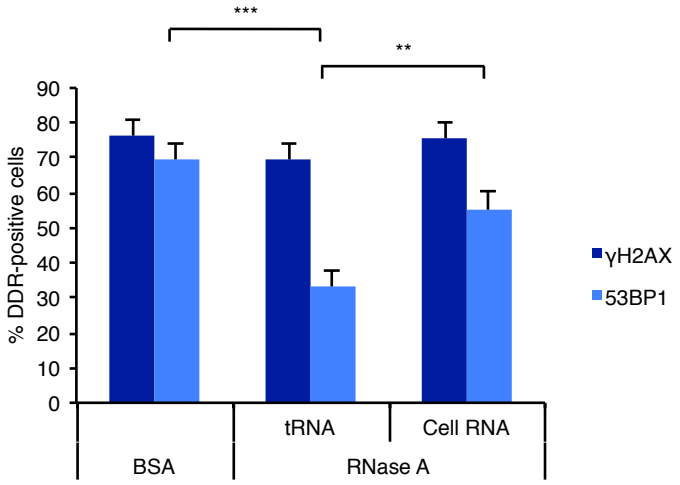

Figure 37. Total cellular RNA can rescue DDR foci at telomeres in RNase A treated cells.

TRF2$^{-/-}$ MEFs cells were permeabilized and treated with BSA or RNase A. RNase A treated cells were incubated with yeast tRNA and RNA coming from TRF2$^{-/-}$ MEFs, in the presence of α-amanitin. Bar graph shows the quantification of γH2AX and 53BP1-positive cells. (** p value < 0.01, *** p value < 0.001, calculated by chi square test; for the quantification shown, around 150 cells per sample were analysed; n = 2 independent experiments; error bars represent s.e.m.)

4.4.2 Telomere induced foci are DICER and DROSHA-dependent

Next I investigated the role of DICER and DROSHA on DDR activation at dysfunctional telomeres. I transiently knocked down DICER or DROSHA in MEFs TRF2$^{-/-}$ (Fig. 38a) and looked at the TIFs formation. Consistent with the published results (Francia et al., 2012), γH2AX foci were not affected by DICER or DROSHA knock down (Fig. 38b,d). Differently from what observed in IR-induced DNA damage (Francia et al., 2012), also 53BP1 was not affected (Fig. 38b,d). However, this apparent inconsistency can be explained by the fact that 53BP1 needs DDRNAs for the localization at the DNA damage site only initially after the DNA damage generation, but it gets eventually recruited in a DDRNA-independent manner (Francia et al., 2012). Since the DNA damage at unprotected telomeres is not acute as studied by Francia et al, but persistent, at the time of the analysis, 53BP1 was expected to localize at the damaged loci.

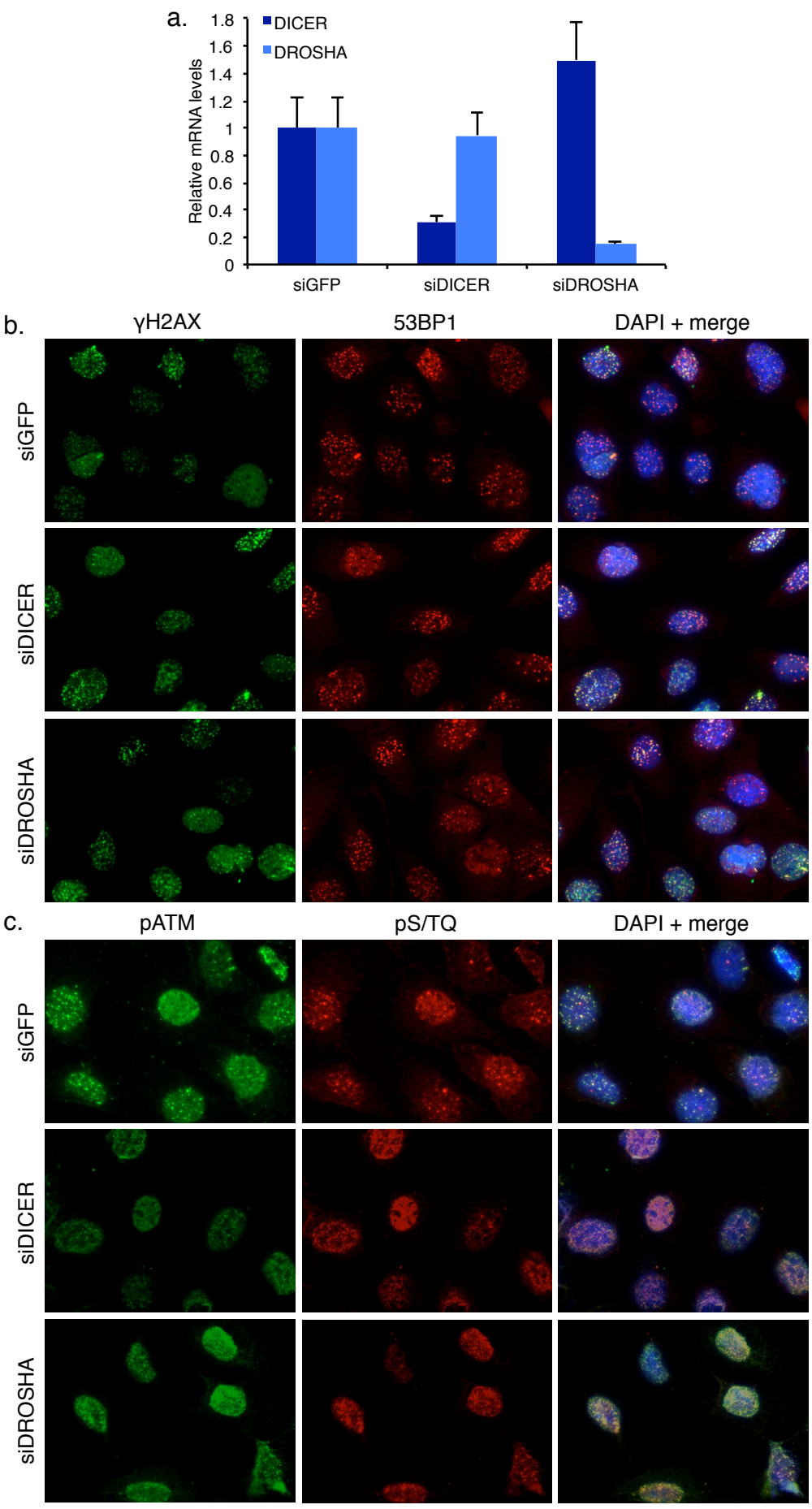
a.
DICER
DROSHA
Relative mRNA levels
1.8
1.6
1.4
1.2
1
0.8
0.6
0.4
0.2
0
siGFP
siDICER
siDROSHA
b.
γH2AX
53BP1
DAPI + merge
siGFP
siDICER
siDROSHA
c.
pATM
pS/TQ
DAPI + merge
siGFP
siDICER
siDROSHA

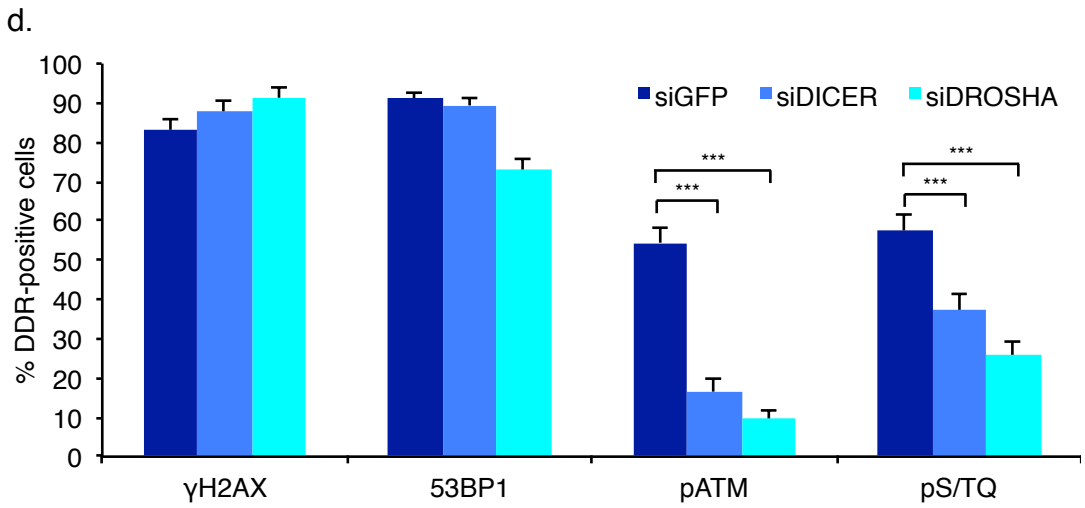

Figure 38. DICER and DROSHA knock down impairs DDR foci formation at uncapped telomeres.

TRF2$^{-/-}$ MEFs were transiently transfected with siDICER, siDROSHA or siGFP as a control. (**a**) Triplicate qPCR reactions with Sybr Green chemistry show the knock down levels of DICER and DROSHA. (**b-c**) Representative images of γH2AX, 53BP1, ATM pS1981, pS/TQ foci, acquired by widefield microscope. (**d**) Quantification of the fraction of DDR-positive cells. (** p value < 0.01, *** p value < 0.001 calculated by chi square test; for the quantification shown, around 150 cells per sample were analysed; n = 2 independent experiments; error bars represent s.e.m.).

Then I extended this observation to other DDR markers; in particular I studied foci containing ATM pS1981, and proteins phosphorylated by ATM or ATR (pS/TQ). While discrete foci were detected in the control cells, upon DICER and DHOSHA knock down, DDR focal signals were reduced or became diffused in the nucleus (Fig. 38c,d). Thus, differently from γH2AX and 53BP1, the recruitment to the unprotected telomeres of ATM and its downstream targets needs DICER and DROSHA.

4.4.3 Chromosomal fusions in TRF2-deficient cells are DICER and DROSHA-dependent

In *Arabidopsis thaliana* diRNAs are necessary for efficient repair by HR (Wei et al., 2012). Chromosomal fusions are repair events mediated mainly by NHEJ (Sfeir and de Lange, 2012) so I asked whether DDRNAs have a role also in this repair pathway. I transiently knocked down DICER or DROSHA in MEFs TRF2$^{-/-}$ cells and analyzed metaphase spreads after colcemid block. Control cells showed massive chromosomal

fusions, as already shown in (Celli and de Lange, 2005). In contrast, both DICER and DROSHA knocked down cells showed a lower degree of fusions (Fig. 39), indicating that DICER and DROSHA are involved also in NHEJ pathway.

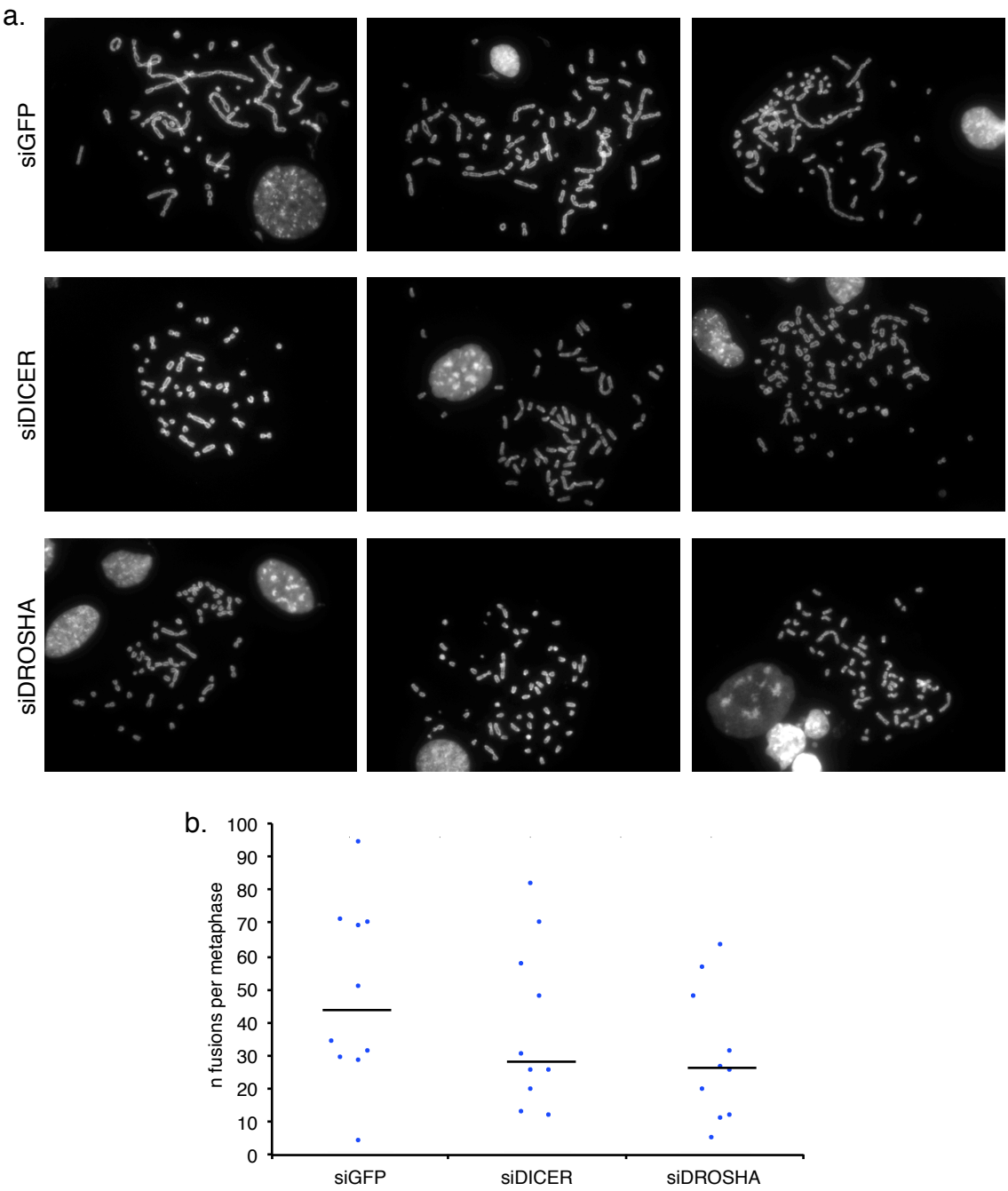

Figure 39. DICER and DROSHA knock down impairs chromosomal fusions.

TRF2$^{-/-}$ MEFs were transiently transfected with siDICER, siDROSHA or siGFP as a control. (**a**) Representative images of metaphase spreads acquired by widefield microscope. (**b**) Dot plot shows the number of fused chromosomes per metaphase spread, solid line indicate the median value. (For the quantification shown, 10 metaphase spreads for each condition from 1 experiment were analysed).

4.4.4 Inhibition of DDRNAs function can revert the senescence phenotype

Cells can accumulate damaged telomeres during ageing, due to telomeric shortening (d'Adda di Fagagna et al., 2003; Harley et al., 1990; Herbig et al., 2004) or to endogenous or exogenous DNA damage occurred at telomeres because they are not repairable (see chapter 4.3). In both cases this persistent DDR activation at telomeres leads to cellular senescence. Based on the preliminary results about the role of RNA, DICER and DROSHA in DDR foci formation and maintenance at dysfunctional telomeres, I hypothesized that DDRNAs with telomeric sequence are generated locally to sustain DDR. Inhibiting their action could suppress DDR activation at the telomeres and potentially prevent or revert the senescence phenotype. To test this, I used a human cell line, T19 fibrosarcoma cells that express an inducible dominant negative (DN) allele of FLAG-tagged TRF2 (van Steensel et al., 1998). The expression of this allele was induced culturing cells in the absence of doxycycline. After 7-8 days of induction, cells expressing the DN TRF2 allele stained positive for FLAG-tag and DNA damage response in the form of 53BP1 foci and they acquired a senescence phenotype (Fig. 40a and (van Steensel et al., 1998)). Most of these DDR foci co-localized with the telomeric PNA probe, indicating that they were caused by telomere uncapping (Fig. 40b and (van Steensel et al., 1998)). To reach a strong and specific inhibition of telomeric DDRNAs, I chose LNAs antisense oligonucleotides. They are modified ribonucleotides with an extra bridge connecting the 2' oxygen and 4' carbon of the sugar that confers higher stability and specificity to the molecule (Jepsen et al., 2004). LNAs have been already used to inhibit miRNAs also *in vivo* (Machlin et al., 2012; Naguibneva et al., 2006; Obad et al., 2011). I used two different LNA inhibitors, one containing few copies of the 5'-TTAGGG-3' repeat (Telo G) and one with the complementary sequence (Telo C), that should in principle bind and inhibit DDRNAs transcribed from the G- and C-rich telomeric strand, respectively. After induction of DN TRF2 expression, I transfected T19 cells with Telo G and Telo C LNA molecules and a control LNA with an unrelated sequence (Cntr).

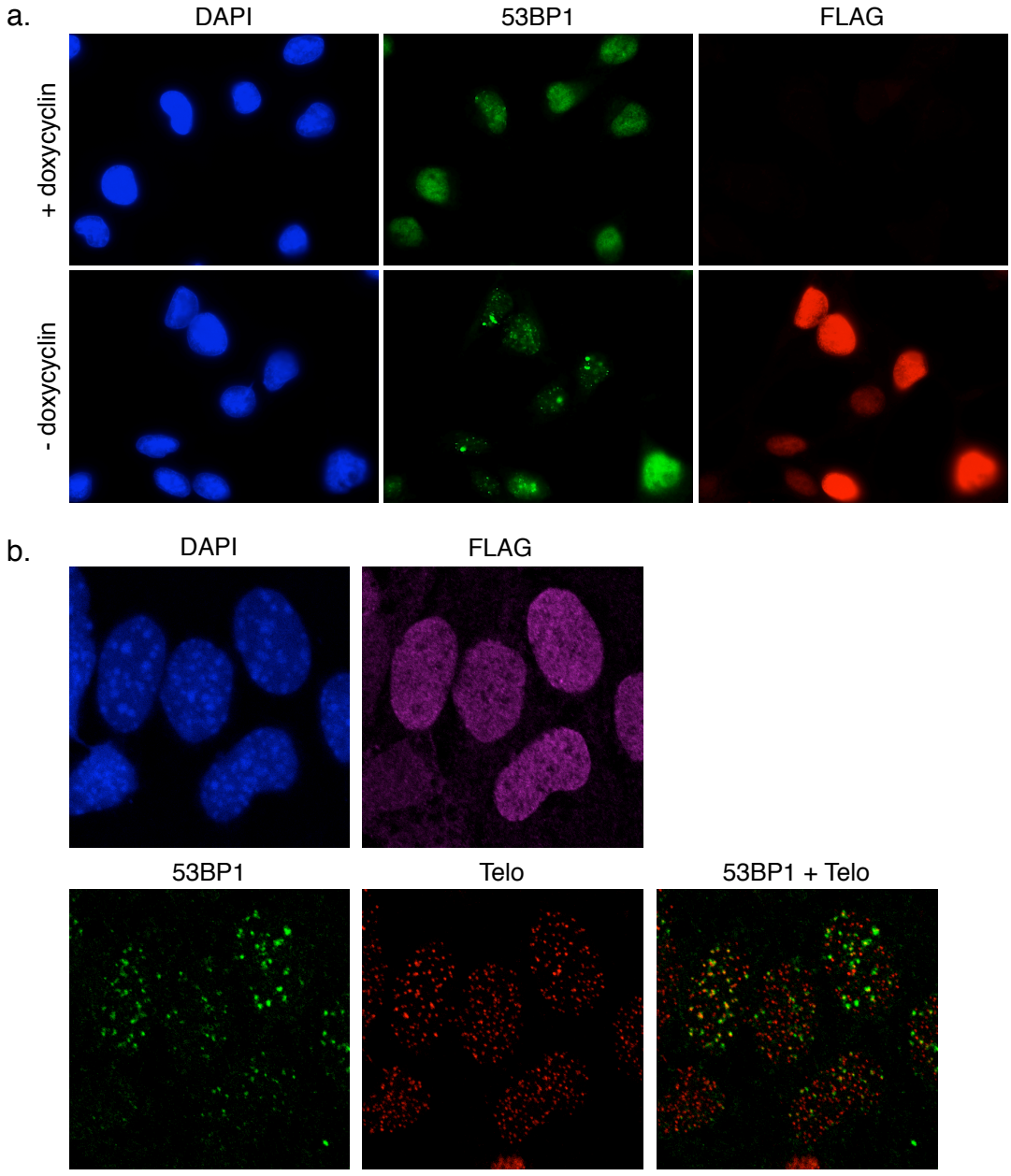

Figure 40. Dominant negative TRF2 expression induces DDR activation at telomeres in T19 cells.

The expression of a dominant negative allele of FLAG-tagged TRF2 was induced by removal of doxycycline from the culturing medium in T19 cells. (**a**) Representative images of FLAG and 53BP1 immunostaining acquired by widefield microscope. (**b**) Representative images of FLAG and 53BP1 immunostaining and telomere signal, detected using a telomeric PNA probe (Telo), acquired by confocal microscope.

I observed that, with time, in cells expressing DN TRF2 (FLAG +), both telomeric LNAs transfected individually decreased the percentage of 53BP1-positive cells, to a different extent, while control LNA had no effect (Fig. 41). Importantly, in non-induced, undamaged cells (FLAG -) LNA molecules did not induce any DNA damage, excluding

that they could be toxic *per se*. Since a constant DDR activation is necessary for senescence maintenance ((d'Adda di Fagagna et al., 2003; Herbig et al., 2004; Sedelnikova et al., 2004; von Zglinicki et al., 2005) and chapter 4.1.2)

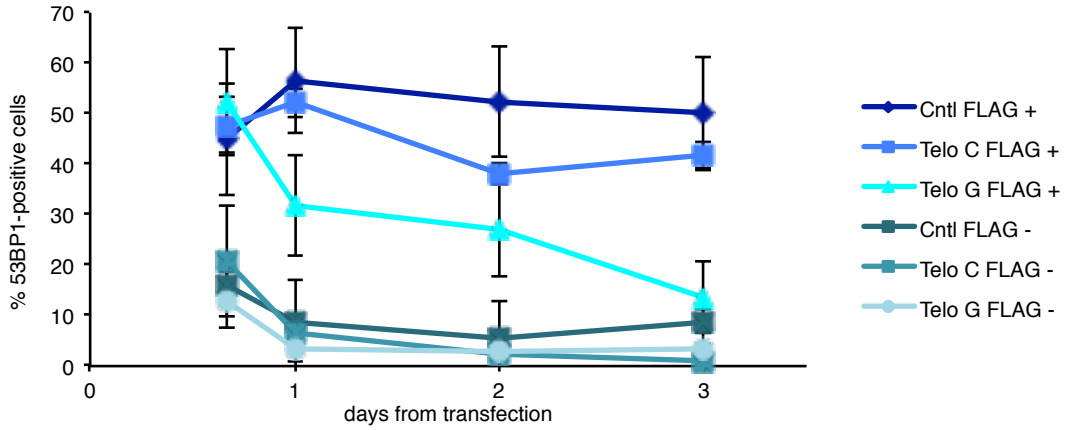

Figure 41. LNA transfection has an impact on DDR in telomere-uncapped cells.

T19 cells were induced by doxycyclin removal and transfected with LNA molecules (200 nM) matching the telomeric G- or C-rich strand (Telo G and C, respectively) and an unrelated control sequence (Cntl). 53BP1 foci-positive cells were scored at the indicated time points post transfection, in telomere-uncapped cells (FLAG +) or uninduced (FLAG -) cells. (For the quantifications shown, around 30-100 cells for each time point from 1 experiment were analysed; error bars represent s.e.m.).

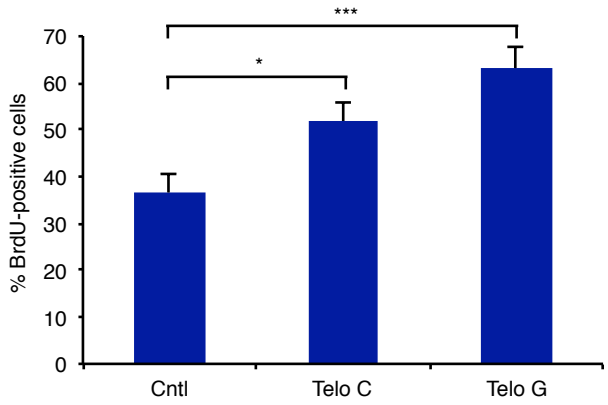

Figure 42. LNA transfection promotes cell cycle progression of senescent cells.

T19 cells were induced by doxycyclin removal and transfected with LNA molecules (200 nM) matching the telomeric G- or C-rich strand (Telo G and C, respectively) and an unrelated control sequence (Cntl). Bar graph shows BrdU incorporation rate after 16 hours of BrdU incubation. (* p value < 0.05, *** p value < 0.001, calculated by chi square test; for the quantification shown, around 150 cells per sample were analysed; n = 3 independent experiments; error bars represent s.e.m.).

I reasoned that inhibiting DDR activation with LNA molecules could be sufficient to prevent the proliferation arrest that occurs at senescence. I thus analyzed the passage through the S phase of cell cycle, by monitoring BrdU incorporation in induced T19 cells after LNA transfection. I observed that cells transfected with both telomeric LNAs, proliferated significantly more than control cells (Fig. 42), suggesting that LNA, by inactivating DDR at telomeres, can promote cell cycle re-entry.

5 Discussion

5.1 Persistent DDR activation at telomeres is the trigger for cellular senescence establishment and maintenance

5.1.1 IR-induced senescence is maintained by a persistent DDR

Replicative senescence is triggered and maintained by DDR, and impairment of DDR factors results in cell cycle re-entry and senescence escape (d'Adda di Fagagna et al., 2003; Herbig et al., 2004; Sedelnikova et al., 2004; von Zglinicki et al., 2005). This conclusion has been a matter of debate, because it has also been reported that activation of the DDR might represent an early and initial step in the process of cellular senescence activation, which is later on inactivated once senescence is fully established (Bakkenist et al., 2004; Chen and Ozanne, 2006). Additional unpublished data from our group show that DDR signalling in the form of nuclear foci are instead very stable in senescent cells and can be detected in two independent batches of senescent human skin fibroblasts, even 3 years after they had stopped proliferating. These fibroblasts have been previously demonstrated to undergo telomere-initiated cellular senescence (Mondello et al., 2003). This data suggest that, at least in some conditions, DDR can indefinitely be maintained. Furthermore, I showed that impairment of DDR cascade by ATM inhibition caused the escape from cell cycle arrest in IrrSen BJ hTERT cells (Figs. 6-8), indicating that senescence status is maintained by a constantly active DDR signalling. The differences observed might derive by a differential response to senescence establishment that can be cell type specific. Indeed, by irradiating in parallel BJ, WI-38 and IMR-90 human fibroblasts, I could observe a reduction of DDR foci with time in IMR-90 only (Fig. 10) but, importantly, this was also associated with considerable cell death (Fig. 11). One explanation could be that IMR-90 cells are more sensitive to standard cell culture conditions and are prone to die by culture shock due to oxidative stress or excessive mitogenic stimuli. Indeed, even in the absence of irradiation, a significant fraction of these cells died after one month in culture, and this effect was exacerbated upon DNA damage generation. However, further

experiments are needed to identify and characterize the mechanisms that explain the reduction of the cell number in a population of senescent cells.

Based on these observations, I can anticipate that, when senescence is a stable condition, it is normally associated with a permanent DDR signalling; if a senescent population is not stable and is characterized by cell death, then a decrease in the number of DDR-positive cells will be observed.

5.1.2 Quality, not quantity, distinguish persistent from transient DNA damage response

The dose of DNA damage used to induce cellular senescence may be considered higher than the levels organisms could normally experience all at once. It thus could be argued that the observed phenotype is the outcome of an artificial system, irrelevant for *in vivo* situations. Nevertheless, I observed a comparable amount of persistent DDR foci even fractionating the same dose over 10 days (Fig. 5), indicating that the observed effect is not ascribable to saturation of cellular DNA repair machinery that cannot cope with an acute relatively high amount of DNA damage. Consistently, persistent DDR foci were induced also by a lower dose of irradiation, although to a lower extent (Fig. 5). This model nicely fits with the hypothesis that DNA damage is randomly generated in the genome and the rupture of telomeric DNA, responsible for the focus persistency, is a stochastic event. Thus it is more likely to occur as the initial amount of DNA damage increases. Doing some simple calculations can be informative. I observed that, at the time of senescence establishment, around 5-8 foci were detectable per cell, and around 1 out of 3-4 of them were at telomeres (Fig 13). This means that, on average, each cell has 1.5-2 TIFs, so most of the cells had at least one TIF, which can trigger senescence. A lower amount of DNA damage would instead induce persistent DDR and senescence in a minor fraction of cells, while all the others that did not receive a telomeric DNA damage would keep proliferating and eventually take over the culture. Thus the need to use a relatively high level of IR to experimentally induce cellular senescence in the bulk population of cells is dictated by the chance to hit at least a telomere in each cell.

The number of persistent DDR foci observed in IrrSen cells is relatively low (Fig. 4), and quite similar to the number observed upon a low dose of irradiation. In addition, IrrSen cells retain the ability to repair additional DNA damage if exposed again to IR (Fumagalli et al., 2012). This suggests that, in the same cell, both transient and persistent DDR foci co-exist and the few persistent DDR foci have some peculiarity that distinguish them from all the other DSBs. The persistent DDR foci have many similarities with the transient ones. They share many components of the DDR machinery such as γH2AX, 53BP1, pATM, and pS/TQ. However, some differences in the downstream DDR signalling pathway can be conceived as possible, which may discriminate between promptly repaired lesions and those that will instead stimulate a more protracted DDR and therefore cellular senescence establishment. Indeed, I found that the downstream kinase CHK2, which is phosphorylated by ATM upon DSB generation, was detected at the persistent DNA damage sites in the form of discrete nuclear foci, differently from what is commonly observed at early time points after irradiation (Fig. 9 and (Lukas et al., 2003)). Thus, differently from repairable DNA damage that is promptly fixed, persistent DDR foci retain also some downstream factors, that normally diffuse into the nucleus. It has recently been shown that dysfunctional telomeres elicit a peculiar DDR, in which ATM is activated, but no ATM-dependent CHK2 phosphorylation at threonine 68 is detectable by immunoblot (Cesare et al., 2013). However, this technique may not be sensitive enough to detect local low accumulation of CHK2, visualized by immunofluorescence. My interpretation is that, upon telomeric DNA damage, ATM phosphorylates CHK2, but the DDR cascade is somehow interrupted at this level. CHK2 is thus retained at the DNA damage site and cannot be fully activated and thus spread the DDR signalling throughout the nucleus. It would be interesting studying the autophosphorylation site of CHK2 that has been shown to be necessary for its full activation following DNA damage (Wu and Chen, 2003).

5.1.3 Telomeric DNA damage triggers cell cycle arrest and cellular senescence

The observation that, with time, persistent DDR co-localize preferentially with telomeres both *in vitro* and *in vivo* (Figs. 13,14), and that a single DSB specifically generated within telomeric repeats induces a more persistent DDR activation (Fig. 16), strongly suggest that telomeres are genomic location that resist repair. This model is further supported by other published results from our group confirming DDR markers accumulation at subtelomeric regions by different approaches, such as ChIP-qPCR and ChIP-seq (Fumagalli et al., 2012). In addition, another group independently reached the same conclusions using a very similar experimental setup (Hewitt et al., 2012).

This model might seem in contrast with previously published works, where authors showed that, in *Saccaromices cerevisiae*, a telomeric DSB induces an anticheckpoint (Michelson et al., 2005; Ribeyre and Shore, 2012). One reason could be the difference in the model system used – yeast *vs* mammals. While in single-cell organism a damaged telomere could be tolerated as the only option for survival, in a complex multicellular organism, telomeric dysfunction can lead to genomic instability and cancer. Importantly however, these studies only focused on the G2/M checkpoint, showing that a damaged telomere do not promote arrest in G2/M, differently from a non-telomeric DSB (Michelson et al., 2005; Ribeyre and Shore, 2012). In most experiments that I performed, cells were arrested in G0 prior to DNA damage induction, and never re-entered the cell cycle upon release from contact inhibition, as monitored by a virtually absent BrdU incorporation, unless upon impairment of DDR activation (Fig. 7). The experimental evidence that I described suggests that a damaged telomere induces a G1/S checkpoint that impedes the cell cycle re-entry and induces a stable G1 senescence condition. This is consistent with a recent report showing that DDR-positive telomeres do not induce the G2/M checkpoint (Cesare et al., 2013). Despite DDR activation, cells progress through the cell cycle and arrest in a stable diploid G1 condition, when a p53-dependent cell cycle arrest is activated.

5.2 TRF2 as an inhibitor of DNA repair at telomeres

5.2.1 Persistent DDR at telomeres is mediated by the telomere-binding protein TRF2

The observed impaired or slower repair kinetics at the telomeres could in principle be explained by different mechanisms. Telomeres and subtelomeres show heterochromatic markers, like histones and DNA methylation (Blasco, 2007), making them potentially difficult to repair (Goodarzi et al., 2008). Nonetheless, neither global chromatin relaxation nor knock down of KAP-1, an important factor for repair in heterochromatin, have an impact on DDR foci persistency at telomeres (Figs. 17,18), indicating that the telomeric DNA *per se* may not be sufficient to explain the observed phenotype.

Shifting my attention from telomeric DNA to the telomere-binding proteins, I tested the role of TRF2 on DDR focus persistency. I ectopically targeted it to a non-telomeric DSB in order to exclude any potential impact of the telomeric DNA. The observed impaired DDR focus resolution in the presence of TRF2 (Fig. 26) strongly indicates that telomere irreparability is, at least in part, mediated by the proteins that bind to it, such as TRF2 and its associated factors. The observation that in IrrSen cells TRF2 was partially down regulated (Fig. 19) has two important implications. It is known that over-expression of TRF2 leads to a decrease in heterochromatin marks at telomeres (Benetti et al., 2008b), suggesting the idea that a down-regulation could have the opposite effect. The second scenario is based on the three-state model of telomeres proposed by Reddel and Karlseder's groups (Cesare et al., 2013; Cesare et al., 2009). According to this model, telomeres can be in three different conditions. In the presence of normal levels of TRF2, telomeres are in the closed or fully capped state, which protects telomeres from both DDR activation and chromosomal fusions. If TRF2 levels at telomeres decrease, because of experimental knock down or during replicative senescence, when telomeric DNA become shorter and can bind to a lower amount of proteins, telomeres are in the intermediate state, they can still resist repair, but activate the DDR. Finally, a complete TRF2 loss, such as the

one achieved by knock out of both alleles, leads to the uncapped state, when the telomere is also prone to fusions.

Based on the evidences reported above, the partial down-regulation of TRF2 in IrrSen cells can contribute to persistent DDR foci at telomeres through two independent mechanisms; by increasing heterochromatin, thus making telomeres harder to repair, or by promoting the intermediate state of telomeres, a structure that activate the DDR. Both these mechanisms however can be excluded, because TRF2 over-expression prior to DNA damage induction did not prevent the DDR foci accumulation at telomeres as well as senescence establishment (Figs. 20-22), revealing that TRF2 is acting in a different way.

5.2.2 TRF2 induces a persistent DDR activation at damaged telomeres while inhibiting DNA repair

Normally telomeres are not recognized as DSBs because TRF2 has been proposed to suppress DDR activation through ATM inhibition. Two possible models can be anticipated; the first one is a direct inhibition of ATM activation by TRF2. This hypothesis is based on the observation that TRF2 and ATM physically interact *in vivo*, and TRF2 over-expression reduces ATM phosphorylation and G2/M checkpoint upon IR (Karlseder et al., 2004). However, in this report, nothing was shown regarding the G1/S checkpoint, which is the one most likely activated in senescent cells. In addition, the effect on the DDR activation induced by irradiation can be explained by a differential role of TRF2 at non-telomeric DSBs. Indeed TRF2 has been reported to transiently localize to DSB sites (Bradshaw et al., 2005). The results that I have shown seem to exclude a direct local inhibition of DDR, since TRF2-coated non-telomeric DSBs elicited a more protracted γH2AX focus (Fig 26) and TRF2 over-expression did not significantly impair persistent DDR foci accumulation at telomeres and consequent senescence establishment (Fig. 20). More direct evidence is the high extent of recruitment of pATM at TRF2-positive telomeres in IrrSen cells (Fig. 23b), indicating that the presence of TRF2 is not impeding ATM activation at telomeres.

A possible explanation that can reconcile these only apparently opposite conclusions comes from experimental results showing that *in vitro* TRF2 can inhibit NHEJ repair only in 5' to 3' direction (Bae and Baumann, 2007). In addition *in vivo* evidences in budding yeast indicate that in the same DSB, Ligase 4 is recruited at the non-telomeric side, but not at the one bearing telomeric repeats (Fumagalli et al., 2012). Thus I can speculate that, upon the generation of a DSB within a telomere, the DDR signalling and repair factors recruitment are activated only on the distal DNA end. It follows that the telomere would result as DDR-positive because of the recruitment of DDR factors on one DNA end, yet it will resist repair because lack of a second available DNA end. Although enticing, this model is not easy to experimentally prove. Indeed, the concomitant targeting of TRF2 at both sides of a DSB in NIH 2/4 cells reduced the DDR activation initially upon break induction (Fig. 28), supporting the directionality model. However, after removal of the DNA damage agent and repair events, the presence of TRF2 on both DNA ends induced a more protracted DDR activation, similarly to that observed with only one TRF2-coated DNA end (compare Figs. 26 and 28).

The second model is based on the ability of TRF2 to maintain the t-loop structure of telomeres (Amiard et al., 2007; Griffith et al., 1999; Stansel et al., 2001), preventing detection of the DNA end by MRE11 and activation of ATM in an indirect manner. I can speculate that the proximal part of a broken telomere loses the t-loop protection and thus elicits a DNA damage response, but still retains TRF2, which is able to inhibit NHEJ. This situation is reminiscent of the intermediate state telomere already described (Cesare et al., 2013; Cesare et al., 2009) but it would be triggered by the loss of the t-loop structure rather than a decrease in TRF2 expression levels. This model is consistent with a recent report, elucidating the dual role of TRF2 in protecting telomeres (Okamoto et al., 2013). The lack of the TRFH dimerization domain of TRF2 induces DDR activation but no chromosomal fusions. This is due to the presence of a specific motif in the Hinge domain of TRF2, called inhibitor of DDR (iDDR) that inhibits the DDR cascade more downstream, at the level of

histone ubiquitylation by RNF8 and RNF168, thus impeding 53BP1 recruitment and NHEJ (Okamoto et al., 2013). Consistently RNF8 knock down has been shown to prevent chromosomal fusions in TRF2 depleted telomeres (Peuscher and Jacobs, 2011). Of note, the TRFH domain is involved in the t-loop formation (Amiard et al., 2007), supporting the model that the initial DDR activation is suppressed by the closed state, mediated by the TRFH domain of TRF2.

Both models can fit with the key observation that a more persistent DDR activation is the result of an impaired DNA repair mediated by TRF2 (Fig. 32). Consequently, although valid and supported by some experimental evidences, no formal proof at the moment can confirm either model and further experiments are needed to shed light on the mechanisms fuelling protracted DDR activation at damaged telomeres.

5.3 Irreparable DNA damage at telomeres: a unifying mechanism for cellular senescence and ageing?

5.3.1 Different types of cellular senescence are all triggered by telomeric DNA damage

Historically cellular senescence has been intrinsically linked to telomeres, since replicative senescence is triggered by telomeric shortening (Harley et al., 1990). More recently, a role of telomeres has been described also in OIS (Suram et al., 2012). Replicative stress induced by RAS activation, causes replication fork stalling and accumulation of DNA damage preferentially at telomeres that behave like fragile sites. This DDR activation can be prevented by telomerase activity, and this leads to the escape from cell cycle arrest. Finally the experimental results presented here reveal that also exogenous sources of DNA damage, like IR, induce cellular senescence through persistent DDR activation at telomeres, which is not due to their shortening.

Taken together, all these suggestions place again telomeres in a central role for the study of cellular senescence, and it is possible to propose that, independently from the stimulus (telomere shortening, oncogene-induced replication stress, exogenous DNA damage), the constantly activated DDR that causes and sustains the senescence status is due to telomere irreparability.

The existence of genomic regions that avoid repair is very dangerous for cell survival. However, inter-chromosome repair of telomeres would lead to fusions and consequent dicentric chromosomes that would trigger genomic instability and cancer initiation, thus in this particular loci, resisting DNA repair appears to be necessary. Taken together, these considerations indicate that, independently from the initial trigger, telomere irreparability and the resulting senescent establishment are an unavoidable drawback for protecting the end of linear chromosomes.

5.3.2 Ageing as a result of irreparable DNA damage at telomeres

In the past years, many studies revealed that ageing is associated with DNA damage accumulation in a plethora of tissues in mice, baboons and humans (Dimri et al., 1995; Herbig et al., 2006; Jeyapalan et al., 2007; Nijnik et al., 2007; Rossi et al., 2007; Rube et al., 2011; Sedelnikova et al., 2004; Wang et al., 2009). In some cases this has been associated with dysfunctional telomeres (Herbig et al., 2006; Jeyapalan et al., 2007), but this is commonly interpreted as the outcome of telomere shortening. This conclusion is based on the fact that this phenotype has been observed in proliferating tissues and that telomere shortening *in vivo* is associated with impairment of stem cells and some features of ageing like hair greying, alopecia, defect in wound healing, as well as a reduction in the life span (Rudolph et al., 1999; Tumpel and Rudolph, 2012).

Of note, I have showed that in post mitotic cells, like hippocampal neurons, DDR foci that accumulated with age in primates were not associated with the shortest telomeres (Figs. 33,34). A similar result was reproduced also in liver, another non-proliferating compartment (Fumagalli et al., 2012), suggesting that telomeric shortening is not the only trigger for DDR accumulation *in vivo*.

These data provide a mechanism for DDR- and senescence-mediated ageing of non-proliferating tissues, which could not be explained solely by telomeric shortening. Accordingly to the model of irreparable DNA damage, during ageing telomere would accumulate persistent DDR markers following exposure to various sources of DNA damage, both endogenous (telomere shortening, ROS, replication stress, oncogene activation) or exogenous (UV, X-Rays), thus promoting cellular senescence and, at the organismal level, the ageing phenotype. Indeed, the DNA damage accumulated in post-mitotic neurons *in vivo* in mice has been shown to promote a senescence-like state, as monitored by SA-β-gal positivity, heterochromatinization and high ROS and IL-6 production (Jurk et al., 2012). In addition mitochondrial oxidative stress, can induce senescence and ageing in the epidermis (Velarde et al., 2012).

In turn deletion of p21, a p53 target in senescent cells, in telomerase-deficient mice rescues the maintenance of hematopoietic cells and intestinal epithelium (Choudhury et al., 2007). Similarly, clearance of p16-positive senescent cells in a mouse model can prevent and partially revert the establishment of age-related disorders (Baker et al., 2011), indicating that cellular senescence is causally implicated in tissue dysfunction and health span.

The existence of genomic loci where DNA damage cannot be repaired would explain the appearance of senescent cells *in vivo* with age. This would lead to impaired cell replacement and consequent tissue, organ and organismal ageing. In summary, since the discovery of replicative senescence, telomeres have been considered as a biological clock, sensitive to the numbers of cell divisions. The novel results described here update this concept, and importantly extend this role also to the more abundant non-proliferating compartments in the organism, adding another mechanism for telomeres sensing the passing of time.

5.4 DDRNAs promote DDR and repair at dysfunctional telomeres

5.4.1 DDRNAs as a novel component of DDR at uncapped telomeres

The interest on non-canonical short ncRNAs such as DDRNAs in the DDR field is increasing and many studies indicate that they are implicated in signalling and repair in various models, including humans (Sharma and Misteli, 2013). The experimental results that I have showed suggest that also at uncapped telomeres DDRNAs are generated and they are necessary for the activation and maintenance of DDR (Figs. 35-38). The existence of short RNAs with G-rich telomeric sequence has already been reported in mouse embryonic stem cells (Cao et al., 2009). However they are DICER-independent, thus they seem to be totally unrelated to DDRNAs.

This evidence gives more hints on the function of DDRNAs, because uncapped telomeres elicit a DDR that is slightly different from the canonical one at other genomic locations (Cesare et al., 2013). For instance, since telomeric DDR does not activate the G2/M checkpoint, it is possible that DDRNAs are mostly involved in the activation of the G1/S checkpoint.

It can be argued that in TRF2$^{-/-}$ cells, telomeres are completely uncapped and also prone to chromosomal fusions, a situation that never occurs in physiological conditions. In senescent cells telomeres retain TRF2 that can inhibit repair events, thus it would be very interesting studying the impact of DDRNAs in the persistent DDR foci that accumulate at telomeres in IrrSen cells. A similar experiment has been already shown in OIS cells that express a constitutively active form of RAS oncogene; upon knock down of DICER or DROSHA, but not GW proteins, DDR foci disassemble and cell proliferation is re-established (Francia et al., 2012).

5.4.2 NHEJ at uncapped telomeres is dependent on DICER and DROSHA

A more intriguing and less predicted result is the decrease in the number of chromosomal fusions in DICER and DROSHA knocked down cells (Fig 39). A role in DNA repair has

been already proposed for diRNAs both in plants and human cells, but limited to the HR pathway (Wei et al., 2012). An impact of DICER and DROSHA on chromosomal fusions suggests a role of DDRNAs also in NHEJ, which is the major DNA repair pathway acting at TRF2-depleted telomeres. Obviously further experiments are needed to clarify if this effect is DDRNA-mediated or instead it is an indirect effect of impaired miRNA biogenesis. For instance, it will be essential to demonstrate that inhibition of fusions is no more evident upon knock down of other downstream components of the miRNA biogenesis pathway, like GW proteins. Importantly, I also plan to treat cells with synthetic short DDRNAs with telomeric sequence, to show that they are sufficient to rescue the chromosomal fusions in DICER and DROSHA-depleted cells. Similarly, I will use antisense LNA oligonucleotides with the telomeric sequences, which I showed are able to counteract DDRNA-mediated DDR activation and proliferation arrest (Figs. 41,42), to inhibit DDRNAs in order to prevent chromosomal fusions.

Since I showed that TRF2 is the main player in repair inhibition at telomeres, it would be very interesting to study the possible interaction between TFR2 and telomeric DDRNAs by cross-linking immunoprecipitation (CLIP) followed by high-throughput RNA sequencing, and, in case, also if it is necessary for the interruption of the downstream DDR events leading to DNA repair. Of note, TRF2 has already been shown to directly interact with another telomeric ncRNA, TERRA, through its amino terminal basic domain (Deng et al., 2009).

5.4.3 Telomeric DDRNAs as a target to prevent and revert cellular senescence and ageing phenotypes

The evidence that DDRNAs generated at uncapped telomeres can be inhibited with antisense LNA molecules, to repress the DDR activation and rescue the senescence-associated proliferation block (Figs. 40-42) opens a novel field of potential drug design for many diseases.

Indeed recently, many reports show that small ncRNAs can be inhibited even *in vivo* by different antisense oligonucleotides (ASOs), which act through base pairing complementarity, and thus used as targets of therapeutic strategies (Esteller, 2011). They have been mainly used to repress miRNAs activity in different diseases in mouse models. For instance in mammary tumours, antagomir targeting miR-10b suppresses metastasis formation (Ma et al., 2010), while LNAs have been used to reduce melanoma metastasis (Pencheva et al., 2012). LNAs have been successfully used in other pathologies like acute myocardial infarction and obesity (Boon et al., 2013; Grueter et al., 2012). Also in primates LNAs have been used to treat deregulated cholesterol metabolism and chronic hepatitis C virus infection (Elmen et al., 2008; Lanford et al., 2010).

Based on these encouraging findings, it would be very interesting to test antisense LNAs *in vivo*, in a mouse model with impaired telomere maintenance, in order to study the efficacy of the treatment on senescence and ageing phenotypes. This would lead to the design of drugs for human diseases linked to telomeric dysfunction, as well as to treat all the phenotypes caused by DDR accumulation at telomeres during ageing.

References

Acosta, J.C., Banito, A., Wuestefeld, T., Georgilis, A., Janich, P., Morton, J.P., Athineos, D., Kang, T.W., Lasitschka, F., Andrulis, M.*, et al.* (2013). A complex secretory program orchestrated by the inflammasome controls paracrine senescence. Nat Cell Biol *15*, 978-990.

Al-Hakim, A., Escribano-Diaz, C., Landry, M.C., O'Donnell, L., Panier, S., Szilard, R.K., and Durocher, D. (2010). The ubiquitous role of ubiquitin in the DNA damage response. DNA repair *9*, 1229-1240.

Amiard, S., Doudeau, M., Pinte, S., Poulet, A., Lenain, C., Faivre-Moskalenko, C., Angelov, D., Hug, N., Vindigni, A., Bouvet, P.*, et al.* (2007). A topological mechanism for TRF2-enhanced strand invasion. Nat Struct Mol Biol *14*, 147-154.

Ancelin, K., Brunori, M., Bauwens, S., Koering, C.E., Brun, C., Ricoul, M., Pommier, J.P., Sabatier, L., and Gilson, E. (2002). Targeting assay to study the cis functions of human telomeric proteins: evidence for inhibition of telomerase by TRF1 and for activation of telomere degradation by TRF2. Mol Cell Biol *22*, 3474-3487.

Arnoult, N., Van Beneden, A., and Decottignies, A. (2012). Telomere length regulates TERRA levels through increased trimethylation of telomeric H3K9 and HP1alpha. Nat Struct Mol Biol *19*, 948-956.

Azzalin, C.M., Reichenbach, P., Khoriauli, L., Giulotto, E., and Lingner, J. (2007). Telomeric repeat containing RNA and RNA surveillance factors at mammalian chromosome ends. Science *318*, 798-801.

Bae, N.S., and Baumann, P. (2007). A RAP1/TRF2 complex inhibits nonhomologous end-joining at human telomeric DNA ends. Mol Cell *26*, 323-334.

Baker, D.J., Wijshake, T., Tchkonia, T., LeBrasseur, N.K., Childs, B.G., van de Sluis, B., Kirkland, J.L., and van Deursen, J.M. (2011). Clearance of p16Ink4a-positive senescent cells delays ageing-associated disorders. Nature 479, 232-236.

Bakkenist, C.J., Drissi, R., Wu, J., Kastan, M.B., and Dome, J.S. (2004). Disappearance of the telomere dysfunction-induced stress response in fully senescent cells. Cancer Res *64*, 3748-3752.

Bartkova, J., Rezaei, N., Liontos, M., Karakaidos, P., Kletsas, D., Issaeva, N., Vassiliou, L.V., Kolettas, E., Niforou, K., Zoumpourlis, V.C.*, et al.* (2006). Oncogene-induced senescence is part of the tumorigenesis barrier imposed by DNA damage checkpoints. Nature *444*, 633-637.

Baumann, P., and Cech, T.R. (2001). Pot1, the putative telomere end-binding protein in fission yeast and humans. Science *292*, 1171-1175.

Begus-Nahrmann, Y., Hartmann, D., Kraus, J., Eshraghi, P., Scheffold, A., Grieb, M., Rasche, V., Schirmacher, P., Lee, H.W., Kestler, H.A.*, et al.* (2012). Transient telomere dysfunction induces chromosomal instability and promotes carcinogenesis. J Clin Invest *122*, 2283-2288.

Bekker-Jensen, S., Lukas, C., Kitagawa, R., Melander, F., Kastan, M.B., Bartek, J., and Lukas, J. (2006). Spatial organization of the mammalian genome surveillance machinery in response to DNA strand breaks. J Cell Biol *173*, 195-206.

Bekker-Jensen, S., Lukas, C., Melander, F., Bartek, J., and Lukas, J. (2005). Dynamic assembly and sustained retention of 53BP1 at the sites of DNA damage are controlled by Mdc1/NFBD1. J Cell Biol *170*, 201-211.

Benetti, R., Gonzalo, S., Jaco, I., Munoz, P., Gonzalez, S., Schoeftner, S., Murchison, E., Andl, T., Chen, T., Klatt, P.*, et al.* (2008a). A mammalian microRNA cluster controls DNA methylation and telomere recombination via Rbl2-dependent regulation of DNA methyltransferases. Nat Struct Mol Biol *15*, 268-279.

Benetti, R., Schoeftner, S., Munoz, P., and Blasco, M.A. (2008b). Role of TRF2 in the assembly of telomeric chromatin. Cell Cycle *7*, 3461-3468.

Bensimon, A., Schmidt, A., Ziv, Y., Elkon, R., Wang, S.Y., Chen, D.J., Aebersold, R., and Shiloh, Y. (2010). ATM-dependent and -independent dynamics of the nuclear phosphoproteome after DNA damage. Sci Signal *3*, rs3.

Bernardes de Jesus, B., and Blasco, M.A. (2013). Telomerase at the intersection of cancer and aging. Trends Genet *29*, 513-520.

Birney, E., Stamatoyannopoulos, J.A., Dutta, A., Guigo, R., Gingeras, T.R., Margulies, E.H., Weng, Z., Snyder, M., Dermitzakis, E.T., Thurman, R.E.*, et al.* (2007). Identification and analysis of functional elements in 1% of the human genome by the ENCODE pilot project. Nature *447*, 799-816.

Blackburn, E.H. (2000). Telomere states and cell fates. Nature *408*, 53-56.

Blasco, M.A. (2007). The epigenetic regulation of mammalian telomeres. Nat Rev Genet *8*, 299-309.

Bodnar, A.G., Ouellette, M., Frolkis, M., Holt, S.E., Chiu, C.P., Morin, G.B., Harley, C.B., Shay, J.W., Lichtsteiner, S., and Wright, W.E. (1998). Extension of life-span by introduction of telomerase into normal human cells. Science *279*, 349-352.

Bombarde, O., Boby, C., Gomez, D., Frit, P., Giraud-Panis, M.J., Gilson, E., Salles, B., and Calsou, P. (2010). TRF2/RAP1 and DNA-PK mediate a double protection against joining at telomeric ends. EMBO J *29*, 1573-1584.

Boon, R.A., Iekushi, K., Lechner, S., Seeger, T., Fischer, A., Heydt, S., Kaluza, D., Treguer, K., Carmona, G., Bonauer, A.*, et al.* (2013). MicroRNA-34a regulates cardiac ageing and function. Nature *495*, 107-110.

Bradshaw, P.S., Stavropoulos, D.J., and Meyn, M.S. (2005). Human telomeric protein TRF2 associates with genomic double-strand breaks as an early response to DNA damage. Nat Genet *37*, 193-197.

Branzei, D., and Foiani, M. (2008). Regulation of DNA repair throughout the cell cycle. Nat Rev Mol Cell Biol *9*, 297-308.

Broccoli, D., Smogorzewska, A., Chong, L., and de Lange, T. (1997). Human telomeres contain two distinct Myb-related proteins, TRF1 and TRF2. Nat Genet *17*, 231-235.

Brown, J.P., Wei, W., and Sedivy, J.M. (1997). Bypass of senescence after disruption of p21CIP1/WAF1 gene in normal diploid human fibroblasts. Science *277*, 831-834.

Buscemi, G., Perego, P., Carenini, N., Nakanishi, M., Chessa, L., Chen, J., Khanna, K., and Delia, D. (2004). Activation of ATM and Chk2 kinases in relation to the amount of DNA strand breaks. Oncogene *23*, 7691-7700.

Cao, F., Li, X., Hiew, S., Brady, H., Liu, Y., and Dou, Y. (2009). Dicer independent small RNAs associate with telomeric heterochromatin. RNA *15*, 1274-1281.

Cao, L., Kim, S., Xiao, C., Wang, R.H., Coumoul, X., Wang, X., Li, W.M., Xu, X.L., De Soto, J.A., Takai, H*., et al.* (2006). ATM-Chk2-p53 activation prevents tumorigenesis at an expense of organ homeostasis upon Brca1 deficiency. EMBO J *25*, 2167-2177.

Celeste, A., Difilippantonio, S., Difilippantonio, M.J., Fernandez-Capetillo, O., Pilch, D.R., Sedelnikova, O.A., Eckhaus, M., Ried, T., Bonner, W.M., and Nussenzweig, A. (2003). H2AX haploinsufficiency modifies genomic stability and tumor susceptibility. Cell *114*, 371-383.

Celli, G.B., and de Lange, T. (2005). DNA processing is not required for ATM-mediated telomere damage response after TRF2 deletion. Nat Cell Biol *7*, 712-718.

Cesare, A.J., Hayashi, M.T., Crabbe, L., and Karlseder, J. (2013). The telomere deprotection response is functionally distinct from the genomic DNA damage response. Mol Cell *51*, 141-155.

Cesare, A.J., Kaul, Z., Cohen, S.B., Napier, C.E., Pickett, H.A., Neumann, A.A., and Reddel, R.R. (2009). Spontaneous occurrence of telomeric DNA damage response in the absence of chromosome fusions. Nat Struct Mol Biol *16*, 1244-1251.

Cesare, A.J., and Reddel, R.R. (2010). Alternative lengthening of telomeres: models, mechanisms and implications. Nat Rev Genet *11*, 319-330.

Chandra, A., Hughes, T.R., Nugent, C.I., and Lundblad, V. (2001). Cdc13 both positively and negatively regulates telomere replication. Genes Dev *15*, 404-414.

Chang, E., and Harley, C.B. (1995). Telomere length and replicative aging in human vascular tissues. Proc Natl Acad Sci U S A *92*, 11190-11194.

Chapman, J.R., Barral, P., Vannier, J.B., Borel, V., Steger, M., Tomas-Loba, A., Sartori, A.A., Adams, I.R., Batista, F.D., and Boulton, S.J. (2013). RIF1 is essential for 53BP1-dependent nonhomologous end joining and suppression of DNA double-strand break resection. Molecular cell *49*, 858-871.

Chapman, J.R., Taylor, M.R., and Boulton, S.J. (2012). Playing the end game: DNA double-strand break repair pathway choice. Mol Cell *47*, 497-510.

Chen, J.H., and Ozanne, S.E. (2006). Deep senescent human fibroblasts show diminished DNA damage foci but retain checkpoint capacity to oxidative stress. FEBS Lett *580*, 6669-6673.

Chiang, Y.J., Calado, R.T., Hathcock, K.S., Lansdorp, P.M., Young, N.S., and Hodes, R.J. (2010). Telomere length is inherited with resetting of the telomere set-point. Proc Natl Acad Sci U S A *107*, 10148-10153.

Choudhury, A.R., Ju, Z., Djojosubroto, M.W., Schienke, A., Lechel, A., Schaetzlein, S., Jiang, H., Stepczynska, A., Wang, C., Buer, J.*, et al.* (2007). Cdkn1a deletion improves stem cell function and lifespan of mice with dysfunctional telomeres without accelerating cancer formation. Nat Genet *39*, 99-105.

Cohen, S.B., Graham, M.E., Lovrecz, G.O., Bache, N., Robinson, P.J., and Reddel, R.R. (2007). Protein composition of catalytically active human telomerase from immortal cells. Science *315*, 1850-1853.

Colgin, L.M., Baran, K., Baumann, P., Cech, T.R., and Reddel, R.R. (2003). Human POT1 facilitates telomere elongation by telomerase. Curr Biol *13*, 942-946.

Collado, M., and Serrano, M. (2010). Senescence in tumours: evidence from mice and humans. Nat Rev Cancer *10*, 51-57.

Coppe, J.P., Desprez, P.Y., Krtolica, A., and Campisi, J. (2010). The senescence-associated secretory phenotype: the dark side of tumor suppression. Annu Rev Pathol *5*, 99-118.

Coppe, J.P., Patil, C.K., Rodier, F., Sun, Y., Munoz, D.P., Goldstein, J., Nelson, P.S., Desprez, P.Y., and Campisi, J. (2008). Senescence-associated secretory phenotypes reveal cell-nonautonomous functions of oncogenic RAS and the p53 tumor suppressor. PLoS Biol *6*, 2853-2868.

Cusanelli, E., Romero, C.A., and Chartrand, P. (2013). Telomeric Noncoding RNA TERRA Is Induced by Telomere Shortening to Nucleate Telomerase Molecules at Short Telomeres. Molecular cell *51*, 780-791.

d'Adda di Fagagna, F., Hande, M.P., Tong, W.M., Roth, D., Lansdorp, P.M., Wang, Z.Q., and Jackson, S.P. (2001). Effects of DNA nonhomologous end-joining factors on telomere length and chromosomal stability in mammalian cells. Curr Biol *11*, 1192-1196.

d'Adda di Fagagna, F., Reaper, P.M., Clay-Farrace, L., Fiegler, H., Carr, P., Von Zglinicki, T., Saretzki, G., Carter, N.P., and Jackson, S.P. (2003). A DNA damage checkpoint response in telomere-initiated senescence. Nature *426*, 194-198.

Dankort, D., Filenova, E., Collado, M., Serrano, M., Jones, K., and McMahon, M. (2007). A new mouse model to explore the initiation, progression, and therapy of BRAFV600E-induced lung tumors. Genes Dev *21*, 379-384.

Davoli, T., and de Lange, T. (2012). Telomere-driven tetraploidization occurs in human cells undergoing crisis and promotes transformation of mouse cells. Cancer Cell *21*, 765-776.

de Lange, T. (2005). Shelterin: the protein complex that shapes and safeguards human telomeres. Genes Dev *19*, 2100-2110.

de Magalhaes, J.P., Chainiaux, F., Remacle, J., and Toussaint, O. (2002). Stress-induced premature senescence in BJ and hTERT-BJ1 human foreskin fibroblasts. FEBS Lett *523*, 157-162.

Deans, A.J., and West, S.C. (2011). DNA interstrand crosslink repair and cancer. Nat Rev Cancer *11*, 467-480.

Deng, Z., Norseen, J., Wiedmer, A., Riethman, H., and Lieberman, P.M. (2009). TERRA RNA binding to TRF2 facilitates heterochromatin formation and ORC recruitment at telomeres. Mol Cell *35*, 403-413.

Di Micco, R., Fumagalli, M., Cicalese, A., Piccinin, S., Gasparini, P., Luise, C., Schurra, C., Garre, M., Nuciforo, P.G., Bensimon, A.*, et al.* (2006). Oncogene-induced senescence is a DNA damage response triggered by DNA hyper-replication. Nature *444*, 638-642.

Di Micco, R., Fumagalli, M., and d'Adda di Fagagna, F. (2007). Breaking news: high-speed race ends in arrest--how oncogenes induce senescence. Trends Cell Biol *17*, 529-536.

Di Virgilio, M., Callen, E., Yamane, A., Zhang, W., Jankovic, M., Gitlin, A.D., Feldhahn, N., Resch, W., Oliveira, T.Y., Chait, B.T.*, et al.* (2013). Rif1 prevents resection of DNA breaks and promotes immunoglobulin class switching. Science *339*, 711-715.

Digweed, M., and Sperling, K. (2004). Nijmegen breakage syndrome: clinical manifestation of defective response to DNA double-strand breaks. DNA Repair (Amst) *3*, 1207-1217.

Dimri, G.P., Lee, X., Basile, G., Acosta, M., Scott, G., Roskelley, C., Medrano, E.E., Linskens, M., Rubelj, I., Pereira-Smith, O.*, et al.* (1995). A biomarker that identifies senescent human cells in culture and in aging skin in vivo. Proc Natl Acad Sci U S A *92*, 9363-9367.

Dominguez-Sola, D., Ying, C.Y., Grandori, C., Ruggiero, L., Chen, B., Li, M., Galloway, D.A., Gu, W., Gautier, J., and Dalla-Favera, R. (2007). Non-transcriptional control of DNA replication by c-Myc. Nature *448*, 445-451.

Doyle, M., Badertscher, L., Jaskiewicz, L., Guttinger, S., Jurado, S., Hugenschmidt, T., Kutay, U., and Filipowicz, W. (2013). The double-stranded RNA binding domain of human Dicer functions as a nuclear localization signal. RNA *19*, 1238-1252.

Elmen, J., Lindow, M., Schutz, S., Lawrence, M., Petri, A., Obad, S., Lindholm, M., Hedtjarn, M., Hansen, H.F., Berger, U.*, et al.* (2008). LNA-mediated microRNA silencing in non-human primates. Nature *452*, 896-899.

Escribano-Diaz, C., Orthwein, A., Fradet-Turcotte, A., Xing, M., Young, J.T., Tkac, J., Cook, M.A., Rosebrock, A.P., Munro, M., Canny, M.D.*, et al.* (2013). A cell cycle-dependent regulatory circuit composed of 53BP1-RIF1 and BRCA1-CtIP controls DNA repair pathway choice. Mol Cell *49*, 872-883.

Esteller, M. (2011). Non-coding RNAs in human disease. Nat Rev Genet *12*, 861-874.

Eulalio, A., Huntzinger, E., and Izaurralde, E. (2008). GW182 interaction with Argonaute is essential for miRNA-mediated translational repression and mRNA decay. Nat Struct Mol Biol *15*, 346-353.

Evan, G.I., and d'Adda di Fagagna, F. (2009). Cellular senescence: hot or what? Curr Opin Genet Dev *19*, 25-31.

Fattah, F., Lee, E.H., Weisensel, N., Wang, Y., Lichter, N., and Hendrickson, E.A. (2010). Ku regulates the non-homologous end joining pathway choice of DNA double-strand break repair in human somatic cells. PLoS Genet *6*, e1000855.

Ferron, S., Mira, H., Franco, S., Cano-Jaimez, M., Bellmunt, E., Ramirez, C., Farinas, I., and Blasco, M.A. (2004). Telomere shortening and chromosomal instability abrogates proliferation of adult but not embryonic neural stem cells. Development *131*, 4059-4070.

Flynn, R.L., Centore, R.C., O'Sullivan, R.J., Rai, R., Tse, A., Songyang, Z., Chang, S., Karlseder, J., and Zou, L. (2011). TERRA and hnRNPA1 orchestrate an RPA-to-POT1 switch on telomeric single-stranded DNA. Nature *471*, 532-536.

Francia, S., Michelini, F., Saxena, A., Tang, D., de Hoon, M., Anelli, V., Mione, M., Carninci, P., and d'Adda di Fagagna, F. (2012). Site-specific DICER and DROSHA RNA products control the DNA-damage response. Nature 488, 231-235.

Fujita, K., Horikawa, I., Mondal, A.M., Jenkins, L.M., Appella, E., Vojtesek, B., Bourdon, J.C., Lane, D.P., and Harris, C.C. (2010). Positive feedback between p53 and TRF2 during telomere-damage signalling and cellular senescence. Nat Cell Biol 12, 1205-1212.

Fumagalli, M., Rossiello, F., Clerici, M., Barozzi, S., Cittaro, D., Kaplunov, J.M., Bucci, G., Dobreva, M., Matti, V., Beausejour, C.M.*, et al.* (2012). Telomeric DNA damage is irreparable and causes persistent DNA-damage-response activation. Nat Cell Biol *14*, 355-365.

Giraud-Panis, M.J., Teixeira, M.T., Geli, V., and Gilson, E. (2010). CST meets shelterin to keep telomeres in check. Mol Cell *39*, 665-676.

Goodarzi, A.A., Noon, A.T., Deckbar, D., Ziv, Y., Shiloh, Y., Lobrich, M., and Jeggo, P.A. (2008). ATM signaling facilitates repair of DNA double-strand breaks associated with heterochromatin. Mol Cell *31*, 167-177.

Gorbunova, V., Seluanov, A., and Pereira-Smith, O.M. (2002). Expression of human telomerase (hTERT) does not prevent stress-induced senescence in normal human fibroblasts but protects the cells from stress-induced apoptosis and necrosis. J Biol Chem *277*, 38540-38549.

Grandori, C., Wu, K.J., Fernandez, P., Ngouenet, C., Grim, J., Clurman, B.E., Moser, M.J., Oshima, J., Russell, D.W., Swisshelm, K.*, et al.* (2003). Werner syndrome protein limits MYC-induced cellular senescence. Genes Dev *17*, 1569-1574.

Greider, C.W., and Blackburn, E.H. (1985). Identification of a specific telomere terminal transferase activity in Tetrahymena extracts. Cell *43*, 405-413.

Griffith, J.D., Comeau, L., Rosenfield, S., Stansel, R.M., Bianchi, A., Moss, H., and de Lange, T. (1999). Mammalian telomeres end in a large duplex loop. Cell *97*, 503-514.

Grueter, C.E., van Rooij, E., Johnson, B.A., DeLeon, S.M., Sutherland, L.B., Qi, X., Gautron, L., Elmquist, J.K., Bassel-Duby, R., and Olson, E.N. (2012). A cardiac microRNA governs systemic energy homeostasis by regulation of MED13. Cell *149*, 671-683.

Gunes, C., and Rudolph, K.L. (2013). The role of telomeres in stem cells and cancer. Cell *152*, 390-393.

Haferkamp, S., Tran, S.L., Becker, T.M., Scurr, L.L., Kefford, R.F., and Rizos, H. (2009). The relative contributions of the p53 and pRb pathways in oncogene-induced melanocyte senescence. Aging (Albany NY) *1*, 542-556.

Hahn, W.C., Counter, C.M., Lundberg, A.S., Beijersbergen, R.L., Brooks, M.W., and Weinberg, R.A. (1999). Creation of human tumour cells with defined genetic elements. Nature *400*, 464-468.

Hardy, C.F., Sussel, L., and Shore, D. (1992). A RAP1-interacting protein involved in transcriptional silencing and telomere length regulation. Genes Dev *6*, 801-814.

Harley, C.B., Futcher, A.B., and Greider, C.W. (1990). Telomeres shorten during ageing of human fibroblasts. Nature *345*, 458-460.

Hayflick, L., and Moorhead, P.S. (1961). The serial cultivation of human diploid cell strains. Exp Cell Res *25*, 585-621.

Hemann, M.T., Strong, M.A., Hao, L.Y., and Greider, C.W. (2001). The shortest telomere, not average telomere length, is critical for cell viability and chromosome stability. Cell *107*, 67-77.

Herbig, U., Ferreira, M., Condel, L., Carey, D., and Sedivy, J.M. (2006). Cellular senescence in aging primates. Science *311*, 1257.

Herbig, U., Jobling, W.A., Chen, B.P., Chen, D.J., and Sedivy, J.M. (2004). Telomere shortening triggers senescence of human cells through a pathway involving ATM, p53, and p21(CIP1), but not p16(INK4a). Mol Cell *14*, 501-513.

Hewitt, G., Jurk, D., Marques, F.D., Correia-Melo, C., Hardy, T., Gackowska, A., Anderson, R., Taschuk, M., Mann, J., and Passos, J.F. (2012). Telomeres are favoured targets of a persistent DNA damage response in ageing and stress-induced senescence. Nat Commun *3*, 708.

Hirao, A., Cheung, A., Duncan, G., Girard, P.M., Elia, A.J., Wakeham, A., Okada, H., Sarkissian, T., Wong, J.A., Sakai, T.*, et al.* (2002). Chk2 is a tumor suppressor that regulates apoptosis in both an ataxia telangiectasia mutated (ATM)-dependent and an ATM-independent manner. Mol Cell Biol *22*, 6521-6532.

Ho, J.N., Lee, Y.H., Park, J.S., Jun, W.J., Kim, H.K., Hong, B.S., Shin, D.H., and Cho, H.Y. (2005). Protective effects of aucubin isolated from Eucommia ulmoides against UVB-induced oxidative stress in human skin fibroblasts. Biol Pharm Bull *28*, 1244-1248.

Hu, H., Du, L., Nagabayashi, G., Seeger, R.C., and Gatti, R.A. (2010). ATM is down-regulated by N-Myc-regulated microRNA-421. Proc Natl Acad Sci U S A *107*, 1506-1511.

Hu, J., Hwang, S.S., Liesa, M., Gan, B., Sahin, E., Jaskelioff, M., Ding, Z., Ying, H., Boutin, A.T., Zhang, H.*, et al.* (2012). Antitelomerase therapy provokes ALT and mitochondrial adaptive mechanisms in cancer. Cell *148*, 651-663.

Huen, M.S., Grant, R., Manke, I., Minn, K., Yu, X., Yaffe, M.B., and Chen, J. (2007). RNF8 transduces the DNA-damage signal via histone ubiquitylation and checkpoint protein assembly. Cell *131*, 901-914.

Iacovoni, J.S., Caron, P., Lassadi, I., Nicolas, E., Massip, L., Trouche, D., and Legube, G. (2010). High-resolution profiling of gammaH2AX around DNA double strand breaks in the mammalian genome. Embo J *29*, 1446-1457.

Iliakis, G., Wang, Y., Guan, J., and Wang, H. (2003). DNA damage checkpoint control in cells exposed to ionizing radiation. Oncogene *22*, 5834-5847.

Indiviglio, S.M., and Bertuch, A.A. (2009). Ku's essential role in keeping telomeres intact. Proc Natl Acad Sci U S A *106*, 12217-12218.

Jackson, S.P., and Bartek, J. (2009). The DNA-damage response in human biology and disease. Nature *461*, 1071-1078.

Jackson, S.P., and Durocher, D. (2013). Regulation of DNA damage responses by ubiquitin and SUMO. Mol Cell *49*, 795-807.

Janzen, V., Forkert, R., Fleming, H.E., Saito, Y., Waring, M.T., Dombkowski, D.M., Cheng, T., DePinho, R.A., Sharpless, N.E., and Scadden, D.T. (2006). Stem-cell ageing modified by the cyclin-dependent kinase inhibitor p16INK4a. Nature *443*, 421-426.

Jaskelioff, M., Muller, F.L., Paik, J.H., Thomas, E., Jiang, S., Adams, A.C., Sahin, E., Kost-Alimova, M., Protopopov, A., Cadinanos, J.*, et al.* (2011). Telomerase reactivation reverses tissue degeneration in aged telomerase-deficient mice. Nature *469*, 102-106.

Jazayeri, A., Falck, J., Lukas, C., Bartek, J., Smith, G.C., Lukas, J., and Jackson, S.P. (2006). ATM- and cell cycle-dependent regulation of ATR in response to DNA double-strand breaks. Nat Cell Biol *8*, 37-45.

Jepsen, J.S., Sorensen, M.D., and Wengel, J. (2004). Locked nucleic acid: a potent nucleic acid analog in therapeutics and biotechnology. Oligonucleotides *14*, 130-146.

Jeyapalan, J.C., Ferreira, M., Sedivy, J.M., and Herbig, U. (2007). Accumulation of senescent cells in mitotic tissue of aging primates. Mech Ageing Dev *128*, 36-44.

Jinek, M., and Doudna, J.A. (2009). A three-dimensional view of the molecular machinery of RNA interference. Nature *457*, 405-412.

Jurk, D., Wang, C., Miwa, S., Maddick, M., Korolchuk, V., Tsolou, A., Gonos, E.S., Thrasivoulou, C., Saffrey, M.J., Cameron, K.*, et al.* (2012). Postmitotic neurons develop a p21-dependent senescence-like phenotype driven by a DNA damage response. Aging Cell *11*, 996-1004.

Kappei, D., Butter, F., Benda, C., Scheibe, M., Draskovic, I., Stevense, M., Novo, C.L., Basquin, C., Araki, M., Araki, K.*, et al.* (2013). HOT1 is a mammalian direct telomere repeat-binding protein contributing to telomerase recruitment. EMBO J *32*, 1681-1701.

Karlseder, J., Hoke, K., Mirzoeva, O.K., Bakkenist, C., Kastan, M.B., Petrini, J.H., and de Lange, T. (2004). The telomeric protein TRF2 binds the ATM kinase and can inhibit the ATM-dependent DNA damage response. PLoS Biol *2*, E240.

Karpenshif, Y., and Bernstein, K.A. (2012). From yeast to mammals: recent advances in genetic control of homologous recombination. DNA Repair (Amst) *11*, 781-788.

Kawai, S., and Amano, A. (2012). BRCA1 regulates microRNA biogenesis via the DROSHA microprocessor complex. J Cell Biol *197*, 201-208.

Kolas, N.K., Chapman, J.R., Nakada, S., Ylanko, J., Chahwan, R., Sweeney, F.D., Panier, S., Mendez, M., Wildenhain, J., Thomson, T.M.*, et al.* (2007). Orchestration of the DNA-damage response by the RNF8 ubiquitin ligase. Science *318*, 1637-1640.

Kreiling, J.A., Tamamori-Adachi, M., Sexton, A.N., Jeyapalan, J.C., Munoz-Najar, U., Peterson, A.L., Manivannan, J., Rogers, E.S., Pchelintsev, N.A., Adams, P.D.*, et al.*

(2011). Age-associated increase in heterochromatic marks in murine and primate tissues. Aging Cell *10*, 292-304.

Krishnamurthy, J., Ramsey, M.R., Ligon, K.L., Torrice, C., Koh, A., Bonner-Weir, S., and Sharpless, N.E. (2006). p16INK4a induces an age-dependent decline in islet regenerative potential. Nature *443*, 453-457.

Kuilman, T., Michaloglou, C., Mooi, W.J., and Peeper, D.S. (2010). The essence of senescence. Genes Dev *24*, 2463-2479.

Lal, A., Pan, Y., Navarro, F., Dykxhoorn, D.M., Moreau, L., Meire, E., Bentwich, Z., Lieberman, J., and Chowdhury, D. (2009). miR-24-mediated downregulation of H2AX suppresses DNA repair in terminally differentiated blood cells. Nat Struct Mol Biol *16*, 492-498.

Lanford, R.E., Hildebrandt-Eriksen, E.S., Petri, A., Persson, R., Lindow, M., Munk, M.E., Kauppinen, S., and Orum, H. (2010). Therapeutic silencing of microRNA-122 in primates with chronic hepatitis C virus infection. Science *327*, 198-201.

Langerak, P., and Russell, P. (2011). Regulatory networks integrating cell cycle control with DNA damage checkpoints and double-strand break repair. Philos Trans R Soc Lond B Biol Sci *366*, 3562-3571.

Lansdorp, P.M., Verwoerd, N.P., van de Rijke, F.M., Dragowska, V., Little, M.T., Dirks, R.W., Raap, A.K., and Tanke, H.J. (1996). Heterogeneity in telomere length of human chromosomes. Hum Mol Genet *5*, 685-691.

Lazzerini Denchi, E., Attwooll, C., Pasini, D., and Helin, K. (2005). Deregulated E2F activity induces hyperplasia and senescence-like features in the mouse pituitary gland. Mol Cell Biol *25*, 2660-2672.

Lazzerini Denchi, E., and de Lange, T. (2007). Protection of telomeres through independent control of ATM and ATR by TRF2 and POT1. Nature *448*, 1068-1071.

Lee, H.C., Chang, S.S., Choudhary, S., Aalto, A.P., Maiti, M., Bamford, D.H., and Liu, Y. (2009). qiRNA is a new type of small interfering RNA induced by DNA damage. Nature *459*, 274-277.

Lieber, M.R. (2010). The mechanism of double-strand DNA break repair by the nonhomologous DNA end-joining pathway. Annu Rev Biochem *79*, 181-211.

Lipps, H.J., and Rhodes, D. (2009). G-quadruplex structures: in vivo evidence and function. Trends Cell Biol *19*, 414-422.

Liu, Q., Guntuku, S., Cui, X.S., Matsuoka, S., Cortez, D., Tamai, K., Luo, G., Carattini-Rivera, S., DeMayo, F., Bradley, A.*, et al.* (2000). Chk1 is an essential kinase that is regulated by Atr and required for the G(2)/M DNA damage checkpoint. Genes Dev *14*, 1448-1459.

Lukas, C., Falck, J., Bartkova, J., Bartek, J., and Lukas, J. (2003). Distinct spatiotemporal dynamics of mammalian checkpoint regulators induced by DNA damage. Nat Cell Biol *5*, 255-260.

Lund, E., and Dahlberg, J.E. (2006). Substrate selectivity of exportin 5 and Dicer in the biogenesis of microRNAs. Cold Spring Harb Symp Quant Biol *71*, 59-66.

Lustig, A.J., Kurtz, S., and Shore, D. (1990). Involvement of the silencer and UAS binding protein RAP1 in regulation of telomere length. Science *250*, 549-553.

Ma, L., Reinhardt, F., Pan, E., Soutschek, J., Bhat, B., Marcusson, E.G., Teruya-Feldstein, J., Bell, G.W., and Weinberg, R.A. (2010). Therapeutic silencing of miR-10b inhibits metastasis in a mouse mammary tumor model. Nat Biotechnol *28*, 341-347.

Machlin, E.S., Sarnow, P., and Sagan, S.M. (2012). Combating hepatitis C virus by targeting microRNA-122 using locked nucleic acids. Curr Gene Ther *12*, 301-306.

Mailand, N., Bekker-Jensen, S., Faustrup, H., Melander, F., Bartek, J., Lukas, C., and Lukas, J. (2007). RNF8 ubiquitylates histones at DNA double-strand breaks and promotes assembly of repair proteins. Cell *131*, 887-900.

Malumbres, M., and Barbacid, M. (2009). Cell cycle, CDKs and cancer: a changing paradigm. Nat Rev Cancer *9*, 153-166.

Marcand, S., Brevet, V., Mann, C., and Gilson, E. (2000). Cell cycle restriction of telomere elongation. Curr Biol *10*, 487-490.

Marcand, S., Pardo, B., Gratias, A., Cahun, S., and Callebaut, I. (2008). Multiple pathways inhibit NHEJ at telomeres. Genes & development *22*, 1153-1158.

Marchion, D.C., Bicaku, E., Daud, A.I., Sullivan, D.M., and Munster, P.N. (2005). Valproic acid alters chromatin structure by regulation of chromatin modulation proteins. Cancer Res *65*, 3815-3822.

Martin, M., Terradas, M., Iliakis, G., Tusell, L., and Genesca, A. (2009). Breaks invisible to the DNA damage response machinery accumulate in ATM-deficient cells. Genes Chromosomes Cancer *48*, 745-759.

Martinez, P., Thanasoula, M., Carlos, A.R., Gomez-Lopez, G., Tejera, A.M., Schoeftner, S., Dominguez, O., Pisano, D.G., Tarsounas, M., and Blasco, M.A. (2010). Mammalian Rap1 controls telomere function and gene expression through binding to telomeric and extratelomeric sites. Nat Cell Biol *12*, 768-780.

Martinez, P., Thanasoula, M., Munoz, P., Liao, C., Tejera, A., McNees, C., Flores, J.M., Fernandez-Capetillo, O., Tarsounas, M., and Blasco, M.A. (2009). Increased telomere fragility and fusions resulting from TRF1 deficiency lead to degenerative pathologies and increased cancer in mice. Genes Dev *23*, 2060-2075.

Marusyk, A., Wheeler, L.J., Mathews, C.K., and DeGregori, J. (2007). p53 mediates senescence-like arrest induced by chronic replicational stress. Mol Cell Biol *27*, 5336-5351.

Mathon, N.F., Malcolm, D.S., Harrisingh, M.C., Cheng, L., and Lloyd, A.C. (2001). Lack of replicative senescence in normal rodent glia. Science *291*, 872-875.

McPherson, J.P., Lemmers, B., Hirao, A., Hakem, A., Abraham, J., Migon, E., Matysiak-Zablocki, E., Tamblyn, L., Sanchez-Sweatman, O., Khokha, R.*, et al.* (2004). Collaboration of Brca1 and Chk2 in tumorigenesis. Genes Dev *18*, 1144-1153.

McVey, M., and Lee, S.E. (2008). MMEJ repair of double-strand breaks (director's cut): deleted sequences and alternative endings. Trends Genet *24*, 529-538.

Meyerson, M. (2000). Role of telomerase in normal and cancer cells. J Clin Oncol *18*, 2626-2634.

Michalik, K.M., Bottcher, R., and Forstemann, K. (2012). A small RNA response at DNA ends in Drosophila. Nucleic Acids Res *40*, 9596-9603.

Michaloglou, C., Vredeveld, L.C., Soengas, M.S., Denoyelle, C., Kuilman, T., van der Horst, C.M., Majoor, D.M., Shay, J.W., Mooi, W.J., and Peeper, D.S. (2005). BRAFE600-associated senescence-like cell cycle arrest of human naevi. Nature *436*, 720-724.

Michelson, R.J., Rosenstein, S., and Weinert, T. (2005). A telomeric repeat sequence adjacent to a DNA double-stranded break produces an anticheckpoint. Genes Dev *19*, 2546-2559.

Mitchell, J.R., Wood, E., and Collins, K. (1999). A telomerase component is defective in the human disease dyskeratosis congenita. Nature *402*, 551-555.

Miyake, Y., Nakamura, M., Nabetani, A., Shimamura, S., Tamura, M., Yonehara, S., Saito, M., and Ishikawa, F. (2009). RPA-like mammalian Ctc1-Stn1-Ten1 complex binds to single-stranded DNA and protects telomeres independently of the Pot1 pathway. Mol Cell *36*, 193-206.

Molofsky, A.V., Slutsky, S.G., Joseph, N.M., He, S., Pardal, R., Krishnamurthy, J., Sharpless, N.E., and Morrison, S.J. (2006). Increasing p16INK4a expression decreases forebrain progenitors and neurogenesis during ageing. Nature *443*, 448-452.

Mondello, C., Chiesa, M., Rebuzzini, P., Zongaro, S., Verri, A., Colombo, T., Giulotto, E., D'Incalci, M., Franceschi, C., and Nuzzo, F. (2003). Karyotype instability and anchorage-independent growth in telomerase-immortalized fibroblasts from two centenarian individuals. Biochem Biophys Res Commun *308*, 914-921.

Moskwa, P., Buffa, F.M., Pan, Y., Panchakshari, R., Gottipati, P., Muschel, R.J., Beech, J., Kulshrestha, R., Abdelmohsen, K., Weinstock, D.M.*, et al.* (2011). miR-182-mediated downregulation of BRCA1 impacts DNA repair and sensitivity to PARP inhibitors. Mol Cell *41*, 210-220.

Munoz, P., Blanco, R., de Carcer, G., Schoeftner, S., Benetti, R., Flores, J.M., Malumbres, M., and Blasco, M.A. (2009). TRF1 controls telomere length and mitotic fidelity in epithelial homeostasis. Mol Cell Biol *29*, 1608-1625.

Naguibneva, I., Ameyar-Zazoua, M., Nonne, N., Polesskaya, A., Ait-Si-Ali, S., Groisman, R., Souidi, M., Pritchard, L.L., and Harel-Bellan, A. (2006). An LNA-based loss-of-function assay for micro-RNAs. Biomed Pharmacother *60*, 633-638.

Nam, E.A., and Cortez, D. (2011). ATR signalling: more than meeting at the fork. Biochem J *436*, 527-536.

Narita, M., Nunez, S., Heard, E., Lin, A.W., Hearn, S.A., Spector, D.L., Hannon, G.J., and Lowe, S.W. (2003). Rb-mediated heterochromatin formation and silencing of E2F target genes during cellular senescence. Cell *113*, 703-716.

Nelson, G., Wordsworth, J., Wang, C., Jurk, D., Lawless, C., Martin-Ruiz, C., and von Zglinicki, T. (2012). A senescent cell bystander effect: senescence-induced senescence. Aging Cell *11*, 345-349.

Nijnik, A., Woodbine, L., Marchetti, C., Dawson, S., Lambe, T., Liu, C., Rodrigues, N.P., Crockford, T.L., Cabuy, E., Vindigni, A.*, et al.* (2007). DNA repair is limiting for haematopoietic stem cells during ageing. Nature *447*, 686-690.

Nussenzweig, A., and Nussenzweig, M.C. (2007). A backup DNA repair pathway moves to the forefront. Cell *131*, 223-225.

O'Donovan, P.J., and Livingston, D.M. (2010). BRCA1 and BRCA2: breast/ovarian cancer susceptibility gene products and participants in DNA double-strand break repair. Carcinogenesis *31*, 961-967.

O'Driscoll, M., Ruiz-Perez, V.L., Woods, C.G., Jeggo, P.A., and Goodship, J.A. (2003). A splicing mutation affecting expression of ataxia-telangiectasia and Rad3-related protein (ATR) results in Seckel syndrome. Nat Genet *33*, 497-501.

O'Sullivan, R.J., and Karlseder, J. (2010). Telomeres: protecting chromosomes against genome instability. Nat Rev Mol Cell Biol *11*, 171-181.

Obad, S., dos Santos, C.O., Petri, A., Heidenblad, M., Broom, O., Ruse, C., Fu, C., Lindow, M., Stenvang, J., Straarup, E.M.*, et al.* (2011). Silencing of microRNA families by seed-targeting tiny LNAs. Nat Genet *43*, 371-378.

Okamoto, K., Bartocci, C., Ouzounov, I., Diedrich, J.K., Yates, J.R., 3rd, and Denchi, E.L. (2013). A two-step mechanism for TRF2-mediated chromosome-end protection. Nature *494*, 502-505.

Palm, W., Hockemeyer, D., Kibe, T., and de Lange, T. (2009). Functional dissection of human and mouse POT1 proteins. Mol Cell Biol *29*, 471-482.

Panier, S., Ichijima, Y., Fradet-Turcotte, A., Leung, C.C., Kaustov, L., Arrowsmith, C.H., and Durocher, D. (2012). Tandem protein interaction modules organize the ubiquitin-dependent response to DNA double-strand breaks. Mol Cell *47*, 383-395.

Parrinello, S., Samper, E., Krtolica, A., Goldstein, J., Melov, S., and Campisi, J. (2003). Oxygen sensitivity severely limits the replicative lifespan of murine fibroblasts. Nat Cell Biol *5*, 741-747.

Pencheva, N., Tran, H., Buss, C., Huh, D., Drobnjak, M., Busam, K., and Tavazoie, S.F. (2012). Convergent multi-miRNA targeting of ApoE drives LRP1/LRP8-dependent melanoma metastasis and angiogenesis. Cell *151*, 1068-1082.

Peuscher, M.H., and Jacobs, J.J. (2011). DNA-damage response and repair activities at uncapped telomeres depend on RNF8. Nat Cell Biol *13*, 1139-1145.

Polo, S.E., and Jackson, S.P. (2011). Dynamics of DNA damage response proteins at DNA breaks: a focus on protein modifications. Genes & development *25*, 409-433.

Porro, A., Feuerhahn, S., Reichenbach, P., and Lingner, J. (2010). Molecular dissection of telomeric repeat-containing RNA biogenesis unveils the presence of distinct and multiple regulatory pathways. Mol Cell Biol *30*, 4808-4817.

Povirk, L.F. (1996). DNA damage and mutagenesis by radiomimetic DNA-cleaving agents: bleomycin, neocarzinostatin and other enediynes. Mutat Res *355*, 71-89.

Price, J.S., Waters, J.G., Darrah, C., Pennington, C., Edwards, D.R., Donell, S.T., and Clark, I.M. (2002). The role of chondrocyte senescence in osteoarthritis. Aging Cell *1*, 57-65.

Prowse, K.R., and Greider, C.W. (1995). Developmental and tissue-specific regulation of mouse telomerase and telomere length. Proc Natl Acad Sci U S A *92*, 4818-4822.

Qi, H., and Zakian, V.A. (2000). The Saccharomyces telomere-binding protein Cdc13p interacts with both the catalytic subunit of DNA polymerase alpha and the telomerase-associated est1 protein. Genes Dev *14*, 1777-1788.

Qian, W., Wang, J., Jin, N.N., Fu, X.H., Lin, Y.C., Lin, J.J., and Zhou, J.Q. (2009). Ten1p promotes the telomeric DNA-binding activity of Cdc13p: implication for its function in telomere length regulation. Cell Res *19*, 849-863.

Rastogi, R.P., Richa, Kumar, A., Tyagi, M.B., and Sinha, R.P. (2010). Molecular mechanisms of ultraviolet radiation-induced DNA damage and repair. J Nucleic Acids *2010*, 592980.

Ribeyre, C., and Shore, D. (2012). Anticheckpoint pathways at telomeres in yeast. Nat Struct Mol Biol *19*, 307-313.

Rodier, F., Coppe, J.P., Patil, C.K., Hoeijmakers, W.A., Munoz, D.P., Raza, S.R., Freund, A., Campeau, E., Davalos, A.R., and Campisi, J. (2009). Persistent DNA damage signalling triggers senescence-associated inflammatory cytokine secretion. Nat Cell Biol *11*, 973-979.

Rodier, F., Munoz, D.P., Teachenor, R., Chu, V., Le, O., Bhaumik, D., Coppe, J.P., Campeau, E., Beausejour, C.M., Kim, S.H.*, et al.* (2011). DNA-SCARS: distinct nuclear structures that sustain damage-induced senescence growth arrest and inflammatory cytokine secretion. J Cell Sci *124*, 68-81.

Rossi, D.J., Bryder, D., Seita, J., Nussenzweig, A., Hoeijmakers, J., and Weissman, I.L. (2007). Deficiencies in DNA damage repair limit the function of haematopoietic stem cells with age. Nature *447*, 725-729.

Rube, C.E., Fricke, A., Widmann, T.A., Furst, T., Madry, H., Pfreundschuh, M., and Rube, C. (2011). Accumulation of DNA damage in hematopoietic stem and progenitor cells during human aging. PLoS One *6*, e17487.

Rudolph, K.L., Chang, S., Lee, H.W., Blasco, M., Gottlieb, G.J., Greider, C., and DePinho, R.A. (1999). Longevity, stress response, and cancer in aging telomerase-deficient mice. Cell *96*, 701-712.

Sahin, E., and Depinho, R.A. (2010). Linking functional decline of telomeres, mitochondria and stem cells during ageing. Nature *464*, 520-528.

Saini, H.K., Griffiths-Jones, S., and Enright, A.J. (2007). Genomic analysis of human microRNA transcripts. Proc Natl Acad Sci U S A *104*, 17719-17724.

Satyanarayana, A., Greenberg, R.A., Schaetzlein, S., Buer, J., Masutomi, K., Hahn, W.C., Zimmermann, S., Martens, U., Manns, M.P., and Rudolph, K.L. (2004). Mitogen stimulation cooperates with telomere shortening to activate DNA damage responses and senescence signaling. Mol Cell Biol *24*, 5459-5474.

Schmitt, C.A. (2003). Senescence, apoptosis and therapy--cutting the lifelines of cancer. Nat Rev Cancer *3*, 286-295.

Schoeftner, S., and Blasco, M.A. (2008). Developmentally regulated transcription of mammalian telomeres by DNA-dependent RNA polymerase II. Nat Cell Biol *10*, 228-236.

Schoeftner, S., and Blasco, M.A. (2009). A 'higher order' of telomere regulation: telomere heterochromatin and telomeric RNAs. EMBO J *28*, 2323-2336.

Schwarz, D.S., Hutvagner, G., Du, T., Xu, Z., Aronin, N., and Zamore, P.D. (2003). Asymmetry in the assembly of the RNAi enzyme complex. Cell *115*, 199-208.

Sedelnikova, O.A., Horikawa, I., Zimonjic, D.B., Popescu, N.C., Bonner, W.M., and Barrett, J.C. (2004). Senescing human cells and ageing mice accumulate DNA lesions with unrepairable double-strand breaks. Nat Cell Biol *6*, 168-170.

Serrano, M., Lin, A.W., McCurrach, M.E., Beach, D., and Lowe, S.W. (1997). Oncogenic ras provokes premature cell senescence associated with accumulation of p53 and p16INK4a. Cell *88*, 593-602.

Sfeir, A., and de Lange, T. (2012). Removal of shelterin reveals the telomere end-protection problem. Science *336*, 593-597.

Sfeir, A., Kosiyatrakul, S.T., Hockemeyer, D., MacRae, S.L., Karlseder, J., Schildkraut, C.L., and de Lange, T. (2009). Mammalian telomeres resemble fragile sites and require TRF1 for efficient replication. Cell *138*, 90-103.

Sharma, V., and Misteli, T. (2013). Non-coding RNAs in DNA damage and repair. FEBS Lett *587*, 1832-1839.

Sherr, C.J., and DePinho, R.A. (2000). Cellular senescence: mitotic clock or culture shock? Cell *102*, 407-410.

Sherr, C.J., and McCormick, F. (2002). The RB and p53 pathways in cancer. Cancer Cell *2*, 103-112.

Shiloh, Y., and Ziv, Y. (2013). The ATM protein kinase: regulating the cellular response to genotoxic stress, and more. Nat Rev Mol Cell Biol *14*, 197-210.

Smogorzewska, A., and de Lange, T. (2002). Different telomere damage signaling pathways in human and mouse cells. EMBO J *21*, 4338-4348.

Soubeyrand, S., Pope, L., and Hache, R.J. (2010). Topoisomerase IIalpha-dependent induction of a persistent DNA damage response in response to transient etoposide exposure. Mol Oncol *4*, 38-51.

Soulas-Sprauel, P., Rivera-Munoz, P., Malivert, L., Le Guyader, G., Abramowski, V., Revy, P., and de Villartay, J.P. (2007). V(D)J and immunoglobulin class switch recombinations: a paradigm to study the regulation of DNA end-joining. Oncogene *26*, 7780-7791.

Soutoglou, E., Dorn, J.F., Sengupta, K., Jasin, M., Nussenzweig, A., Ried, T., Danuser, G., and Misteli, T. (2007). Positional stability of single double-strand breaks in mammalian cells. Nat Cell Biol *9*, 675-682.

Soutoglou, E., and Misteli, T. (2008). Activation of the cellular DNA damage response in the absence of DNA lesions. Science *320*, 1507-1510.

Sperka, T., Wang, J., and Rudolph, K.L. (2012). DNA damage checkpoints in stem cells, ageing and cancer. Nat Rev Mol Cell Biol *13*, 579-590.

Stansel, R.M., de Lange, T., and Griffith, J.D. (2001). T-loop assembly in vitro involves binding of TRF2 near the 3' telomeric overhang. EMBO J *20*, 5532-5540.

Stewart, G.S., Maser, R.S., Stankovic, T., Bressan, D.A., Kaplan, M.I., Jaspers, N.G., Raams, A., Byrd, P.J., Petrini, J.H., and Taylor, A.M. (1999). The DNA double-strand break repair gene hMRE11 is mutated in individuals with an ataxia-telangiectasia-like disorder. Cell *99*, 577-587.

Stewart, G.S., Panier, S., Townsend, K., Al-Hakim, A.K., Kolas, N.K., Miller, E.S., Nakada, S., Ylanko, J., Olivarius, S., Mendez, M.*, et al.* (2009). The RIDDLE syndrome protein mediates a ubiquitin-dependent signaling cascade at sites of DNA damage. Cell *136*, 420-434.

Stewart, G.S., Stankovic, T., Byrd, P.J., Wechsler, T., Miller, E.S., Huissoon, A., Drayson, M.T., West, S.C., Elledge, S.J., and Taylor, A.M. (2007). RIDDLE immunodeficiency syndrome is linked to defects in 53BP1-mediated DNA damage signaling. Proc Natl Acad Sci U S A *104*, 16910-16915.

Stracker, T.H., Couto, S.S., Cordon-Cardo, C., Matos, T., and Petrini, J.H. (2008). Chk2 suppresses the oncogenic potential of DNA replication-associated DNA damage. Mol Cell *31*, 21-32.

Stucki, M., Clapperton, J.A., Mohammad, D., Yaffe, M.B., Smerdon, S.J., and Jackson, S.P. (2005). MDC1 directly binds phosphorylated histone H2AX to regulate cellular responses to DNA double-strand breaks. Cell *123*, 1213-1226.

Sulli, G., Di Micco, R., and d'Adda di Fagagna, F. (2012). Crosstalk between chromatin state and DNA damage response in cellular senescence and cancer. Nat Rev Cancer *12*, 709-720.

Suram, A., Kaplunov, J., Patel, P.L., Ruan, H., Cerutti, A., Boccardi, V., Fumagalli, M., Di Micco, R., Mirani, N., Lal Gurung, R.*, et al.* (2012). Oncogene-induced telomere dysfunction enforces cellular senescence in human cancer precursor lesions. EMBO J.

Takai, H., Smogorzewska, A., and de Lange, T. (2003). DNA damage foci at dysfunctional telomeres. Curr Biol *13*, 1549-1556.

Tang, D.G., Tokumoto, Y.M., Apperly, J.A., Lloyd, A.C., and Raff, M.C. (2001). Lack of replicative senescence in cultured rat oligodendrocyte precursor cells. Science *291*, 868-871.

Teixeira, M.T., Arneric, M., Sperisen, P., and Lingner, J. (2004). Telomere length homeostasis is achieved via a switch between telomerase- extendible and -nonextendible states. Cell *117*, 323-335.

Toussaint, O., Medrano, E.E., and von Zglinicki, T. (2000). Cellular and molecular mechanisms of stress-induced premature senescence (SIPS) of human diploid fibroblasts and melanocytes. Exp Gerontol *35*, 927-945.

Tumpel, S., and Rudolph, K.L. (2012). The role of telomere shortening in somatic stem cells and tissue aging: lessons from telomerase model systems. Ann N Y Acad Sci *1266*, 28-39.

van Steensel, B., and de Lange, T. (1997). Control of telomere length by the human telomeric protein TRF1. Nature *385*, 740-743.

van Steensel, B., Smogorzewska, A., and de Lange, T. (1998). TRF2 protects human telomeres from end-to-end fusions. Cell *92*, 401-413.

Vasile, E., Tomita, Y., Brown, L.F., Kocher, O., and Dvorak, H.F. (2001). Differential expression of thymosin beta-10 by early passage and senescent vascular endothelium is modulated by VPF/VEGF: evidence for senescent endothelial cells in vivo at sites of atherosclerosis. FASEB J *15*, 458-466.

Velarde, M.C., Flynn, J.M., Day, N.U., Melov, S., and Campisi, J. (2012). Mitochondrial oxidative stress caused by Sod2 deficiency promotes cellular senescence and aging phenotypes in the skin. Aging (Albany NY) *4*, 3-12.

Venteicher, A.S., Abreu, E.B., Meng, Z., McCann, K.E., Terns, R.M., Veenstra, T.D., Terns, M.P., and Artandi, S.E. (2009). A human telomerase holoenzyme protein required for Cajal body localization and telomere synthesis. Science *323*, 644-648.

von Zglinicki, T., Saretzki, G., Ladhoff, J., d'Adda di Fagagna, F., and Jackson, S.P. (2005). Human cell senescence as a DNA damage response. Mech Ageing Dev *126*, 111-117.

Wang, C., Jurk, D., Maddick, M., Nelson, G., Martin-Ruiz, C., and von Zglinicki, T. (2009). DNA damage response and cellular senescence in tissues of aging mice. Aging Cell *8*, 311-323.

Wang, H., Perrault, A.R., Takeda, Y., Qin, W., and Iliakis, G. (2003). Biochemical evidence for Ku-independent backup pathways of NHEJ. Nucleic Acids Res *31*, 5377-5388.

Wang, Y., Huang, J.W., Calses, P., Kemp, C.J., and Taniguchi, T. (2012). MiR-96 downregulates REV1 and RAD51 to promote cellular sensitivity to cisplatin and PARP inhibition. Cancer Res *72*, 4037-4046.

Watson, J.D. (1972). Origin of concatemeric T7 DNA. Nat New Biol *239*, 197-201.

Wei, W., Ba, Z., Gao, M., Wu, Y., Ma, Y., Amiard, S., White, C.I., Rendtlew Danielsen, J.M., Yang, Y.G., and Qi, Y. (2012). A role for small RNAs in DNA double-strand break repair. Cell *149*, 101-112.

Woo, R.A., and Poon, R.Y. (2004). Activated oncogenes promote and cooperate with chromosomal instability for neoplastic transformation. Genes Dev *18*, 1317-1330.

Wright, W.E., Piatyszek, M.A., Rainey, W.E., Byrd, W., and Shay, J.W. (1996). Telomerase activity in human germline and embryonic tissues and cells. Dev Genet *18*, 173-179.

Wu, P., Takai, H., and de Lange, T. (2012). Telomeric 3' overhangs derive from resection by Exo1 and Apollo and fill-in by POT1b-associated CST. Cell *150*, 39-52.

Wu, X., and Chen, J. (2003). Autophosphorylation of checkpoint kinase 2 at serine 516 is required for radiation-induced apoptosis. J Biol Chem *278*, 36163-36168.

Yan, D., Ng, W.L., Zhang, X., Wang, P., Zhang, Z., Mo, Y.Y., Mao, H., Hao, C., Olson, J.J., Curran, W.J.*, et al.* (2010). Targeting DNA-PKcs and ATM with miR-101 sensitizes tumors to radiation. PLoS One *5*, e11397.

Ye, J., Lenain, C., Bauwens, S., Rizzo, A., Saint-Leger, A., Poulet, A., Benarroch, D., Magdinier, F., Morere, J., Amiard, S.*, et al.* (2010). TRF2 and apollo cooperate with topoisomerase 2alpha to protect human telomeres from replicative damage. Cell *142*, 230-242.

Ye, J.Z., and de Lange, T. (2004). TIN2 is a tankyrase 1 PARP modulator in the TRF1 telomere length control complex. Nat Genet *36*, 618-623.

Ye, J.Z., Donigian, J.R., van Overbeek, M., Loayza, D., Luo, Y., Krutchinsky, A.N., Chait, B.T., and de Lange, T. (2004a). TIN2 binds TRF1 and TRF2 simultaneously and stabilizes the TRF2 complex on telomeres. J Biol Chem *279*, 47264-47271.

Ye, J.Z., Hockemeyer, D., Krutchinsky, A.N., Loayza, D., Hooper, S.M., Chait, B.T., and de Lange, T. (2004b). POT1-interacting protein PIP1: a telomere length regulator that recruits POT1 to the TIN2/TRF1 complex. Genes Dev *18*, 1649-1654.

Zhang, R., Poustovoitov, M.V., Ye, X., Santos, H.A., Chen, W., Daganzo, S.M., Erzberger, J.P., Serebriiskii, I.G., Canutescu, A.A., Dunbrack, R.L.*, et al.* (2005). Formation of MacroH2A-containing senescence-associated heterochromatin foci and senescence driven by ASF1a and HIRA. Dev Cell *8*, 19-30.

Zhang, X., Wan, G., Berger, F.G., He, X., and Lu, X. (2011). The ATM kinase induces microRNA biogenesis in the DNA damage response. Mol Cell *41*, 371-383.

Zimmermann, M., Lottersberger, F., Buonomo, S.B., Sfeir, A., and de Lange, T. (2013). 53BP1 regulates DSB repair using Rif1 to control 5' end resection. Science *339*, 700-704.

Ziv, Y., Bielopolski, D., Galanty, Y., Lukas, C., Taya, Y., Schultz, D.C., Lukas, J., Bekker-Jensen, S., Bartek, J., and Shiloh, Y. (2006). Chromatin relaxation in response to DNA double-strand breaks is modulated by a novel ATM- and KAP-1 dependent pathway. Nat Cell Biol *8*, 870-876.

Acknowledgments

I would like to thank many people, whose support has been essential for this research project.

My supervisor, Dr. Fabrizio d'Adda di Fagagna, for giving me the possibility to join his group, for advices, patience, and his ability to be a great boss.

Prof. Marco Foiani from IFOM (Milan, Italy) and Dr. Maria Blasco from CNIO (Madrid, Spain), for taking time out from their busy schedules to serve as my internal and external co-supervisors, respectively.

Prof. Karl Lenhard Rudolph from Leibniz Institute for Age Research (Jena, Germany) and Dr. Gioacchino Natoli from IEO (Milan, Italy), for accepting to be my examiners and for reading my thesis.

The IFOM-IEO-Campus facilities, in particular the Cell Culture, the Imaging, the RT-PCR and the Kitchen units, for their important help in my work.

Marzia, for teaching me everything I had to know to perform this job in the best way.

Aurora and Flavia, with whom I shared joys and pains of the PhD period till the thesis writing, and Valentina, who helped me for any problem in the lab and outside; they used to be my colleagues, but then became my dear friends.

The FDADF people, for being the best research group I could work in.

The lab F people, for making the workplace so fun.

All my friends, in particular Aida and Luca, for making me smile at home at the end of the long working days.

Giacomo, for supporting me in any pleasant or stressful moment, without asking anything in return. His high motivation in this job was to me an example to follow.

My family, for giving me the chance to chose my own way to happiness and to make all my decisions without interfering.